INFORMATION TO USERS

This manuscript has been reproduced from the microfilm master. UMI films the text directly from the original or copy submitted. Thus, some thesis and dissertation copies are in typewriter face, while others may be from any type of computer printer.

The quality of this reproduction is dependent upon the quality of the copy submitted. Broken or indistinct print, colored or poor quality illustrations and photographs, print bleedthrough, substandard margins, and improper alignment can adversely affect reproduction.

In the unlikely event that the author did not send UMI a complete manuscript and there are missing pages, these will be noted. Also, if unauthorized copyright material had to be removed, a note will indicate the deletion.

Oversize materials (e.g., maps, drawings, charts) are reproduced by sectioning the original, beginning at the upper left-hand corner and continuing from left to right in equal sections with small overlaps.

Photographs included in the original manuscript have been reproduced xerographically in this copy. Higher quality 6" x 9" black and white photographic prints are available for any photographs or illustrations appearing in this copy for an additional charge. Contact UMI directly to order.

Bell & Howell Information and Learning
300 North Zeeb Road, Ann Arbor, MI 48106-1346 USA
800-521-0600

Study of Circularly Symmetrical Two-dimensional Digital Filters Possessing Separable Denominator Transfer Functions

Seetharaman Swarnamani

A Thesis

in

The Department

of

Electrical and Computer Engineering

Presented in Partial Fulfillment of the Requirements

for the Degree of Master of Applied Science at

Concordia University

Montreal, Quebec, Canada

June 2000

Abstract

Study of Circularly Symmetrical Two-dimensional Digital Filters Possessing Separable Denominator Transfer Functions

Seetharaman Swarnamani

Multi-dimensional signal processing has many applications in modern-day devices and softwares. Specifically, two-dimensional signal processing and analysis has evoked a lot of interest among researchers due to their numerous advantages in areas such as image processing. Two-dimensional digital filters are being widely used in modern image processing software for various types of processing and analysis. In such applications, the signal does not have any preferred spatial direction and so the required filter function, possessing circularly symmetric frequency response characteristics, is of great importance.

The main objective of this Thesis has been to implement two-dimensional filter functions using simple design procedures and to study the presence of circular symmetry in such designed filters by parameter modifications. In keeping with the simple design criteria, the two-dimensional filters studied in this thesis have been designed starting from two one-dimensional filters as an independent product. Only IIR Filters have been considered for this purpose due to their capability of approximating the required response with low order filters and also their flexibility in terms of altering filter parameters to obtain new filters. The filters have been checked for stability before analysis. The design has made use of the fact that varying the feedback factor "k" in an IIR filter produces a near-circular

symmetric response for certain values of "k" between specific magnitude ranges.

Algorithms have been obtained to check the extent of circular symmetry under specific magnitude ranges and to correct the feedback factor "k" in order to obtain the maximum proximity to circular symmetry. The lowpass filter has been primarily chosen to illustrate the objective of the thesis. Both Butterworth and Chebyshev cases have been studied. This study has also focussed on the effect of changing the pole-parameters(polar angles) in two-dimensional lowpass filter functions and its contribution to circular symmetry.

The most common filter kinds, as well as their combination, have been studied and analysed for circular symmetry.

Considerable success has been achieved in obtaining near-circular symmetry especially among the two-dimensional lowpass filters. It has also been found that there exists numerous possibilities to achieve near circular symmetry based on the parameter modifications and magnitude range of the filter under study.

Acknowledgements

At the outset, I would like to sincerely thank Prof.Venkat Ramachandran, my thesis supervisor, for his guidance in carrying out this research all the way through to its completion. He introduced me to this exciting area of filters and was a constant source of inspiration.

I would also like to thank Prof.Rama.B.Bhat who was instrumental in providing me with this opportunity to pursue my graduate studies here in Concordia University and has been available for advice whenever I needed it. I would also like to thank him in the preparation of this thesis.

I would like to express my appreciation to Dr.J.C.Giguere for his valuable suggestions to improve the presentation of this Thesis.

My parents have always been a source of inspiration and this work would have been almost impossible without their constant encouragement and support from beyond seas.

I would like to express my heart-felt appreciation to my colleagues and friends namely Jyothsna, Rachit, Mahesh, Vijay Jain, Tanushri, Roli, Daksha, Jasjit, Helen, Meghana, Subhashini, Vijay Pisini, Zhiling and other colleagues from the Graduate students office. I spent most of my time during graduate work with these people and they have seen me through the thick and thins of my life as a student and if not for their support, this would not have been a smooth ride.

Table of Contents

List of Figures x

List of Tables xv

List of Important Symbols and Special Characters xvi

1 Introduction **1**

1.1 Two-Dimensional Digital filters 3

1.1.1 Finite Impulse Response Filters (FIR Filters) 3

1.1.2 Infinite Impulse Response Filters (IIR Filters) 4

1.2 Types of Symmetries associated with 2-D Transfer Functions 5

1.2.1 Displacement(Identity) Symmetry 6

1.2.2 Rotational Symmetry 6

1.2.3 Centro - Symmetry 7

1.2.4 Reflection Symmetry 7

1.2.5 Quadrantal Symmetry 8

1.2.6 Diagonal Fourfold Reflection Symmetry 8

1.2.7 Octagonal Symmetry 8

1.2.8 Circular Symmetry 9

1.3 Realization of the 2-D Filter Functions 10

1.3.1 Direct Method 10

1.3.2 Parallel Realization 10

1.3.3 Cascade Realization 11

1.3.4 Wave Realization 11
1.4 Scope of the Thesis 11

2 Generation of Stable Lowpass IIR 2-D Transfer Functions Possessing Near-circular Symmetry **14**

2.1 Introduction 14
2.2 Stability 16
2.3 Circular Symmetry: Importance and Significance 20
2.4 Design Methods for 2-D FIR Digital Filters 21
2.4.1 Frequency Transformation Method 22
2.4.2 Linear Programming Method 24
2.4.3 Window Method 24
2.5 Design Methods for 2-D IIR Digital Filters 26
2.6 Design of 2-D Butterworth Filters using Separable 1-D Transfer Functions 28
2.6.1 Design of 2-D IIR Lowpass Butterworth Filter using Separable Transfer Functions 29
2.7 Generation of Stable 2-D IIR Product Separable Denominator Transfer Functions and Test for Circular Symmetry 35
2.8 Algorithm to Check the Extent of Circular Symmetry for a Given Magnitude Range 45
2.9 Design of 2-D IIR Chebyshev Lowpass Filter 52
2.9.1 The Chebyshev Lowpass Characteristics 52
2.9.2 2-D Chebyshev Lowpass Characteristics and Test for Circular Symmetry 53

2.10 Pole-Parameter Transformation and Analysis of Lowpass Butterworth Filters 62
2.10.1 Introduction 62
2.10.2 Pole-parameter Representation 63
2.10.3 Complementary Symmetry 64
2.10.4 Symmetrical Swinging of Butterworth Poles Preserving the CPP Property 67
2.10.5 Low-Q Filters(LQF) 71
2.10.6 High-Q Filters(HQF) 73
2.10.7 Implementation of Pole Parameter Transformation 75
2.10.8 Two-dimensional CPPF 81
2.10.9 Summary and Discussion 93

3 Generation of Stable 2-D Bandpass, Bandstop and Highpass Filters and their Approximation to Circular Symmetry **95**
3.1 Bandpass Filter 96
3.2 Bandstop Filter 104
3.3 Highpass Filter 113
3.4 Summary and Discussion 121

4 Combination Filters **122**
4.1 Lowpass and Bandpass Combination Filter 123
4.2 Lowpass and Lowpass Combination Filter 128
4.3 Lowpass and Highpass Combination Filter 133
4.4 Summary and Discussion 139

5 Conclusions **140**

5.1 Circular Symmetry of 2-D Filters 141

5.1.1 Study of Circular Symmetry in Lowpass Filters 142

5.1.2 Study of Circular Symmetry in Complementary Pole-pair Filters 144

5.1.3 Study of Circular Symmetry in 2-D Highpass, Bandpass and Bandstop Filters 145

5.1.4 Study of Circular Symmetry in 2-D Combination Filters . . . 147

List of Figures

2.1 2-D IIR Butterworth LPF, Order-4 (a) Magnitude plot (b) Contour plot 34

2.2 Basic structure for the 2-D transfer function expressed as a signal flow graph. 36

2.3 Plot of Eqn.(2.23) for k=0.5. (a) Magnitude plot (b) Contour plot . . 39

2.4 Contour plots for 2-D IIR Butterworth LPF for (a) k=-0.6 (b) k=-0.4 40

2.5 Contour plot for 2-D IIR Butterworth LPF for k=-0.3 41

2.6 Contour plots for 2-D IIR Butterworth LPF for (a) k=-0.2 (b) k=0 . 42

2.7 2-D IIR Butterworth LPF response and test for circular symmetry under magnitude range 0.49<Mag<0.51 for (a) k=-0.6 (b) k=-0.4. . . 49

2.8 2-D IIR Butterworth LPF response and test for circular symmetry under magnitude range 0.49<Mag<0.51 for k=-0.3. 50

2.9 2-D IIR Butterworth LPF response and test for circular symmetry under magnitude range 0.49<Mag<0.51 for (a) k=-0.2 (b) k=0. . . . 51

2.10 2D Chebyshev LPF characteristics for (a) k=-1.0 and (b) k=-0.8. . . 55

2.11 2D Chebyshev LPF characteristics for (a) k=-0.64 56

2.12 2D Chebyshev LPF characteristics for (a) k=-0.4 and (b) k=0.4. . . . 57

2.13 Plots to show the extent of circular symmetry for the case where $\epsilon = 0.1526$. These plots are shown for the same corresponding values of k as shown in Figs.(2.10), (2.11), (2.12). All the plots show the magnitude range $0.28 < Mag < 0.32$. 58

2.14 2D Chebyshev lowpass filter characteristics for the second case considered for ripple width $\epsilon = 0.3493$. Plots (a)-(e) are shown for different values of k close to circular symmetry. 60

2.15 Plots to show the extent of circular symmetry for the second case where $\epsilon = 0.3493$. The plots are shown for the same corresponding values of k as in Fig.(2.14). All the plots show the magnitude range $0.28 < Mag < 0.32$. 61

2.16 Pole parameter representation 63

2.17 Pole plot for a 1-D filter of order $n = 16$. 66

2.18 Pole parameter swinging and shifting of the adjacent pole-pair towards each other. 68

2.19 (a) Polar plot for 1-D filter of order $n = 8$. (b) Shifting of the poles by $\pm 5^o$. 80

2.20 Magnitude response of the CPP filters : comparitive study 81

2.21 Shift of poles by angle of $\pm 5^o$ for the two independent transfer functions. 82

2.22 2-D CPPF before pole parameter transformation showing near circular symmetry at $k = k_1 = k_2 = -0.3$. (a) Magnitude Plot (b) Contour Plot 85

2.23 2-D CPPF after pole parameter transformation of $\theta_o = +5^o$ showing near circular symmetry at $k = k_1 = k_2 = -0.48$. 86

2.24 Plots to illustrate the extent of circular symmetry obtained after shifting the poles of the original transfer function by $+5^o$. 87
2.25 2-D CPPF after pole parameter transformation of $\theta_o = -5^o$ showing near circular symmetry at $k = k_1 = k_2 = -0.67$. 88
2.26 2-D CPPF after pole parameter transformation of $\theta_o = +3^o$ showing near circular symmetry at $k = k_1 = k_2 = -0.08$. 89
2.27 2-D CPPF after pole parameter transformation of $\theta_o = -3^o$ showing near circular symmetry at $k = k_1 = k_2 = -0.04$. 90
2.28 2-D CPPF after pole parameter transformation of $\theta_o = +7^o$ showing near circular symmetry at $k = k_1 = k_2 = 0.18$. 91
2.29 2-D CPPF after pole parameter transformation of $\theta_o = -7^o$. It is noted that there is clearly no circular symmetry in this case. 92

3.1 2-D IIR Butterworth Bandpass filter of 4^{th} order - contour plots. . . 102
3.2 Plots to show the extent of circular symmetry of the responses shown in Fig.(3.1). The magnitude range under consideration is 0.8<Mag<1. 103
3.3 2-D IIR Butterworth Bandstop Filter of 4th order-contour plots. . . 111
3.4 Plots to show the extent of circular symmetry of the responses shown in Fig.(3.3). The magnitude range under consideration is 0.45<Mag<0.55. 112
3.5 2-D IIR Butterworth Highpass Filter of 4th order-contour plots. . . . 119
3.6 Plots to show the extent of circular symmetry of the responses shown in Fig.(3.5). The magnitude range under consideration is 0.45<Mag<0.55. 120

4.1 A one-dimensional interpretation of the Lowpass+Bandpass combination. 123

4.2 Plots showing (a) the response of the Lowpass filter (b) approximation to circular symmetry between magnitude range [0.7,0.9](normalised) derived from Program A3. 125
4.3 Plot showing the response of the combination filter. 126
4.4 Plot showing the extent of circular symmetry in the combination of a Lowpass and a Bandpass filter. Magnitude range under study=[0.7 0.9](normalised) derived from Program A3. 126
4.5 A one-dimensional interpretation of the two Lowpass filter combination. 128
4.6 Plots (a) and (c) showing the response of the Lowpass filters (1) and (2) respectively and plots (b) and (d) showing their approximation to circular symmetry for a specific magnitude range [0.2, 0.4](normalised) derived from Program A3. 130
4.7 Plots (a) and (b) showing the response of the combination filter(magnitude and contour plots respectively) and plot (c) showing the extent of circular symmetry in this response between the magnitude range[0.2, 0.4](normalised) derived from Program A3. 131
4.8 A one-dimensional interpretation of the Lowpass+Highpass combination. 133
4.9 Plot (a) showing the response of the Lowpass filter and plot (b) showing its approximation to circular symmetry between magnitude range [0.2, 0.4](normalised) derived from Program A3. 135
4.10 Plot (a) showing the response of the Highpass filter and plot (b) showing its extent of circular symmetry for $k = -0.52$ and in the magnitude range [0.2, 0.4](normalised) derived from Program A3. 136

4.11 Plot to show the extent of circular symmetry in the combination of a Lowpass and a Highpass filter. Magnitude range under study=[0.2 0.4](normalised) derived from Program A3. 137

List of Tables

2.1 Filter Specifications for the Butterworth Lowpass Filter. Scripts 1 and 2 refer to the two-dimensions respectively. 31

2.2 Analysis results for the extent of circular symmetry in 2-D Chebyshev lowpass transfer functions for two different values of ripple width. The magnitude range under study for both the above cases is 0.49<Mag<0.51. 59

2.3 Summary of the results obtained due to the analysis of the pole parameter transformation filters. 79

2.4 Summary of the results achieved due to different values of angular shift in the complex poles and their corresponding values of k for circular symmetry. The range of magnitude chosen for all the above cases is 0.49<Mag<0.51. 93

4.1 Combination filter parameters - Lowpass + Bandpass Filter. 123

4.2 Combination filter parameters - Lowpass - Lowpass Filter. 129

4.3 Combination filter parameters - Lowpass + Highpass filter. 134

List of Important Symbols and Special Characters

z_1, z_2	Z-domain parameter in first and second dimension.
s_1, s_2	Laplace domain parameter in first and second dimension.
ω_1, ω_2	Frequencies in radians in the analog domain in first and second dimension(also w_1, w_2).
k_1, k_2	Feedback factor in an IIR Transfer function in first and second dimension.
$\sum$	Summation.
$\forall$	For all values.
$\in$	Belongs to.
$\prod$	Product of.
α	Gain of a transfer function in decibels.
β	Polar angle in degrees.
$\beta_1, \beta_2, \beta_3$	Poles of a transfer function.
ϵ	Ripple width of a Chebyshev filter.
ω_{pk}, θ_{pk}	Magnitude and Angle(in degrees) of a pole-phasor.
Q	Q-factor.
W_p	Pass-band edge cut-off frequency of a filter in the analog domain(radians).

W_s	Stop-band edge cut-off frequency of a filter in the analog domain(radians).
W_n	Natural frequency of a Butterworth filter in the analog domain(radians).
R_p	Loss in the pass-band region of a filter in the analog domain(decibels).
R_s	Loss in the stop-band region of a filter in the analog domain(decibels).

Chapter 1

Introduction

The topic of Multidimensional system (MDS) analysis and design has attracted considerable attention during recent years and is still receiving increased attention by theorists and practitioners. Because of its important applications in many practical systems, this subject is still being investigated. Different aspects of problems have been thoroughly studied and these include modeling, stability, structure analysis and realizations, digital filter design, multidimensional signal processing, reconstruction and so on. Many important results have been obtained.

Specifically, interest has been directed by researchers into the area of two-dimensional (2-D) digital systems due to several reasons: high efficiency due to high-speed computations; permitting better image processing and analysis; great application flexibility and adaptivity; decreasing cost of software or hardware implementations due to the large expansion and evolution of standard computers, microcomputers, microprocessors, and high-integration digital circuits. These two-dimensional digital systems are being used increasingly to replace analog systems in important areas such as facsimile, television, sonar, radar, bio-medicine, remote sensing, underwater acoustics,

moving-objects recognition, robotics and so on.

Important operations that can be performed by two-dimensional digital systems include the following: two-dimensional digital filtering, two-dimensional digital transformations, local space processing, data compression, and pattern recognition. Digital filtering, digital transformations, and local space operators play important roles in preprocessing of images, performing smoothing, enhancement, noise reduction, extracting boundaries and edges before pattern recognition, data compression operations permitting the reduction of large number of data representing the images in digital form and solving or minimizing transmission and storage problems. Pattern recognition operations permit the extraction of significant information and configurations from the images for final interpretation and utilization.

Over the past decade, researchers have shown particular interest in two-dimensional filters, both recursive and non-recursive. These two-dimensional filters find increasing applications in many fields, such as image processing and seismic signal processing. In many of these applications, the signal does not have any preferred spatial direction, and so the required filter functions, possessing circularly symmetric frequency response characteristics are finding great importance. Also two dimensional filters find increasing applications in image restoration and enhancement. As an example, two dimensional highpass filtering removes the unwanted background noise from an image so that the details contained in the higher spatial frequencies are easier to perceive.

1.1 Two-Dimensional Digital filters

In general, similar to one-dimensional(herewith referred to as 1-D) digital filters, two-dimensional digital(herewith referred to as 2-D) filters can be classified into two main groups. The first group comprises a finite sequence transfer function and so the filters in this group are called Finite Impulse Response (FIR) filters. The second group comprises an infinite sequence transfer function and so the filters in this group are called Infinite Impulse Response (IIR) filters.

1.1.1 Finite Impulse Response Filters (FIR Filters)

The transfer function of 2-D FIR filters can be described by using 2-D z-transform as follows:

$$H(z_1, z_2) = \sum_{n_1=0}^{M} \sum_{n_2=0}^{N} A_{n_1 n_2} z_1^{-n_1} z_2^{-n_2} \tag{1.1}$$

Eqn.(1.1) means that some of the 1-D design methods can be directly extended to two(2-D) or more dimensions(m-D) by appropriate modifications in the design procedures. It should also be noted that a straightforward extension of 1-D technique to 2-D design may not always be possible. In the 2-D FIR filters, problems of stability do not occur since the impulse response is bounded and exists only for finite time or the stability of $H(z_1, z_2)$ is guaranteed. Therefore

$$\sum_{n_1=0}^{M} \sum_{n_2=0}^{N} |h(z_1, z_2)| < \infty \tag{1.2}$$

for all finite values of M and N.

1.1.2 Infinite Impulse Response Filters (IIR Filters)

The transfer function of 2-D IIR filters can be described by using 2-D z-transform [1] and can be expressed as a ratio of two variable polynomials as follows:

$$H(z_1, z_2) = \frac{N(z_1, z_2)}{D(z_1, z_2)} = \frac{\sum_{i=0}^{K} \sum_{j=0}^{J} a_{ij} z_1^{-i} z_2^{-j}}{\sum_{k=0}^{K} \sum_{l=0}^{L} b_{kl} z_1^{-k} z_2^{-l}} \tag{1.3}$$

where $b_{00} = 1$, $a_{ij}$and b_{kl} are real coefficients.

For any input signal $X(z_1, z_2)$, the output of the filter is given by,

$$Y(z_1, z_2) = H(z_1, z_2) \cdot X(z_1, z_2) \tag{1.4}$$

In the 2-D IIR filters, one important problem to be dealt with is stability. According to stability theorem [2], [3], the 2-D IIR filter is guaranteed to be stable in the bounded-input bounded-output(BIBO) sense, if there exists no value of z_1 and z_2 for which

$$D(z_1, z_2) = 0 \; for \; both \; |z_1| \geq 1 \; and \; |z_2| \geq 1 \tag{1.5}$$

exists simultaneously [1]. This means it is highly preferable that the given analog transfer function must have Very Strictly Hurwitz Polynomial (VSHP) denominator [3], [4]. In the Laplace domain, the polynomial $D(s_1, s_2)$ is said to be very strictly Hurwitz polynomial if $(1/D(s_1, s_2))$ does not possess any singularities in the region (s_1, s_2) with $Re(s_1) \geq 0$ and $Re(s_2) \geq 0$. Therefore, the design of a 2-D IIR filter requires obtaining the coefficients a_{ij} and b_{kl} in Eqn.(1.3) so that $H(e^{j\omega_1 t_1}, e^{j\omega_2 t_2})$ approximates a given response $G(j\omega_1, j\omega_2)$ where ω_1 and ω_2 are horizontal and vertical spatial frequencies respectively, which also ensures the stability of the filter. If we obtain

a transfer function whose denominator is a VSHP and then obtain a corresponding digital transfer function by using the double bilinear transformation given by

$$s_i \rightarrow \frac{z_i - 1}{z_i + 1}, i = 1, 2 \tag{1.6}$$

then we can guarantee stability in the digital domain also.

1.2 Types of Symmetries associated with 2-D Transfer Functions

Two and higher dimensional systems may possess different types of symmetries. These symmetries have been used to reduce the complexity of the design and implementation of systems.

To understand how symmetry concept is extended to mathematical functions, consider a real function $f(x_1, x_2)$ of two independent variables x_1 and x_2. The function $f(x_1, x_2)$ assigns a unique value to each pair of values of x_1 and x_2 and so may be represented by a three dimensional object having the (x_1, x_2) plane as the base and the value of the function at each point in the plane as the height. We may say that a function possesses a symmetry, if a pair of operations, performed simultaneously, one on the base of the function object (i.e.,(x_1, x_2) plane), and the other on the height of the object(function value) leaves the function undisturbed.

In other words, existence of symmetry in a function implies that the value of the function at (x_{1T}, x_{2T}) meets a certain requirement or condition, where (x_{1T}, x_{2T}) is obtained by some operation on (x_1, x_2), and this condition being satisfied for all

points in the region.

Most of the applications require that a 2-D digital filter shall have a certain symmetry in its magnitude response. This symmetry property can be used in the reduction of the number of multiplications in the implementation of these filters and also in the reduction of the number of variables in the optimization procedure. The following gives a brief review of the different symmetry constraints [5].

1.2.1 Displacement(Identity) Symmetry

If a function possesses displacement identity symmetry with a displacement of d, the symmetry conditions on the function can be expressed as

$$f(x+d) = f(x) \; \forall \; x \in X \tag{1.7}$$

1.2.2 Rotational Symmetry

Choosing the rotational center as the origin and the rotation angle as $\pi/2$ radians, we get the four-fold rotational symmetry condition as

$$f(x_1, x_2) = f(-x_2, x_1) \; \forall \; x \in X \tag{1.8}$$

following which we have

$$f(x_1, x_2) = f(-x_1, x_2) = f(-x_1, -x_2) = f(x_1, -x_2) \tag{1.9}$$

1.2.3 Centro - Symmetry

In the two-variable case, twofold rotational symmetry (rotation by π radians) is called centro-symmetry. The required condition for centro-symmetry is

$$f(-x_1, -x_2) = f(x_1, x_2) \; \forall \; x \in X \tag{1.10}$$

In a similar way, conditions for centro-anti-, centro-conjugate and centro-conjugate antisymmetries may be stated.

1.2.4 Reflection Symmetry

Reflections about the x_1 axis, the x_2 axis, and the diagonals $x_1 = x_2$ and $x_1 = -x_2$ line, respectively, result in reflection symmetries which could be any one of the following:

$$x_1 \; axis \; reflection \; \rightarrow f(x_1, -x_2) = f(x_1, x_2) \tag{1.11}$$

$$x_2 \; axis \; reflection \; \rightarrow f(-x_1, x_2) = f(x_1, x_2) \tag{1.12}$$

$$x_1 = x_2 \; line \; intersection \; \rightarrow f(x_2, x_1) = f(x_1, x_2) \tag{1.13}$$

$$x_1 = -x_2 \; line \; intersection \; \rightarrow f(-x_2, -x_1) = f(x_1, x_2) \tag{1.14}$$

$$180^\circ \; rotation \; about \; the \; origin \; \rightarrow f(-x_1, -x_2) = f(x_1, x_2) \tag{1.15}$$

$$90^\circ \; rotation \; about \; the \; origin \; \rightarrow f(x_2, -x_1) = f(x_1, x_2) \tag{1.16}$$

1.2.5 Quadrantal Symmetry

The condition on the function to possess quadrantal identity symmetry is

$$f(x_1, x_2) = f(x_1, -x_2) = f(-x_1, x_2) = f(-x_1, -x_2) \tag{1.17}$$

It is easy to verify that the four quadrants of the X-plane correspond to the four symmetry regions. Hence this symmetry is called quadrantal symmetry.

1.2.6 Diagonal Fourfold Reflection Symmetry

Similar to the quadrantal case, if the function possesses reflection symmetry with respect to the $x_1 = x_2$ line and the $x_1 = -x_2$ line simultaneously, it is supposed to possess diagonal fourfold reflection symmetry

$$f(x_1, x_2) = f(x_2, x_1) = f(-x_2, -x_1) = f(-x_1, -x_2) \tag{1.18}$$

As in quadrantal symmetry, the function possesses two-fold rotational symmetry when it possesses diagonal fourfold reflection symmetry.

1.2.7 Octagonal Symmetry

In this case the function possesses quadrantal symmetry and diagonal symmetry simultaneously. The conditions for a function to posses octagonal symmetry are given

by

$$f(x_1, x_2) = f(x_1, -x_2) = f(-x_1, x_2) = f(x_2, x_1) = f(-x_2, -x_1) = f(-x_1, -x_2)$$
$$= f(x_2, -x_1) = f(-x_2, x_1) \tag{1.19}$$

1.2.8 Circular Symmetry

Mathematically, circular symmetry in 2-D filter responses can be defined as the filter response being able to satisfy the general equation of a circle, according to which,

$$\omega_1^2 + \omega_2^2 = M \tag{1.20}$$

where ω_1 *and* ω_2 are the frequencies in the two dimensions, and M is the magnitude response which needs to be a constant in order to satisfy the circular symmetry property.

However, it has been clearly proved in [7], [14] that, it is not possible to obtain exact circularly symmetric stable rational transfer function with denominator other than unity in the analog domain. In order to approximate circular symmetry, a product separable function given by,

$$H(s_1, s_2) = h_1(s_1)\, h_2(s_2) \tag{1.21}$$

is considered.

From the above the following can be deduced:

(1) Any separable function $H(s_1, s_2) = h_1(s_1) \times h_2(s_2)$ is quadrantally symmetric.

(2) When $h_1(.) = h_2(.)$, $H(s_1, s_2)$ is also octagonally symmetric, where $h_1(.)$ is a

single variable function.

(3) For the magnitude of circular symmetry being the main criterion, $|h_1(j\omega_1)|^2$ should approximate $\lambda e^{\alpha\omega_1^2}$ for suitable values of λ and α.

(4) When stable all-pole 2-D transfer functions are constrained to possess quadrantal symmetry, they turn out to be separable.

1.3 Realization of the 2-D Filter Functions

The realization of the filter networks from the transfer function can be accomplished using the following important methods:

1.3.1 Direct Method

All 2-D transfer functions can be realized using this method. This realization follows from the algorithm given by Shank [8].

It can be shown that Eqn.(1.3) can be written as

$$Y(z_1,z_2)=\left(\sum_{i=0}^{I}\sum_{j=0}^{J}a_{ij}z_1^{-i}z_2^{-j}\star X(z_1,z_2)\right)-\left(\sum_{k=0}^{K}\sum_{l=0}^{L}b_{kl}z_1^{-k}z_2^{-l}\star Y(z_1,z_2)\right) \quad (1.22)$$

The above equation can be directly realized using different approaches [9]. However, one main limitation of direct realization is that it results in high round-off errors.

1.3.2 Parallel Realization

In this case the given 2-D transfer function is to be expanded,where possible, into partial fractions.

1.3.3 Cascade Realization

Here, it is required that the given 2-D transfer function is expressed as a product of several lower order 2-D transfer functions which may not be possible since a 2-variable polynomial, in general, is not factorizable. It is noted here that when the 2-D function may be expressed as a product of realizable low-order functions, then a cascade type of realisation can be used.

1.3.4 Wave Realization

This realization starts from a given analog network which is transformed into digital domain by a double bilinear transformation. As is evident, exact realizations of the product separable transfer functions are not possible [10].

1.4 Scope of the Thesis

Finite impulse frequency response (FIR) filter functions possessing nearly circular symmetric responses can be generated from 1-D FIR functions [11]. This procedure cannot, however, be used to generate 2-D infinite impulse response (IIR) functions approximating circular symmetry, as the application of such a transformation to a 1-D IIR function results in a 2-D IIR function which is not, in general, factorizable into a set of quarter plane or half-plane stable functions without further effort [12].

It has been recently proved that if a quarter plane filter possesses quadrantal symmetry in its magnitude response, then its denominator can be expressed as a product of two 1-D polynomials [13], [14]. It can be easily verified that the presence of circular symmetry implies the presence of octagonal, and hence, quadrantal symmetries.

Therefore it is reasonable to constrain the desired function to possess octagonal symmetry in its magnitude response and to choose the filter function with a product separable denominator. The main scope of this thesis is to choose and study such filter functions. Such a choice eliminates the necessity for checking the stability of the filter during the approximation stage of the design. For filters which do not possess quadrantal symmetry in their frequency responses, this constraint, namely the denominator being product separable, restricts the domain of functions over which approximation is carried out resulting in suboptimal solutions. Also, since there is no constraint on the numerator polynomials, the types of responses one can approximate using separable denominator filter functions seems to be practically unlimited.

In this thesis, the most common types of filter responses namely Lowpass, Highpass, Bandpass and Bandstop have been considered in detail with respect to the above mentioned theory. Separable denominator transfer functions will be considered in all the above cases. This means that the 2-D filters will be studied as an extension to the 1-D counterpart. All the 2-D filter designs, considered in this thesis work, will therefore be derivations from two 1-D filters. This, in effect, is also the simplest of all conventional 2-D filter designs and therefore gives a lot of scope for future work.

In Chapter-2, Lowpass filters obtained from Butterworth, Chebyshev and pole-parameter transformations will be utilized in-order to design 2-D filters of approximate circular symmetry. The Lowpass filter will be chosen as the basis of comparison for the distinctly different types of filters, studied in this chapter. The effect of pole-parameter transformation and its effect on performance of the filter will then be studied. In this respect, first we point out that the pole vectors of the Butterworth filters(of order $n=2^k$) can be subjected to "prescribed symmetrical swinging"

[15], such that certain symmetry properties present in the original pole-pattern can be maintained invariant. Here we introduce a new family of filters called "2-D Complementary Pole-Pair Filters (2-D CPPF's)", generated by exploiting the symmetry invariant property as mentioned above. The performance of the new filters obtained are studied. The effect of this symmetrical swinging affecting the circular symmetry of these types of filters will also be studied.

In Chapter-3, Butterworth transformations of the Highpass, Bandpass and Bandstop filters will be implemented and their approximation to near-circular symmetry for each case will be studied. The Chebyshev filter design for these types of filters and their comparison to the Butterworth counterpart will be left as a scope for future study.

In Chapter-4, we will investigate the possibilities of combining different 2-D Butterworth filters to form unique transfer functions and therefore unique filter responses. The possibility of circular symmetry after the combination of two transfer functions will be studied. It is possible to obtain user specific filter responses by such combination filters. In this chapter, three different designs of combination filters will be considered and studied.

The basic goal, underlying in all of the above study, is to emphasise on the possibilty of near circular symmetry starting with filters possessing separable denominators and their combinations. Circular symmetry as we know is one of the most important aspect of commonly used filters, in emerging fields such as image processing. The main goal of this thesis is to obtain the nearest approximation to such filters with the simplest design methods possible.

Chapter 2

Generation of Stable Lowpass IIR 2-D Transfer Functions Possessing Near-circular Symmetry

2.1 Introduction

In order to design a filter having required specifications, one can suitably choose a transfer function with no common factors between the numerator and the denominator. Specifically in 1-D systems in the s-domain, let

$$H_a(s) = \frac{N_a(s)}{D_a(s)} \tag{2.1}$$

be the transfer function in the analog domain with $N_a(s)$ and $D_a(s)$ being relatively prime. For the above function to be stable, we must have $D_a(s)$ to be a Strictly Hurwitz Polynomial (SHP). A strictly Hurwitz polynomial is one which contains its

zeros strictly in the left-half of s-plane. In a similar manner, if

$$H_d(z) = \frac{N_d(z)}{D_d(z)} \tag{2.2}$$

is a transfer function in the discrete domain with $N_d(z)$ and $D_d(z)$ being relatively prime, then $D_d(z)$ should be a Schur polynomial in order that $H_d(z)$ shall be stable. A Schur polynomial contains its zeros strictly within the unit circle.

A simple method to generate a 2-D transfer function is to combine two 1-D transfer functions as a product. In other words, the eventual 2-D sequence is separable as two 1-D sequences that can be expressed as

$$h(x_1, x_2) = f(x_1)g(x_2) \tag{2.3}$$

where $f(x_1)$ and $g(x_2)$ are 1-D functions of independent variables x_1 and x_2, respectively. Such sequences are a special class of 2-D sequences. The 2-D sequence h(x_1,x_2) of this type has $(N_1 - 1)(N_2 - 1)$ degrees of freedom where

the region of support of f(x_1) : $0 \leq x_1 \leq N_1 - 1$ and

the region of support of g(x_1) : $0 \leq x_2 \leq N_2 - 1$

In the 2-D analog case in the s-domain, the transfer function may be expressed as

$$H_a(s_1, s_2) = \frac{N_a(s_1, s_2)}{D_a(s_1, s_2)} \tag{2.4}$$

The numerator $N_a(s_1, s_2)$ and the denominator $D_a(s_1, s_2)$ are polynomials in s_1 and s_2 with both even and odd terms. It may be possible that both the even and the odd parts of the polynomial become zero at specified sets of points, but not in their

neighborhood. If this occurs in the denominator of the transfer function, it is called a non-essential singularity of the first kind(NSFK). If in the 2-D transfer functions both numerator and denominator polynomials become zero simultaneously at a given set of points, it is known as non-essential singularity of the second kind(NSSK)[19]. The above two cases may be expressed as follows:

(a) $D_a(s_1, s_2) = 0$ and $N_a(s_1, s_2) \neq 0$ constitute non-essential singularity of the first kind at (s_1, s_2).

(b) $D_a(s_1, s_2) = 0$ and $N_a(s_1, s_2) = 0$ constitute non-essential singularity of the second kind at (s_1, s_2).

In the case of 2-D discrete or digital systems, a similar situation exists.

A well known method of designing digital filters is to start from the analog filter transfer function and then apply bilinear transformations $s_i \rightarrow \frac{z_i - 1}{z_i + 1}$, i=1, 2, to obtain the corresponding digital filter transfer function. In 1-D systems, such a transformation does not pose any problems. However in 2-D systems, this could pose problems concerning stability. In such cases, the denominator polynomial may cause problems because of non-essential singularities of first or the second kind. The occurrence of non-essential singularity of the first kind[4] always results in an unstable filter. The occurrence of non-essential singularity of the second kind could result in instability. However, it is not possible to determine, by inspection, if such a transfer function is stable or not [4], [20]. The next section discusses on the stability issue of filters.

2.2 Stability

As mentioned before, 2-D filters can be classified into two main categories namely the Finite Impulse Response Filters(FIR) and the Infinite Impulse Response Filters(IIR).

The Finite Impulse Response Filters have transfer functions resulting from a finite sequence and the Infinite Impulse Response Filters have transfer functions resulting from an infinite sequence.

One important issue concerning both the above types of Filters is the stability of the filter. Now it is known that Finite Impulse Response Filters are inherently stable. Infinite Impulse Response Filters may or may not be stable depending upon the transfer function.

The most commonly used definition for stability is based on the bounded-input bounded-output(BIBO) criterion. This criterion states that a filter is stable if its response to a bounded input is also bounded. Mathematically, it is possible to show that for causal linear shift-invariant systems, this corresponds to the condition that

$$\sum_{n_1=0}^{\infty} \sum_{n_2=0}^{\infty} \mid h(n_1, n_2) \mid < \infty \tag{2.5}$$

where $h(n_1, n_2)$ is the impulse response of the filter.

The above definition points out an important observation that the stability criterion is always verified if the number of terms of the impulse response is finite, which is the case with FIR Filters. However, the above condition does not prove feasible to the test of stability for IIR filters. In the 1-D case, it is possible to relate the BIBO stability condition to the positions of the z-transfer function poles which have to be within the unit circle and it is possible to test the stability by determining the zeros of the denominator polynomial. Similarly, in the 2-D case, a theorem establishing the relationship between the stability of the filter and the zeros of the denominator polynomial, can be formulated. This theorem states that [8], for causal quadrant filters, if $B(z_1, z_2)$ is a polynomial in z_1 and z_2, the expansion of $1/B(z_1, z_2)$ in the

negative powers of z_1 and z_2 converges absolutely if and only if

$$B(z_1, z_2) \neq 0 \quad for \quad \{| z_1 | \geq 1, | z_2 | \geq 1\} \tag{2.6}$$

The above theorem has the same form as in the 1-D case, i.e., it relates the stability of the filter to the singularities of the z-transform. However, in the 2-D case such a formulation for stability condition does not produce an efficient method for stability test, as in 1-D, due to the lack of appropriate factorization theorem of algebra. Therefore, it is necessary in principle, to use an infinite number of steps to test the stability. Also, even if it is possible to find methods to test conditions equivalent to Eqn.(2.6) in a finite number of steps [21], computationally it is not easy to incorporate them in a design method and there is a problem of stabilizing the filters which may become unstable.

From the point of view of stability tests, there can be two different approaches that can be considered, in designing an IIR filter. One method is to carry out the stability test in every stage of the filter design so that the eventual filter is stable. In the second method, stability is not considered as a part of the design and a magnitude-squared transfer function is first designed. Then a stable filter is obtained, by choosing the poles in the stability region. Such an approach is convenient, because squared-magnitude functions can be in a simple form and it is easy to find the poles of the filter.

However, in the 2-D case, poles in the stability region cannot be substituted for poles in the instability regions. This is because, unlike in the 1-D case, it is not possible to substitute the 2-D pole-pair combination by taking the inverse pole-pair transformation. Therefore different methods have to be used in arriving at a solution.

One possible solution can be obtained by considering this as a deconvolution problem. In the quadrant filter case, a filter $H(z_1, z_2)$ can be divided as a product of four filters ${}^{++}H(z_1, z_2)$, ${}^{+-}H(z_1, z_2)$, ${}^{--}H(z_1, z_2)$, ${}^{-+}H(z_1, z_2)$ each of which correspondingly represents their transfer function in the first, second, third and fourth quadrant, respectively, and each of which is stable, if computed through suitable sequence of computation. In view of the property that multiplication in the z-domain corresponds to a convolution in the space domain, the problem corresponds to the reconstruction of the four sequences. Similar procedures may be applied for unsymmetrical half-plane filters as well. In this case, the coefficient matrix, corresponding to the squared magnitude function, can be considered as the convolution of two unsymmetrical half-plane sequences. Thus it is possible to decompose the sequence into two half-plane filters. However in both the above cases there are problems which can arise, as the cepstra obtained using the above procedure are not finite in extent and some amount of truncation is necessary. This again modifies the transfer function and also the minimum phase property cannot be guaranteed after truncation. It is possible to observe that half-plane filters constitute a more general class than the quadrant ones since completely general transfer functions with real impulse response can be generated. The decomposition of a squared-magnitude function in four different quadrant filters or two half-plane filters, each being stable if a suitable sequence of computation is chosen, can give a direct method of obtaining linear phase filtering with IIR implementation. This is especially important when visual images have to be processed, because the shape of the object is related primarily to the phase information.

2.3 Circular Symmetry: Importance and Significance

Of the various types of symmetry that we have discussed in Chapter-1, the symmetry that is of interest to us in this thesis is the circular symmetry of 2-D filters. In many of the applications such as image processing and seismic signal processing, the signal does not possess any preferred spatial direction. Therefore it is desirable to process images with filters whose frequency response is approximately circularly symmetric. As mentioned earlier, FIR filter functions possessing nearly circularly symmetric frequency response can be generated using 1-D FIR functions[11]. But the same is not possible in the case of IIR functions, since the 2-D IIR function is not, in general, factorizable into a set of quarter-plane or half-plane functions. Moreover, the incorporation of the stability constraints in the approximation procedure, is yet another difficulty experienced in the design of IIR Filters. As a solution to this problem, it has been recently proved that if a quarter-plane filter possesses quadrantal symmetry in its magnitude response, then its denominator can be expressed as a product of 2-D polynomials [13], [14]. It can be readily verified that the specification of circular symmetry, implies the presence of the lower order symmetries namely, octagonal and hence, quadrantal symmetries. Therefore it may be reasonable to constrain the desired transfer function of the filter to possess octagonal symmetry(say) and choose the filter function with a product separable denominator. In cases where the filter function is not even quadrantally symmetric, the separable denominator constraint restricts the domain of functions over which approximation is carried out and results in sub-optimal solutions. But since the circular symmetry condition must also include quadrantal symmetry, the separable denominator condition does not prevent us from attaining optimal solutions. One another important aspect is that

there is no constraint over the numerator polynomials in any of the above designs. Hence the types of responses that can be obtained using separable denominator filter function is practically endless. The following two sections give a brief overview of the general design methods of FIR and IIR Filters following which the design method adopted in obtaining circular symmetry of Lowpass filters is described in detail.

2.4 Design Methods for 2-D FIR Digital Filters

FIR filters have transfer functions resulting from a finite sequence. Their main characteristic is that they can be designed to approximate a required frequency response that can be a modified by a linear phase term, if suitable symmetries are required to be present in the impulse response.

Let us consider a 2-D filter having the orders N and M odd in its non-causal form. By means of a translation of its impulse response it is possible to obtain the causal form. This introduces a linear phase term in the transfer function. Therefore the frequency response of the filter can be written in the form

$$H(e^{j\omega_1}, e^{j\omega_2}) = \sum_{k=-(M-1)/2}^{(M-1)/2} \sum_{l=-(N-1)/2}^{(N-1)/2} a_{nc} e^{-j(k\omega_1 + l\omega_2)} \tag{2.7}$$

From the above equation, if the coefficients $a_{nc}(k,l)$ has the symmetry property

$$a_{nc}(k,l) = a_{nc}(k,-l) = a_{nc}(-k,-l) = a_{nc}(-k,l) \tag{2.8}$$

with respect to the axes in the four quadrants, the frequency response is given by

the following expression

$$H(e^{j\omega_1}, e^{j\omega_2}) = \sum_{m=0}^{(M-1)/2} \sum_{n=0}^{(N-1)/2} a(m,n)cos(m\omega_1)cos(n\omega_2) \tag{2.9}$$

where $a(0,0) = a_{nc}(0,0)$

$a(m,0) = 2a_{nc}(m,0)$ where $m = 1, ..., \frac{M-1}{2}$

$a(0,n) = 2a_{nc}(0,n)$ where $m = 1, ..., \frac{N-1}{2}$

$a(m,n) = 4a_{nc}(m,n)$ where $m = 1, ..., \frac{M-1}{2}; n = 1, ..., \frac{N-1}{2}$

In the above case, it is obvious that the frequency response is symmetric with respect to the axes. This can be verified with a simple sign change of ω_1 and ω_2 in Eqn.(2.7). From Eqn.(2.7), the frequency response of the causal filter can be obtained by multiplying the equation by a linear phase term, corresponding to the shift of the impulse response.

This linear phase term can be written as $\exp(-j\{[(M-1)/2]\omega_1 + [(N-1)/2]\omega_2\})$.

The design problem now reduces to the evaluation of the coefficient matrix $a(k,l)$ so as to meet a set of specifications in the space or frequency domain. Several different methods have been proposed some of which are a direct generalization from their 1-D counterparts. Few of the most commonly used methods are discussed in brief, as follows.

2.4.1 Frequency Transformation Method

A suboptimum design method is based on the transformation of the frequency response of the 1-D filter into the frequency response of the 2-D filter [11]. Let us consider, a linear phase 1-D filter with N odd. The frequency response of such a filter

dropping the linear phase term can be written as

$$H(e^{j\omega}) = \sum_{k=0}^{(N-1)/2} a(k)cos(k\omega) \tag{2.10}$$

If for the above, a transformation of variables given by

$$cos(\omega) = Acos\omega_1 + Bcos\omega_2 + Ccos\omega_1 cos\omega_2 + D \tag{2.11}$$

is carried out, using the properties of trigonometric functions and Chebyshev polynomials, it is possible to obtain a 2-D function of the type

$$H(e^{j\omega_1}, e^{j\omega_2}) = \sum_{k=0}^{(N-1)/2} \sum_{l=0}^{(N-1)/2} a(k,l)cos(k\omega_1)cos(l\omega_2) \tag{2.12}$$

The above equation is formally identical to a linear phase 2-D filter, as in Eqn.(2.9).

For instance, if Eqn.(2.9) is solved for ω_1 as a function of ω_2, it is possible to draw the curves in the (ω_1,ω_2) plane, wherein the frequency response of the 2-D filter assumes the same value as the 1-D filter in ω. This means that the filter can be designed in 1-D and then can be transformed into 2-D if A, B, C, D can be chosen to obtain useful transformation contours. With the choice $A = B = C = -D = \frac{1}{2}$, the mapping contours are approximately circular, atleast for small values of ω and circularly symmetric filters can therefore be designed. This design procedure is very convenient from the computational point of view, and can be generalized to the use of transformation relations more complex than the simple relation of Eqn.(2.10) [22]. However, some care has to be given in carrying out the transformation, which is sensitive to numerical error when the number of coefficients becomes high.

2.4.2 Linear Programming Method

Another design methodology is possible using linear programming approach [23] and the multiple exchange ascent algorithm [24]. The main problem with these methods, is the computation time. This limits the maximum length of the impulse response of the filters obtained to about 9 x 9 in the linear programming case and to about 15 x 15 in the multiple exchange ascent case. This design problem can be more tractable by reducing the number of variables in the linear programming by means of frequency sampling approach [23]. In this case, a grid of points is chosen in the frequency domain and most of the frequency sample values are fixed through a direct translation of the filter specifications.

2.4.3 Window Method

The design of FIR filters can be carried out using another efficient and simple technique called the window method. Here we start with the fact that the 2-D frequency response being periodic, it is possible to represent it as a Fourier series, whose coefficients are proportional to the samples of the impulse response of the filter. This is based on the 2-D sampling theorem. Therefore, it is now possible to obtain, either analytically or by using an approximation method based on discrete inverse Fourier transform, the sampled impulse response, starting from the frequency domain specifications. The problem here is that the resulting impulse response is, in general, of infinite order and has to be truncated to obtain a digital filter that is usable in practice.

This truncation can be performed using a rectangular or circular window with an abrupt transition between the value "1" in the zone where the impulse response

has to be retained and "0" in the truncation region. However, such a truncation usually results in a large error in the frequency response for all practical applications. This is due to the fact that convolution in the frequency domain corresponds to multiplication in the sequence domain. Therefore, having a transform containing a wide main lobe and high side lobes as the truncation sequence, discontinuities in the theoretical frequency response are smoothened and oscillations appear. The problem is therefore, to truncate the impulse response by introducing as minimum error as possible, in the frequency response. To achieve this purpose, the sampled impulse response $h(k,l)$ values are multiplied by a window function of samples $w(k,l)$, whose transform presents a suitable trade-off between the width of the main lobe and the area under the sidelobes.

For an illustration, a 2-D window, having circular symmetry properties, can be defined starting from a 1-D window as [25]

$$w(x,y) = w\left(\sqrt{x^2+y^2}\right) \tag{2.13}$$

A number of windowing functions have been proposed to design filters in the 1-D case. For the 2-D case, extensions to the 2-D domain are normally used. The different types of window functions are (a) the Lanczos extension window (b) the Cappellini window (c) the Kaiser window (d) the Weber-type approximation windows (Cappellini windows 2 and 3)[25]. These vary in their primary function definition. Their discussion is beyond the scope of this thesis.

2.5 Design Methods for 2-D IIR Digital Filters

IIR Filters have transfer functions resulting from an infinite sequence. In general, it is more difficult to design a 2-D IIR filter than a 1-D IIR filter. 1-D techniques normally depend on the factorizability of one-variable polynomials, resulting in simple algorithms for the stability test and stabilization of unstable filters. Such techniques, unfortunately, are not directly generalizable to the 2-D case.

From the 2-D IIR filter function in Eqn.(1.3), it can be seen that the coefficients a_{kl} and b_{kl} have to be chosen to approximate the desired frequency response with a stable recursive implementation. The stability is an important problem of the recursive or IIR filters. Different design methods have been proposed, of which two design methods are the most common.

The first method involves spectral transformation from one-dimension to two-dimensions. The second method is based on parameter optimization, using classes of filter structures, as for example the cascade connection of second order filter sections, wherein stability of the filter is introduced using approximation algorithms.

The first method, as proposed in [8], consists of transformation from one-dimension to two-dimensions. This involves a mapping operation from 1-D to 2-D, with a rotation operation. Given a 1-D continuous filter in the factored form, its transfer function can be seen as one of a 2-D filter varying in one direction only:

$$H(s_1, s_2) = H_1(s_2) = H_0 \left[\frac{\prod_{i=1}^{m}(s_2 - q_i)}{\prod_{i=1}^{m}(s_2 - p_i)} \right] \tag{2.14}$$

where q_i and p_i are the zeros and poles of the filter.

As was mentioned before, a rotation operation, needs to be performed with the

transformation operation. A rotation of the (s_1, s_2) axes by an angle β may be performed by means of the transformation

$$s_1 = s_1' cos\beta + s_2' sin\beta \qquad s_2 = -s_1' sin\beta + s_2' cos\beta \tag{2.15}$$

Thus we obtain a filter whose frequency response is a function of s_1 and s_2 and corresponds to a rotation by an angle -β of Eqn.(2.15). From this a digital filter can be obtained by applying bilinear z-transforms to both the continuous variables. This method has been used to obtain simple rotated blocks which can be combined to obtain the design of circularly symmetric recursive filters [29]. Here the conditions of stability have also been proved.

Another method in the similar sense, involves transformation of the squared magnitude function of a 1-D filter to the 2-D domain, followed by a suitable decomposition of the resulting filter.

Given a causal filter(first quadrant filter), it is possible to define the corresponding second, third and fourth quadrant filters, according to the relations given by

$$h_1(k,l) = h_2(k,-l) = h_3(-k,-l) = h_4(-k,l) \tag{2.16}$$

with the following transfer functions given by

$$H_1(z_1,z_2) = H_2(z_1,z_2^{-1}) = H_3(z_1^{-1},z_2^{-1}) = H_4(z_1^{-1},z_2) \tag{2.17}$$

If the above four filters are cascaded, we obtain a zero-phase digital filter whose frequency response is defined by the coefficients $p(k,l)$ and $q(k,l)$ determined through

the convolution of the coefficients of the four filters and is of the following form:

$$G(e^{j\omega_1}, e^{j\omega_2}) = \frac{\sum_{k=0}^{N}\sum_{l=0}^{N} p(k,l)cos(k\omega_1)cos(l\omega_2)}{\sum_{k=0}^{K}\sum_{l=0}^{K} q(k,l)cos(k\omega_1)cos(l\omega_2)} \tag{2.18}$$

If we take a squared magnitude function of a 1-D IIR filter, and apply the transformation of Eqn.(2.11) to its numerator and denominator, then the above equation can be obtained. The squared magnitude function obtained has to be factorized to obtain stable recursive filters.

Based on the review given so far, in what follows, we consider the generation of 2-D filters having circular symmetry. Although it has been clearly proved in [7], [14] that it is not possible to obtain exact circularly symmetric filters, we consider the extent to which such filters can be designed by using separable 1-D transfer functions. In this Chapter we only consider the design of circularly symmetric Lowpass filters. The design of other filters namely Highpass, Bandpass and Bandstop filters will be dealt with in the subsequent chapters.

2.6 Design of 2-D Butterworth Filters using Separable 1-D Transfer Functions

The simplest way to design a 2-D filter is to obtain it as a product of two 1-D Filter transfer functions. Depending upon the requirement, it could be either an FIR or an IIR transfer function. As mentioned earlier, an FIR filter is one which has a transfer function resulting from a finite sequence and the IIR Filter is one which has a transfer function resulting from an infinite sequence. This section deals with the direct design

of 2-D IIR filters using separable transfer functions of two 1-D cases, which are exactly equal in all respects.

2.6.1 Design of 2-D IIR Lowpass Butterworth Filter using Separable Transfer Functions

Depending upon the frequency requirements to be met, filters, in general, are usually classified as

(a) Lowpass Filters - These filter out the high-frequency components of a signal and pass only the low-frequency signal below a certain frequency, in each dimension.

(b) Highpass Filters - These filter out the low-frequency components of a signal and pass only the high-frequency signal above a certain frequency, in each dimension.

(c) Bandpass filters - These filter out a band of frequencies, one below a low frequency and another above a high-frequency, in each dimension and passes the rest of the signal.

(d) Bandstop filters - These filter out a band of frequencies, one above a low frequency and another below a high-frequency, in each dimension and passes the rest of the signal.

In this chapter, only the implementation of the Lowpass Filter design is being considered.

Lowpass Filter

The design of a 2-D IIR Butterworth filter is carried out by first designing the 1-D Butterworth filter and then combining two similar 1-D transfer functions as a product. The program to implement the above has been written using MATLAB

using the various built-in subroutines to achieve the filter specifications. The following procedure has been adopted to design the filter:

(1) Given the specifications namely pass-band edge (W_p), stop-band edge (W_s), losses in the pass-band (R_p) and stop-band (R_s), the order of the filter (N) and the Butterworth natural frequency (W_n) are determined using the MATLAB function *"buttord"*. The procedure, so far, is in single dimension only.

(2) Knowing the order of the filter (N) and the Butterworth natural frequency (W_n), the filter's poles, zeros and the scalar gain (K) is determined using the MATLAB function *"butter"*.

(3) Having determined the poles, zeros and the scalar gain of the filter, the numerator (zeros) and the denominator (poles) polynomials are determined using the MATLAB function *"poly"*.

(4) Now we have the transfer function of the 1-D filter. The same procedure as above, is extended to the second dimension and the transfer function for the second dimension is obtained.

(5) The product of the two 1-D polynomials is determined.

(6) A general subroutine, suitable for any order of the filter has been written to determine the frequency response of the 2-D filter. The corresponding magnitude and contour plots are plotted using the MATLAB functions *"mesh"* and *"contour"*.

The following MATLAB algorithm (Program A1) has been written for the Lowpass filter specifications as shown in Table (2.1).

All frequencies are in radians.

The values of W_p, W_s, R_p, R_s for both the dimensions, can be changed in the program, based on the required design.

$W_p1 = W_p2$	$W_s1 = W_s2$	$R_p1 = R_p2(dB)$	$R_s1 = R_s2(dB)$	N	$W_n1 = W_n2$
0.15	0.65	0.5	45	4	0.2675

Table 2.1: Filter Specifications for the Butterworth Lowpass Filter. Scripts 1 and 2 refer to the two-dimensions respectively.

Program-A1

```
%% 2-D LOWPASS BUTTERWORTH IIR FILTER(lowpass.m) - (for Fig.(2.1))
    clear all;
    close all;
    %% Specification of the 1st 1-D Filter
    Wp1 = 0.15;
    Ws1 = 0.65;
    Rp1 = 0.5;
    Rs1 = 45;
    %% To determine the order-N1 and natural frequency-Wn1
    [N1, Wn1] = buttord(Wp1, Ws1, Rp1, Rs1);
    %% Specification of the 2nd 1-D Filter
    Wp2 = 0.15;
    Ws2 = 0.65;
    Rp2 = 0.5;
    Rs2 = 45;
    %% To determine the order-N2 and natural frequency-Wn2
    [N2, Wn2] = buttord(Wp2, Ws2, Rp2, Rs2);
    %% To determine the poles and zeros and the scalar gain of the 1st 1-D filter
    [Z1,P1,K1] = butter(N1,Wn1);
    Nmr1 = real(poly(Z1));
    Dnr1 = real(poly(P1));
    %% To determine the poles and zeros and the scalar gain of the 2nd 1-D filter
    [Z2,P2,K2] = butter(N2,Wn2);
    Nmr2 = real(poly(Z2));
    Dnr2 = real(poly(P2));
    %% To determine the 2-D transfer function as a product of 2 1-D transfer functions
    %% as Numerator(N) and Denominator(D)
    for m=1:1:size(Nmr1,2)
```

```
for n=1:1:size(Nmr2,2)
N(m,n)= Nmr1(m)*Nmr2(n);
end
end
for m=1:1:size(Dnr1,2)
for n=1:1:size(Dnr2,2)
D(m,n)= Dnr1(m)*Dnr2(n);
end
end
%% To determine the frequency response of the 2-D Lowpass filter
lim=pi;
c1=0;
for w1 = -lim:lim/20:lim
c2=0;
c1=c1+1;
for w2 = -lim:lim/20:lim
c2=c2+1;
for col=1:1:size(Nmr2,2)
NRow(1,col)=cos((size(Nmr2,2)-col)*w2) - j *sin((size(Nmr2,2)-col)*w2);
end
for row=1:1:size(Nmr2,2)
NCol(row,1)=cos((size(Nmr1,2)-row)*w1) - j *sin((size(Nmr1,2)-row)*w1);
end
NR = NRow * N' * NCol;
a=real(NR);
b=imag(NR);
for col=1:1:size(Dnr2,2)
DRow(1,col)=cos((size(Dnr2,2)-col)*w2) - j *sin((size(Dnr2,2)-col)*w2);
end
for row=1:1:size(Dnr2,2)
DCol(row,1)=cos((size(Dnr1,2)-row)*w1) - j *sin((size(Dnr1,2)-row)*w1);
end
DR = DRow * D' * DCol;
c=real(DR);
d=imag(DR);
MOD(c1,c2) = K1*K2*(sqrt((a*c + b*d)^2 + (b*c - a*d)^2))/(c^2+d^2);
end
```

```
end
%% To plot the frequency response of the 2-D Lowpass filter
w1=-lim:lim/20:lim;
w2=-lim:lim/20:lim;
[ww1,ww2]=meshgrid(w1,w2);
zz=MOD/(max(max(MOD)));
mesh(w1,w2,zz);
axis ('image');
xlabel('w1');
ylabel('w2');
zlabel('Magnitude Response');
title(' (b)2-D IIR Butterworth LPF - Order-4(Contour Plot)','FontSize',18);
grid on;
figure;
contour(ww1,ww2,zz);
axis('image');
xlabel('w1');
ylabel('w2');
zlabel('Magnitude Response');
title(' (b)2-D IIR Butterworth LPF - Order-4(Contour Plot)','FontSize',18);
grid on;
%% End of program
```

The results of the algorithm namely the magnitude and the contour plots are as shown in Fig.(2.1). It is noted that the contours are not circularly symmetric.

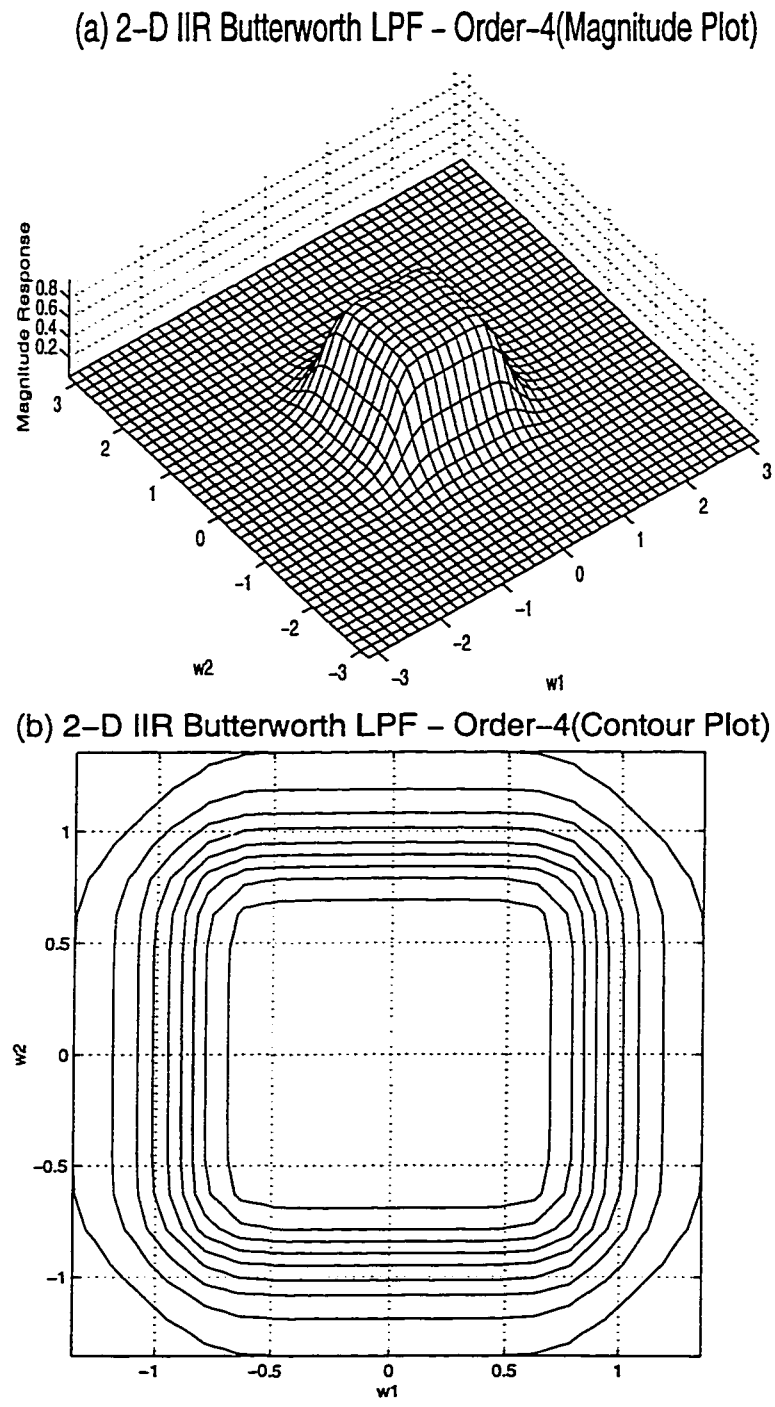

Figure 2.1: 2-D IIR Butterworth LPF, Order-4 (a) Magnitude plot (b) Contour plot

2.7 Generation of Stable 2-D IIR Product Separable Denominator Transfer Functions and Test for Circular Symmetry

In order to obtain a required symmetry, the magnitude response of the filter has to be varied. One way to do it is to vary the coefficients of the filter. This necessarily perturbs the pole-zero locations of the filter in each dimension and thus varies the filter characteristics. But there is a possibility that the filter may become unstable as a result. If FIR filters are used, then we do not have to worry about stability, as it is a known fact that FIR filters are inherently stable. However FIR filters may require high order filters to satisfy the change in magnitude characteristics and thus its implementation could be difficult. If however, we use an IIR filter, by using one or more feedback paths in the design, we may achieve the above purpose. But we need to take care of the stability of the filter. In the case of 2-D systems, the complexity of testing the stability of the system is quite high. Therefore it is necessary to obtain the bounds of one or more coefficients, in order to ensure that the designed filter is stable. In this section, we design a filter transfer function possessing variable characteristics in their frequency response depending upon certain assigned variables.

The basic structure that will be used to explain this, is shown by a signal flow graph in Fig.(2.2).

From Fig.(2.2), the overall transfer function can be deduced as

$$T_{ac} = \frac{V_c}{V_a} = \frac{T_{ab}T_{bc}}{1 - T_{bc}T_{cb}} \tag{2.19}$$

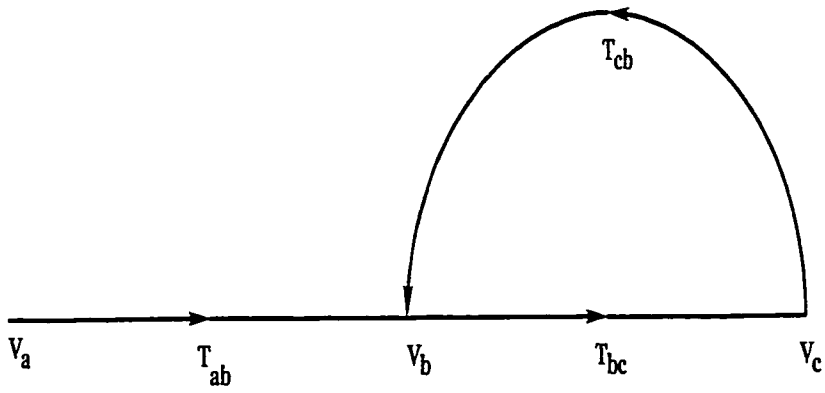

Figure 2.2: Basic structure for the 2-D transfer function expressed as a signal flow graph.

From Eqn.(2.19) (Mason's formula), it can be seen that any change in T_{ab} will result in a scale change in the magnitude response of the filter. Also, it has to be ensured that the eventual transfer function T_{ac} is stable. Now in order to change the magnitude characteristics of the transfer function, one of the transmittance should be changed. This is always possible by using T_{cb} as a variable quantity. This results in a Variable Characteristic Transfer Function(VCTF) [3].

As mentioned in the previous section, one of the simplest ways to generate a 2-D IIR VCTF is to obtain it as a product of two stable 1-D Strictly Hurwitz Polynomials(SHP), one in the s_1 domain and the other in the s_2 domain, and from this we can obtain the denominator polynomial. The numerator polynomial can either be product separable or non-product separable. Then the application of bilinear transformation results in a transfer function which is stable in the discrete domain.

For our case, let us consider a 2-D transfer function $T(s_1, s_2)$ given as a product of two 1-D functions $T_1(s_1)$ and $T_2(s_2)$ each having the form as shown in Eqn.(2.19). Therefore,

$$T_3(s_1, s_2) = T_1(s_1)\ T_2(s_2) \tag{2.20}$$

Let $T_1(s_1) = \frac{1}{g_1(s_1)+f_1(s_1)}$ where $g_1(s_1)$ is a third order butterworth polynomial given by

$g_1(s_1) = s_1^3 + 2s_1^2 + 2s_1 + 1$ and $f_1(s_1) = k_1$.

Similarly for $g_2(s_2)$ and $f_2(s_2)$ in the second dimension, the expressions to obtain $T_2(s_2)$ are given by

$g_2(s_2) = s_2^3 + 2s_2^2 + 2s_2 + 1$ and $f_2(s_2) = k_2$.

A third order polynomial is considered for purposes of illustration. The example can be of any order.

In our case let us focus our attention on the case when $k_1 = k_2 = k$.

In order to determine the range of k over which the filter is stable, we apply the stability condition[30]. According to this condition if $Q_a(s) = m(s) + n(s)$ where $m(s)$ is an even polynomial and $n(s)$ is an odd polynomial and if $m_1(s)$ is an even polynomial, then $Q_a(s) + m_1(s)$ is a strictly Hurwitz polynomial if and only if, in the partial fraction expansion,

$$\frac{m(s) + m_1(s)}{n(s)} = K_\infty s + \sum_{i=1} \frac{K_i s}{s^2 + \beta_i^2} + \frac{K_0}{s} \tag{2.21}$$

with $\beta_i^2 < \beta_{i+1}^2$ ($\beta' s$ being real), we have the conditions

(i) $K_\infty \geq 0$, (ii) $K_i > 0$ for all values of i and (iii) $K_0 > 0$.

From the above condition we have, in our present case, letting $m = 2s^2 + 1$, $m_1 = k$ *and* $n = s^3 + 2s$,

$$\frac{m(s) + m_1(s)}{n(s)} = \frac{2s^2 + 1 + k}{s^3 + 2s} = \frac{\frac{1+k}{2}}{s} + \frac{\frac{3-k}{2}s}{s^2 + 2} \tag{2.22}$$

Evaluating the above conditions from Eqn.(2.22), we have $k = 3$ or $k = -1$. Therefore

the range of k is $-1 < k < 3$.

From Eqn.(2.20) we have $T_3(s_1, s_2) = (\frac{1}{s_1^3+2s_1^2+2s_1+1})(\frac{1}{s_2^3+2s_2^2+2s_2+1})$. Substituting $s_1 = j\omega_1$ and $s_2 = j\omega_2$ in the above equation and simplifying the transfer function by eliminating all the higher powers of ω_1 and ω_2 and retaining only the second degree powers, we have in two dimensions, the relationship to be satisfied as

$$\left\{4k(1+k)^2\omega_1^2 + 4k(1+k)^2\omega_2^2 = (1+k)^4 - \epsilon\right\} \tag{2.23}$$

where ε =response of the transfer function.

Plotting a direct response for Eqn.(2.23) for a value of $k = 0.5$, we have the magnitude and contour plots as shown in Fig.(2.3).

As we notice from Fig.(2.3), it is a circularly symmetric response corresponding to the Eqn.(2.23) which, in general terms, is the equation of a circle. If however, the contour plots of $T_3(s_1, s_2)$ are drawn after bilinear transformation for $k = -0.6$, $k = -0.4$, $k = -0.3$, $k = -0.2$, $k = 0$, we obtain the results as shown in Figs.(2.4), (2.5) and (2.6). It can be seen that circularly symmetric response is possible only in a limited frequency range, since the contribution due to the higher frequencies is not considered.

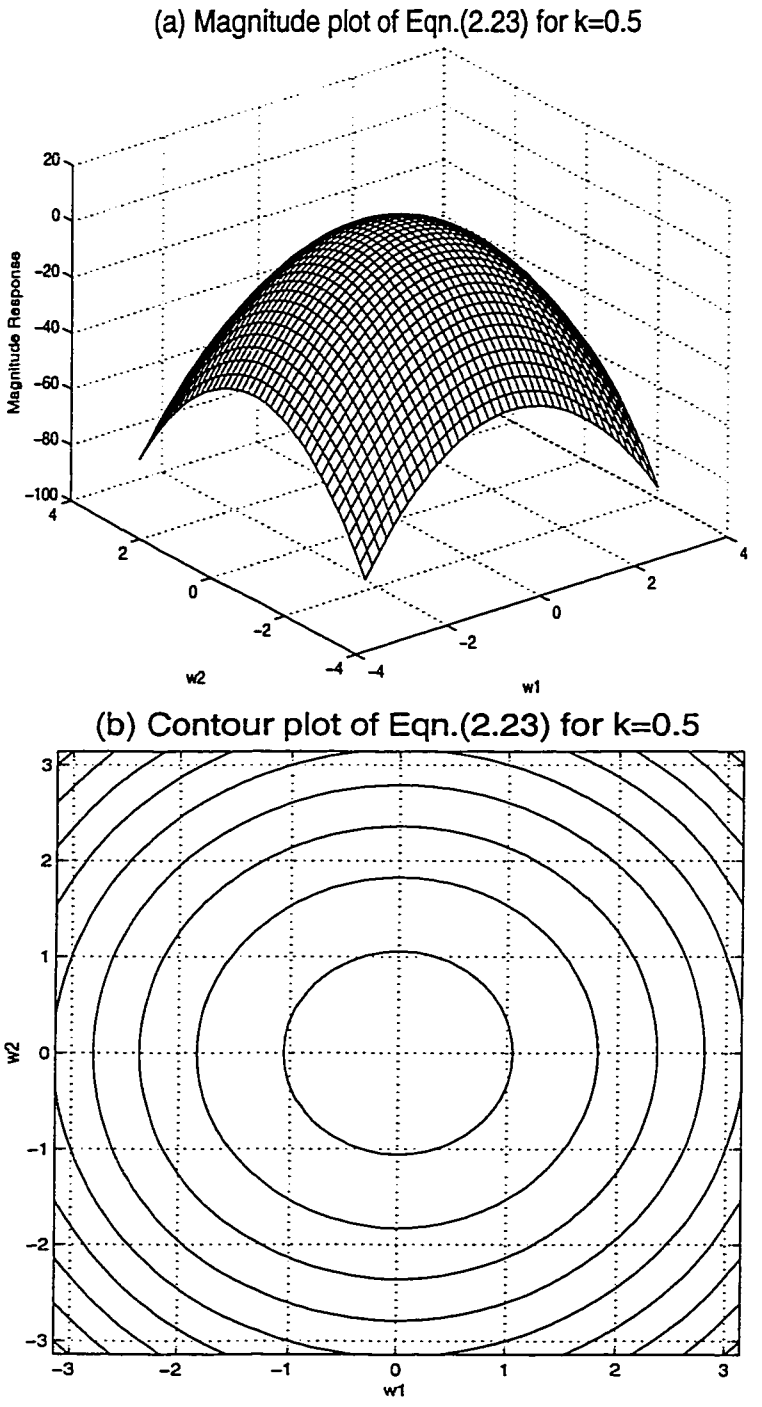

Figure 2.3: Plot of Eqn.(2.23) for k=0.5. (a) Magnitude plot (b) Contour plot

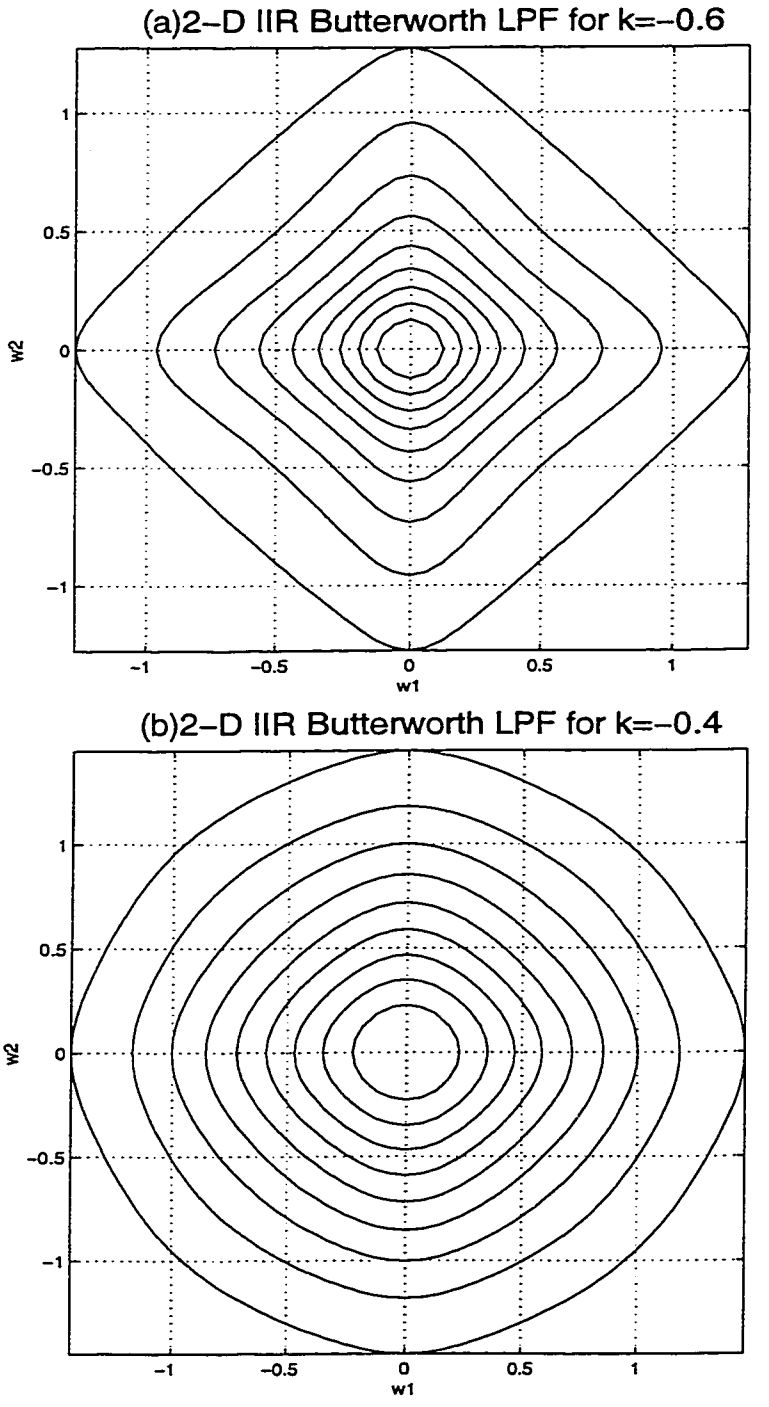

Figure 2.4: Contour plots for 2-D IIR Butterworth LPF for (a) k=-0.6 (b) k=-0.4

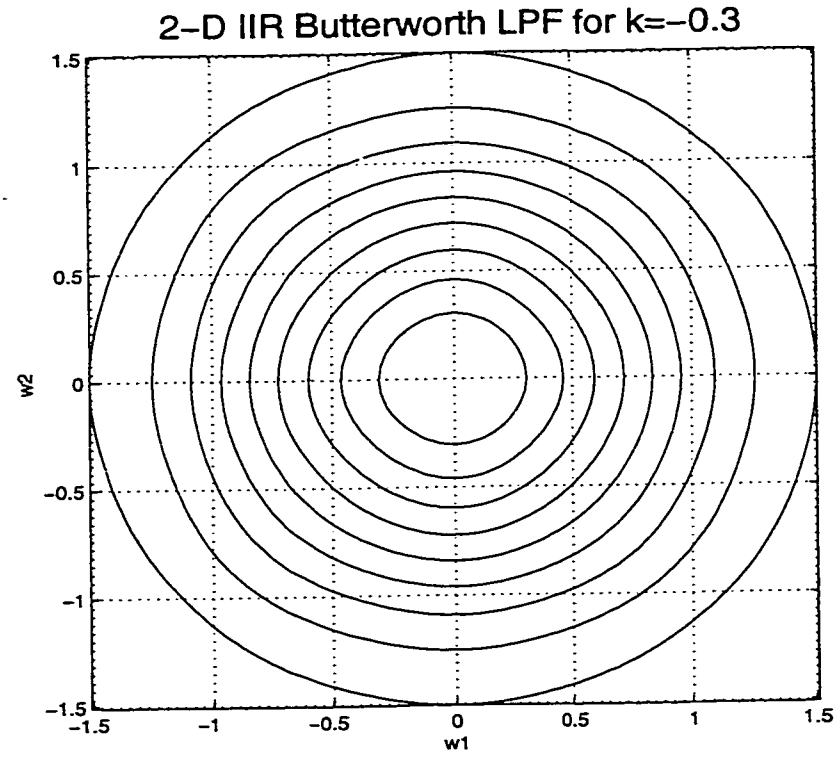

Figure 2.5: Contour plot for 2-D IIR Butterworth LPF for k=-0.3

From the Figs.(2.4), (2.5), (2.6), it can be deduced that for a certain range of k, in and around $k = -0.3$, the filter exhibits circular symmetry. The program for obtaining the above results (Program A2) has been written using MATLAB.

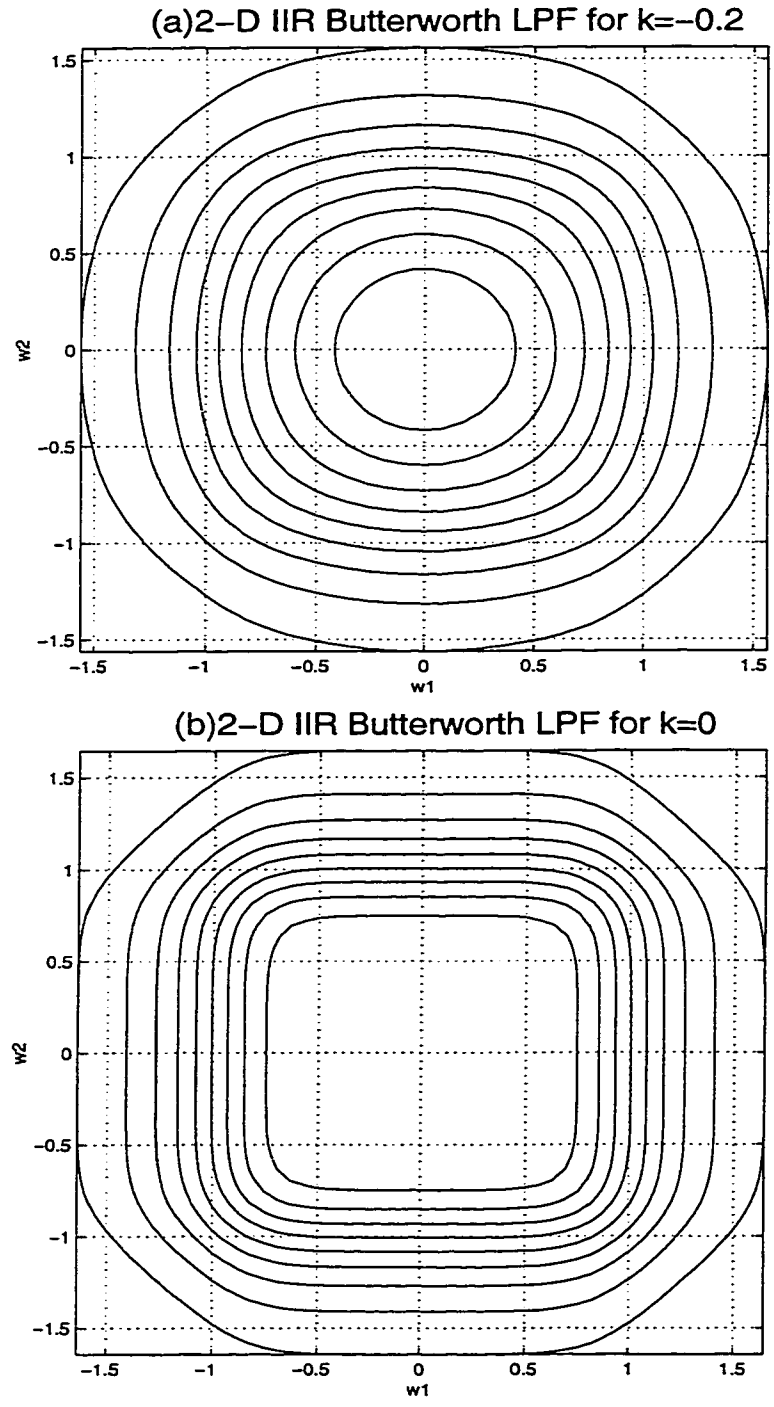

Figure 2.6: Contour plots for 2-D IIR Butterworth LPF for (a) k=-0.2 (b) k=0

Program A2

```
%% Function to determine the transfer function of the filter for
    %% a given k1,k2(garg_rama_mag_copy.m) - for Figs.(2.4), (2.5), (2.6).
    k1=-0.3;
    B1=[1];
    A1=[1 2 2 1];
    B2=B1;
    [R C]=size(A1);
    A1(C)=A1(C)+k1;
    A2=A1;
    k2=k1;
    %% Bilinear transformation of the transfer function
    [N1,D1]=bilinear(B1,A1,1);
    [N2,D2]=bilinear(B2,A2,1);
    %% To determine the 2-D transfer function of the IIR Filter
    for m=1:1:size(N1,2)
    for n=1:1:size(N2,2)
    N(m,n)= N1(m)*N2(n);
    end
    end
    for m=1:1:size(D1,2)
    for n=1:1:size(D2,2)
    D(m,n)= D1(m)*D2(n);
    end
    end
    lim=pi;
    interval=pi/50;
    c1=0;
    for w1 = -lim:interval:lim
    c2=0;
    c1=c1+1;
    for w2 = -lim:interval:lim
    c2=c2+1;
    for col=1:1:size(N2,2)
    NRow(1,col)=(cos(w2) + j *sin(w2))^(size(N2,2)-col);
    end
```

```
for row=1:1:size(N2,2)
NCol(row,1)=(cos(w1) + j *sin(w1))^(size(N1,2)-row);
end
NR = NRow * N' * NCol;
a=real(NR);
b=imag(NR);
for col=1:1:size(D2,2)
DRow(1,col)=(cos(w2) + j *sin(w2))^(size(D2,2)-col);
end
for row=1:1:size(D2,2) DCol(row,1)=(cos(w1) + j *sin(w1))^(size(D1,2)-row);
end
DR = DRow * D' * DCol;
c=real(DR);
d=imag(DR);
MOD(c1,c2) = (sqrt((a*c + b*d)^2 + (b*c - a*d)^2))/(c^2+d^2);
end
end
%% To plot the frequency response plots
w1=-lim:interval:lim;
w2=-lim:interval:lim;
[ww1,ww2]=meshgrid(w1,w2);
zz=MOD/(max(max(MOD)));
figure;
contour(ww1,ww2,zz);
axis('image');
xlabel('w1');
ylabel('w2');
zlabel('Magnitude Response');
title('2-D IIR Butterworth LPF for k=-0.3','FontSize',18);
grid on;
%% End of Program
```

2.8 Algorithm to Check the Extent of Circular Symmetry for a Given Magnitude Range

From the above study, it is seen that, for a given value of k, it becomes necessary to determine whether, at a certain value of the magnitude range, the filter exhibits circular symmetry. An iterative algorithm, has been written in MATLAB, to check the extent of circular symmetry under a given magnitude range and if required, alter the value of the variable quantity(in this case k) so as to obtain the circular symmetric condition.

As a particular case, the initial value of k has been taken as $k = -0.6$. The magnitude range under check is 0.49<Mag<0.51.

The algorithm has been written as follows.

(1) Program A3 is the main program showing the inputs to be given for the circular symmetry test. The filter is first designed given the transfer function in terms of numerator and denominator polynomials.

(2) The transfer function of the 2-D filter is determined using a separate subroutine(same as program A2) which is called from the main program. This subroutine returns the 2-D transfer function of the filter.

(3) The subroutine for the circular symmetry test is then called(Program A3-b).

(4) The basic idea underlying Program A3-b is explained as follows. The magnitude range for the circular symmetry check for the derived frequency response is defined. In this case this value is between (0.49, 0.51).

(5) The magnitude values falling under this range is isolated into a separate matrix and their frequency positions with respect to both the dimensions are noted.

(6) To check if these isolated values of magnitude fall under a circle, their individual magnitude values are noted and a percentage error of 5% is used to include the points into a circle. If desired, any other percentage value can also be chosen.

(7) If all the radius values fall under this limit then the given magnitude range is considered to be fairly circularly symmetric and if this is not the case, the value of k is decreased by a value of 0.1 and the whole process is carried out from the beginning.

Thus this algorithm is highly useful in determining the extent of circular symmetry in 2-D Filters. It is noted that this procedure can be used for testing the circular symmetry of any filter, given the transfer function. In cases where circular symmetry is not very obvious, the value of the percentage error inside the program can be varied in order that the best match for circular symmetry can be obtained.

For this particular case, the algorithm gave a circular symmetry result for the above mentioned magnitude range when the value of $k = -0.3$. The program for the above procedure (Program A3, A3-b) has been written in MATLAB and is shown as follows:

Program A3

```
%% Program to design a filter and check the extent of circular symmetry
    %% for a specific filter transfer function that is input by the user.
    %%(garg_rama_circular.m) for Figs.(2.7), (2.8), (2.9)
    %% This program calls two subroutines.
    %% Define the numerator(B1) and denominator(A1) polynomials of the transfer function
    %% for which circular symmetry is to be tested
    B1=[1]; A1=[1 2 2 1];
    %% Increment the value of k and output the result for each k.
    for k1=-0.9:0.1:0
    %% This defines the range of k that is to be tested.
    %% Calls the sub-routine to design the filter for a specific k (same as Program A2)
```

```
Mag = garg_rama_mag(B1,A1,k1);
%% Calls the subroutine to test extent of circular symmetry (Program A3-b)
[output]=garg_rama_circ(Mag)
end
%% End of program
```

Sub-routine A3-b

```
%% Program to check the extent of circular symmetry for a designed filter
%% given the Magnitude transfer function
function [output]=garg_rama_circ(Mag);
%% To isolate the necessary magnitudes
j1=0; var_circ =0.1;
for i=1:size(Mag,1)
for j=1:size(Mag,2)
if Mag(i,j)>0.49 & Mag(i,j)<0.51
j1=j1+1; points(1,j1) = Mag(i,j);
else
Mag(i,j)=0;
end
end
end
%% To plot the frequency response of the isolated magnitudes
lim=pi;
interval=pi/100;
w1=-lim:interval:lim; w2=-lim:interval:lim;
[ww1,ww2]=meshgrid(w1,w2);
figure;
contour(ww1,ww2,Mag);
axis('image'); xlabel('w1'); ylabel('w2'); grid on;
title(' Test for circular symmetry for k=-0.3 ','FontSize',18);
%% To get the w1,w2 values for the non-zero elements of Mag
count=0;
for i = 1:size(Mag,1)
for j = 1:size(Mag,2)
if Mag(i,j) ~=0
count=count+1;
x(count) = ww1(i,j); y(count) = ww2(i,j);
```

```
end
end
end
%% Check for radius
count1=0; clear Radius;
for i = 1:size(x,2)
x1 = x(i); y1 = y(i); z1=sqrt(x1^2 + y1^2);
count1=count1+1; Radius(count1) = z1;
end
max_Radius = max(Radius); min_Radius = min(Radius);
Radius_vector = (max_Radius - min_Radius)/max_Radius;
%% Output the result of test for circular symmetry
if Radius_vector < 0.02
output = char('Circularly Symmetric');
else
output = char('Not Circularly Symmetric');
end
%% End of program
```

The results are plotted as shown in Figs.(2.7), (2.8) and (2.9) for different values of k. The magnitude range under study is varied between the lowest to the highest value within ranges of 10% of the magnitude. From this, the region of interest (where the filter is approximately circularly symmetric) is found and further simulations are carried on with a 2% magnitude range within the reduced region of interest and eventually, after repeated simulations of Program A3, results show that for a value of $k = -0.3$, for this specific transfer function, optimum circular symmetry is achieved. Going beyond this value of k resulted in degradation of circular symmetry. Figs.(2.7), (2.8) and (2.9) show the final plots of the filter for different values of k. The magnitude values under study in these figures are in the range 0.49<Mag<0.51.

Fig.(2.7) shows the plots for $k = -0.6$ and $k = -0.4$. Here we see that with higher value of k the plot tends to a circle.

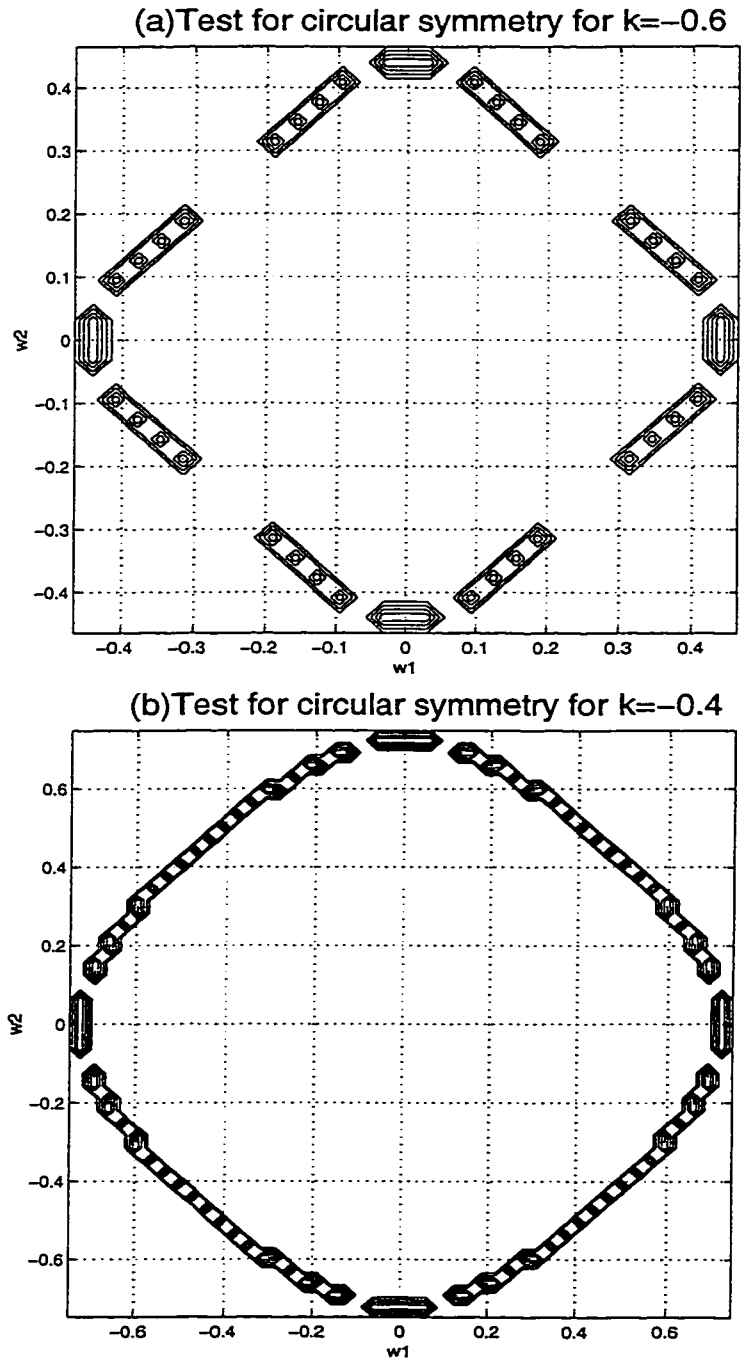

Figure 2.7: 2-D IIR Butterworth LPF response and test for circular symmetry under magnitude range 0.49<Mag<0.51 for (a) k=-0.6 (b) k=-0.4.

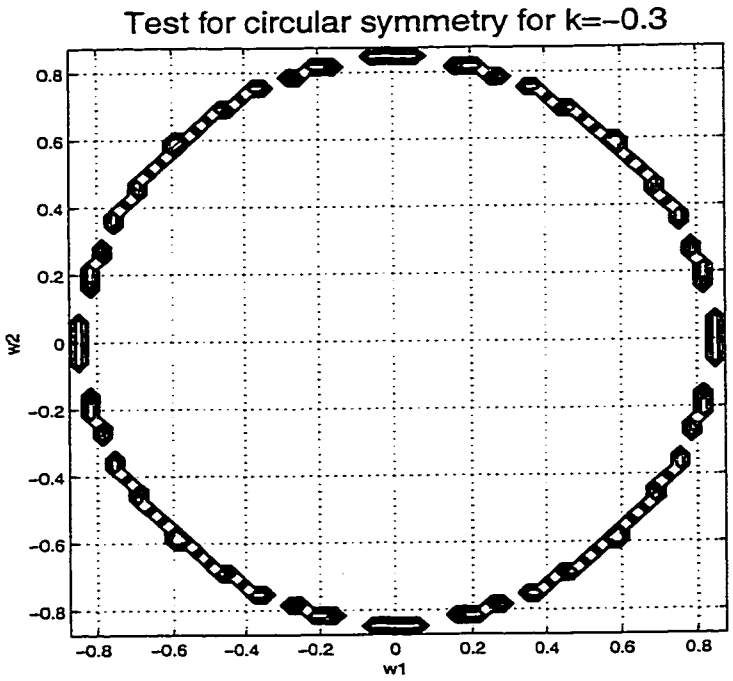

Figure 2.8: 2-D IIR Butterworth LPF response and test for circular symmetry under magnitude range 0.49<Mag<0.51 for k=-0.3.

Fig.(2.8) shows the plot for $k = -0.3$ for which, it is clear that we have circular symmetry exists between the magnitude under study.

Fig.(2.9) shows that as the value of k increase beyond $k = -0.3$ circular symmetry ceases to exist, under the given magnitude range under study.

We have considered, by and far, filters of third order. In a similar manner, simulations can be extended to higher order filters. However with higher order filters, the computations become more complex. Therefore only third order filters have been considered in this work.

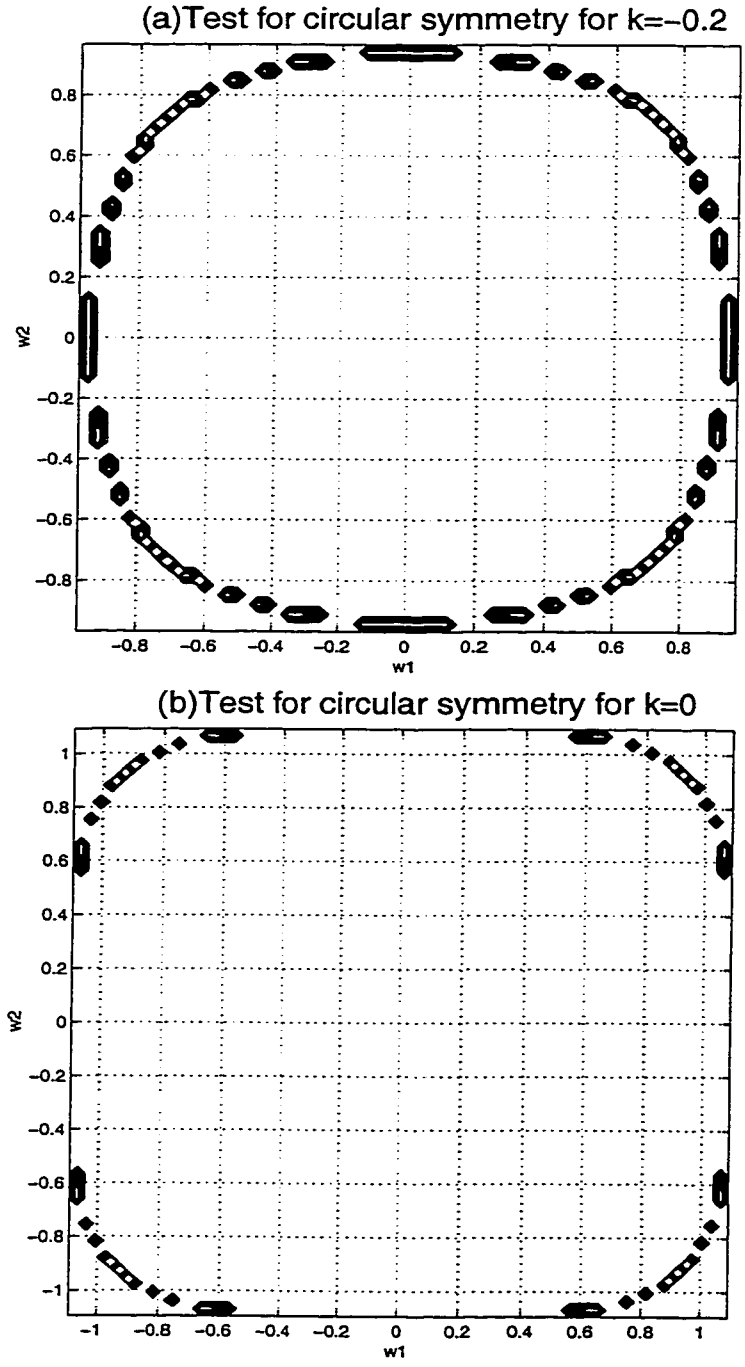

Figure 2.9: 2-D IIR Butterworth LPF response and test for circular symmetry under magnitude range 0.49<Mag<0.51 for (a) k=-0.2 (b) k=0.

2.9 Design of 2-D IIR Chebyshev Lowpass Filter

We have discussed, so far, in detail about the implementation of 2-D Lowpass Butterworth filter design and specifically, its contribution to circular symmetry. In this section, we will discuss about the 2-D Lowpass chebyshev filter design and its approximation to circular symmetry.

The Chebyshev lowpass filter makes use of the Chebyshev polynomial[31]. It is well known that Chebyshev characteristics has an equi-ripple variation in the pass-band and a fast monotonic decrease in gain, outside the pass-band. Inorder to design a 2-D Chebyshev lowpass filter from the 1-D design, as before in the Butterworth design, we will consider it as a product of two 1-D transfer functions.

2.9.1 The Chebyshev Lowpass Characteristics

For the Lowpass characteristics, we chose the value of the transfer function within the range, such that $\omega \leq 1$.

We know that $\mid C_n(\omega) \mid \leq 1$ for $\omega \leq 1$. Therefore we chose a small number ϵ such that

$F(\omega^2) = \epsilon^2 C_n^2(\omega)$.

Therefore we will have

$$\mid H(j\omega) \mid^2 = \frac{1}{1 + \epsilon^2 C_n^2(\omega)} \tag{2.24}$$

Eqn.(2.24) will have its values that fall between 1 and $\frac{1}{(1+\epsilon^2)}$ in the range $0 \leq \omega \leq 1$.

For $\omega \gg 1$, and from Eqn.(2.24)

$$| H(j\omega) |^2 \approx \frac{1}{\epsilon^2 2^{2(n-1)} \omega^{2n}} \tag{2.25}$$

Therefore the gain $\alpha(\omega)$ can be calculated as

$$\alpha(\omega) \approx -10 \log(\epsilon^2 2^{2(n-1)} \omega^{2n} = -20 \log \epsilon - 20(n-1) \log 2 - 20n \log \omega \tag{2.26}$$

2.9.2 2-D Chebyshev Lowpass Characteristics and Test for Circular Symmetry

As has been discussed before in the 2-D IIR Butterworth filter function derivation, the simplest way to obtain a 2-D filter function for Chebyshev filter is to cascade the transfer function of two 1-D filter functions.

As we have discussed in Section 2.7, let us consider a 2-D transfer function given as a product of two 1-D functions.

$$C_3(s_1, s_2) = C_1(s_1) \;\; C_2(s_2) \tag{2.27}$$

Let $C_1(s_1) = \frac{1}{g_1(s_1)+f_1(s_1)}$ where $g_1(s_1)$ is a third order Chebyshev polynomial given by [31].

$g_1(s_1) = s_1^3 + 1.9388 s_1^2 + 2.6294 s_1 + 1.6380$ and $f_1(s_1) = k_1$.

Similarly for $g_2(s_2)$ and $f_2(s_2)$ the expressions to obtain $T_2(s_2)$are given by

$g_2(s_2) = s_2^3 + 1.9388 s_2^2 + 2.6294 s_2 + 1.6380$ and $f_2(s_2) = k_2$.

These functions have a ripple width $\epsilon = 0.1526$.

For symmetry purpose, let us focus our attention on the case when $k_1 = k_2 = k$.

According to the stability condition of Eqn.(2.21) we determine the range of $k = k_1 = k_2$ for which the 1-D transfer function is stable.

From Eqn.(2.21) it is found that this range of k is $-1.6380 < k < 4.0978$.

Plotting the response for the above range of k gives near circularly symmetric response between the range $-1.0 < k < -0.4$. The plots corresponding to the above range are shown in the Figs.(2.10), (2.11) and (2.12) and these correspond to a ripple width of $\epsilon = 0.1526$. These have been plotted using the same Program A2 but with different input values.

The figures also show a plot for $k = 0.4$. Using Program A3 the values of k mentioned in the figures, are tested for circular symmetry within the magnitude range $0.28 < Mag < 0.32$. This magnitude range essentially depends upon the necessity of the specific user and it may be chosen based on the magnitude study of interest. The same study can also be done for other magnitude ranges. In this specific case of magnitude range, it is found that, circular symmetry is obtained for a value of $k = -0.64$. This result has been achieved after extensive simulations of Program A3. The plots shown in Fig.(2.13) show the results of the applying Program A3 to the transfer function achieved for the above case of Chebyshev filter.

Fig.(2.12) also shows the plot for $k = 0.4$. This plot shows that, a Chebyshev type response analogous to its 1-D counterpart, can be achieved for values of k beyond 0.4 and within stability limits.

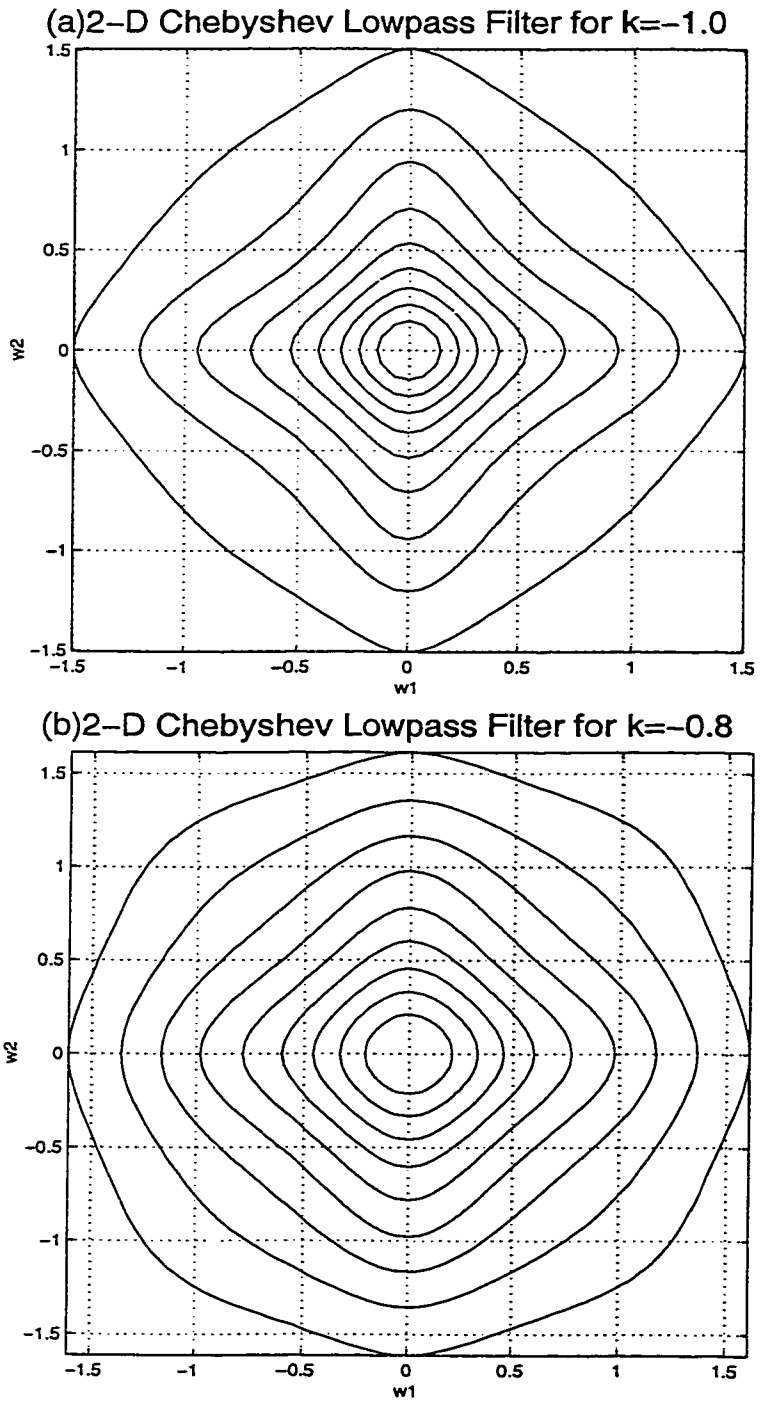

Figure 2.10: 2D Chebyshev LPF characteristics for (a) k=-1.0 and (b) k=-0.8.

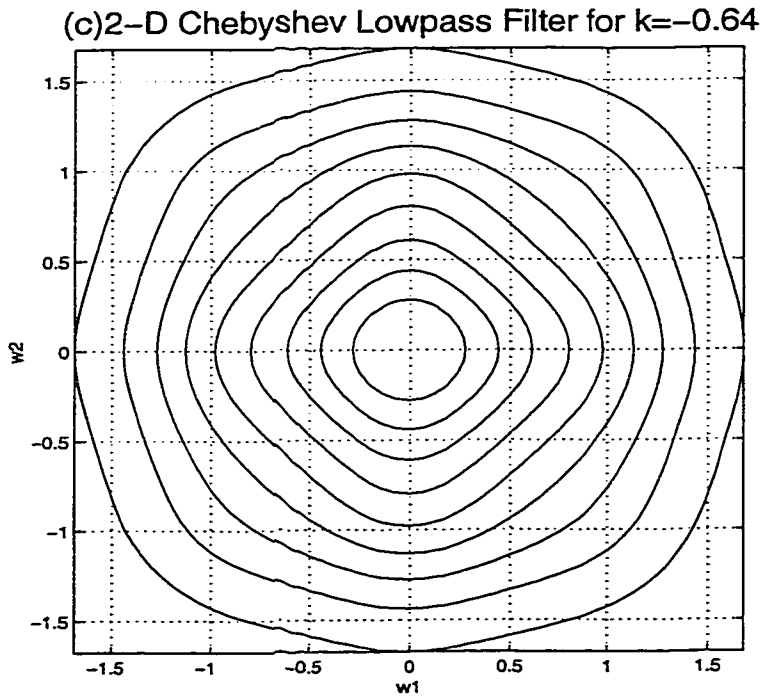

Figure 2.11: 2D Chebyshev LPF characteristics for (a) k=-0.64

As an example, another value of ripple width $\epsilon = 0.3493$ has been considered. In this case the equation for $g_1(s_1)$ and $g_2(s_2)$ is given by

$g_1(s_1) = s_1^3 + 1.2529s_1^2 + 1.5349s_1 + 0.7157.$

$g_2(s_2) = s_2^3 + 1.2529s_2^2 + 1.5349s_2 + 0.7157.$

The rest of the expression being the same, it has been found that for the above equation, the stability range of k is given by $-0.7157 < k < 0.9230$. Contour plots are obtained for the above range and the plots for which near circular symmetry is obtained, are shown as in Fig.(2.14(a)-(e)). These have been plotted using Program A2 with appropriate input values.

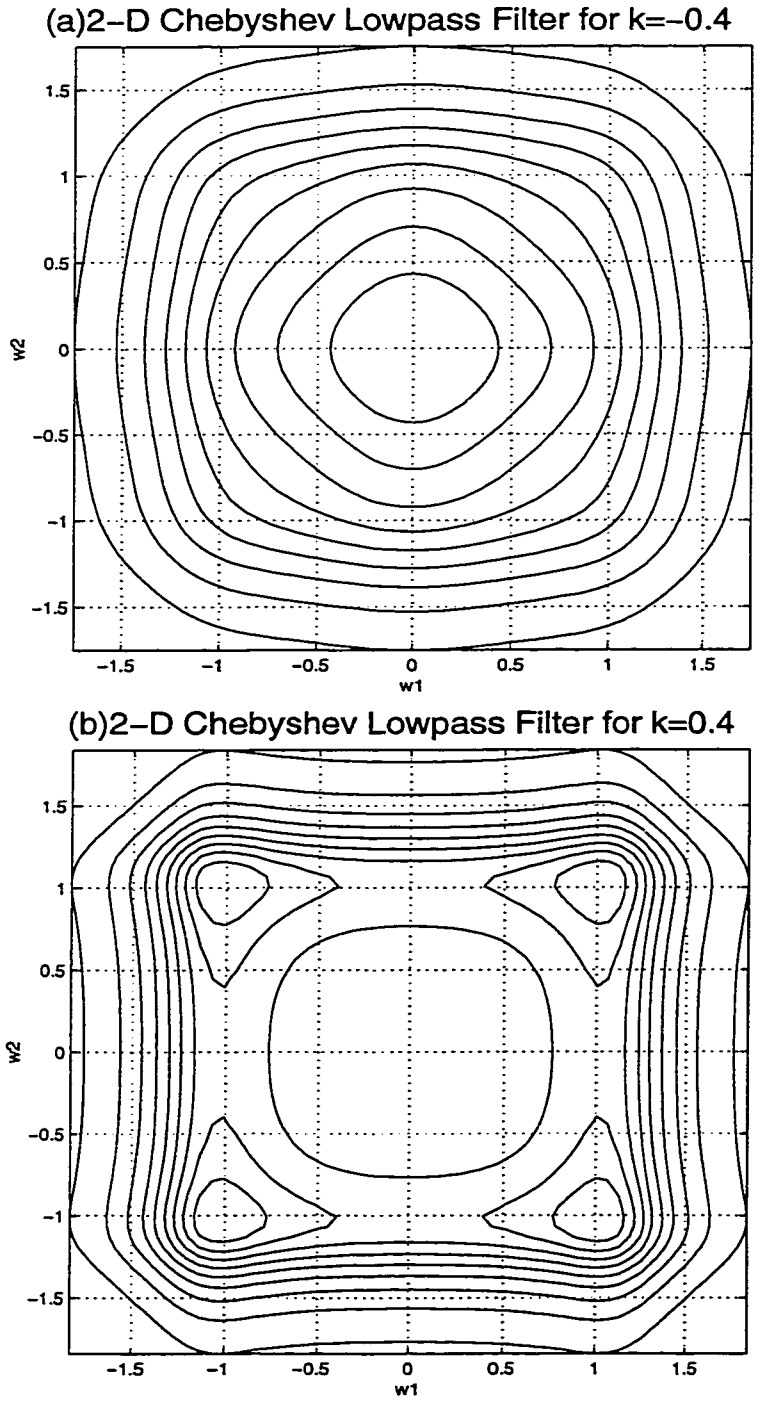

Figure 2.12: 2D Chebyshev LPF characteristics for (a) k=-0.4 and (b) k=0.4.

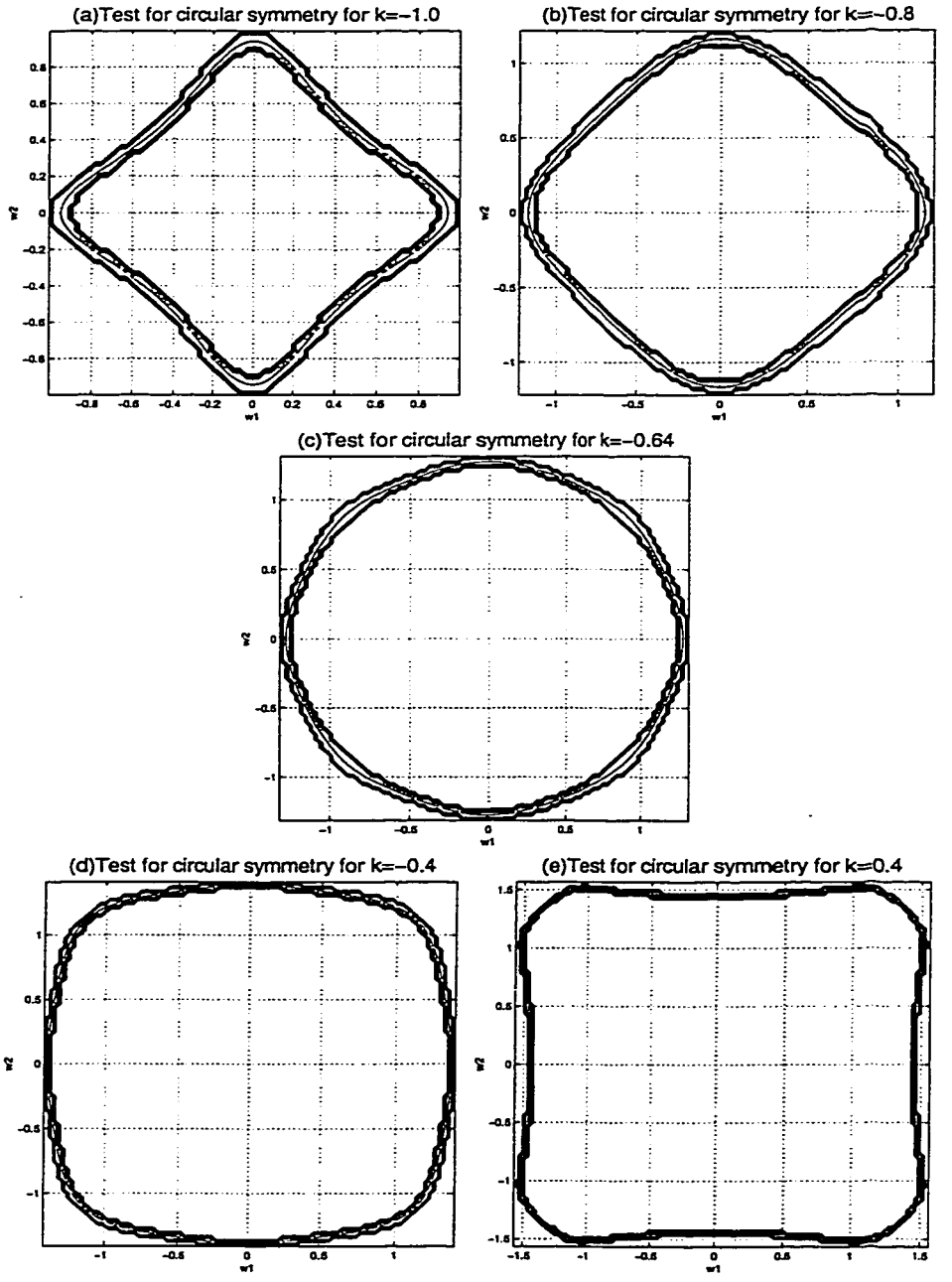

Figure 2.13: Plots to show the extent of circular symmetry for the case where $\epsilon = 0.1526$. These plots are shown for the same corresponding values of k as shown in Figs.(2.10), (2.11), (2.12). All the plots show the magnitude range $0.28 < Mag < 0.32$.

Applying Program A3 to this case of transfer function, the extent of circular symmetry is calculated between the range $0.49 < k < 0.51$. The plots in Fig.(2.15) show these results.

Comparing the above two cases where the plots have been shown for two different cases, it can be seen that, the value of k changes for near circular symmetry (in the second case being $k = -0.25$). It is noted that this is the closest one can approach to circular symmetry for test under the specified magnitude range. It is possible that for another range better symmetry can be obtained.

Table (2.2) summarizes the above two cases.

Ripple Width (ϵ)	Stability range of k	Value of k for near circular symmetry
0.1526	$-1.6380 < k < 4.0978.$	-0.64
0.3493	$-0.7157 < k < 0.9230$	-0.25

Table 2.2: Analysis results for the extent of circular symmetry in 2-D Chebyshev lowpass transfer functions for two different values of ripple width. The magnitude range under study for both the above cases is 0.49<Mag<0.51.

From Table(2.2) it can be noted that, depending on the value of ϵ and therefore the transfer function, the value of k changes for circular symmetry for a chosen value of magnitude range and the same can be obtained by Program A3. The 2-D Chebyshev lowpass filter characteristics have thus been analyzed and its approximation to circular symmetry has been studied and shown in this section.

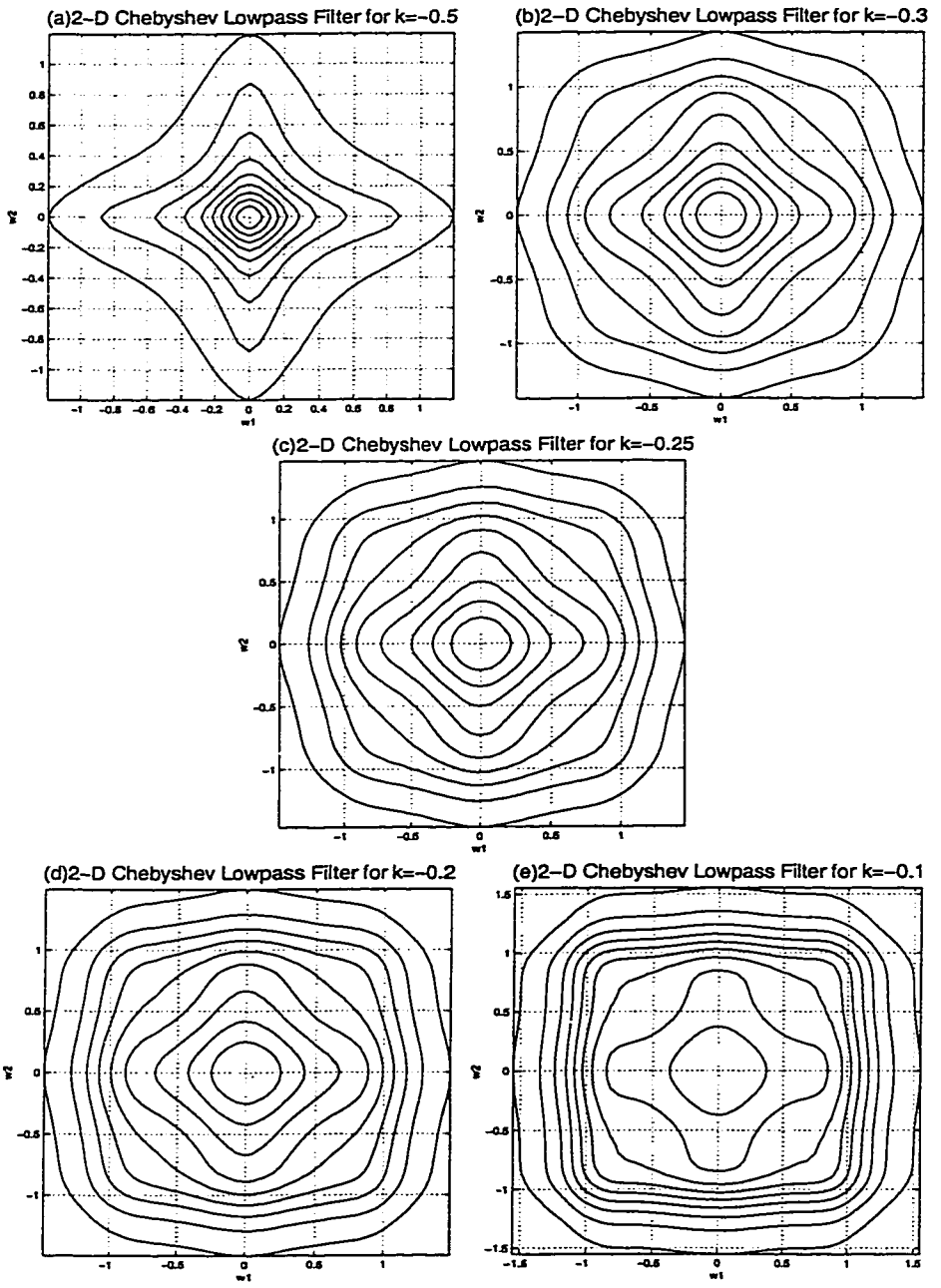

Figure 2.14: 2D Chebyshev lowpass filter characteristics for the second case considered for ripple width $\epsilon = 0.3493$. Plots (a)-(e) are shown for different values of k close to circular symmetry.

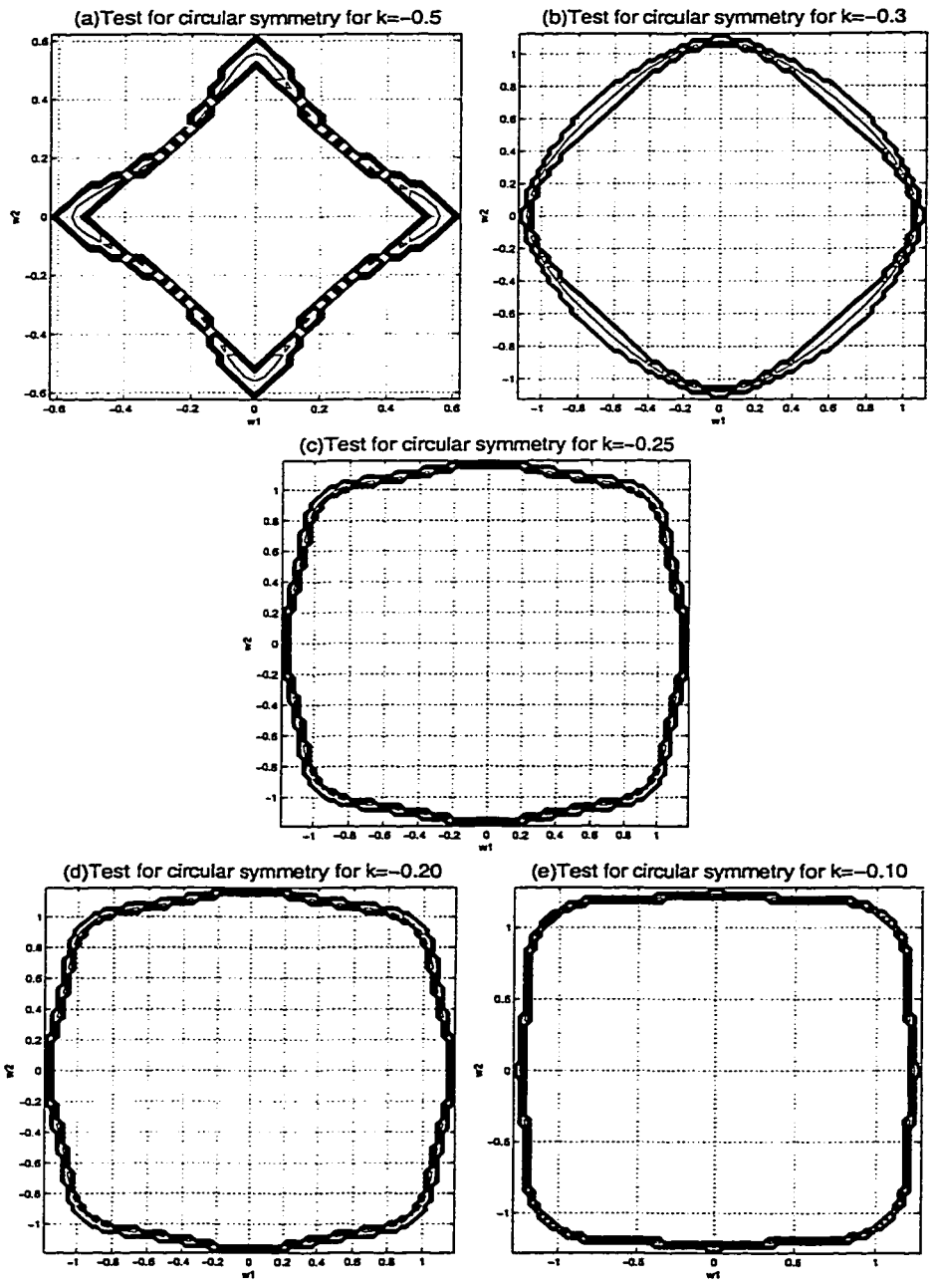

Figure 2.15: Plots to show the extent of circular symmetry for the second case where $\epsilon = 0.3493$. The plots are shown for the same corresponding values of k as in Fig.(2.14). All the plots show the magnitude range $0.28 < Mag < 0.32$.

2.10 Pole-Parameter Transformation and Analysis of Lowpass Butterworth Filters

2.10.1 Introduction

Having discussed in detail the implementation of filters possessing separable denominator 2-D filter transfer functions for the Butterworth and Chebyshev filters, we now go on to study another interesting aspect of filter design namely the pole-parameter transformation[15] and their analysis. In this respect, we will discuss this topic with respect to the Lowpass Butterworth filter design in particular. A brief review of this topic is as follows[15].

The Butterworth filter approximation is based on the fact that all the poles of the filter are uniformly placed on the unit circle in the s-plane. This section deals with a new family of transitional filters, whose design is based on the judicious positioning of the poles in the s-plane. The transitional feature of the new family, dealt with here, is between two Butterworth filters of specific even orders. The poles of these filters constitute a specific reference pole pattern. They lie along the arc of a circle between the reference poles of two specific Butterworth filters. The pole-phasors of each member of the family are of equal magnitude ω_p, not necessarily of unit radius. If the order of the Butterworth filter is a binary power (i.e., $n = 2^k$, k being an integer), then the pole-locations of the filter exhibit very interesting symmetry properties. The pole-locations are such that they are symmetric about the horizontal axis reference such that a single quadrant pole-parameter synthesis is representative of all the poles of the filter. A new family of Butterworth filters can now be formed by what is called "prescribed symmetrical swinging" of the poles of the filter by specific angles such

that the symmetry constraint of the original pole-pattern is not altered. Also, various performance characteristics such as selectivity of magnitude response, sensitivity or critical Q factor, can be smoothly varied by changing the polar angles appropriately. The transitional family of filters following this method have the same bandwidth and hence comparison among the various members of the family is more realistic[15].

2.10.2 Pole-parameter Representation

It is well known that the poles of a Butterworth filter of a specific order, are located uniformly on the unit circle in the s-plane. The line joining any pole with the origin of the coordinates is called the pole-phasor having a magnitude ω_p or the "pole-frequency" and angle θ_p or the polar-angle as shown in the following figure.

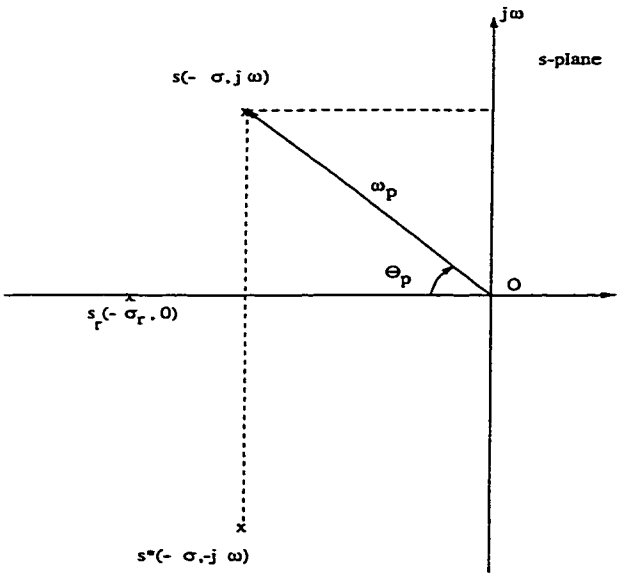

Figure 2.16: Pole parameter representation

The pole parameters shown in Fig.(2.16) correspond to the negative real pole (s_τ) and a complex-conjugate pole-pair (s, s^*). There is a high degree of geometrical

symmetry exhibited by the pole-phasors of a Butterworth filter of even order which is being exploited in the synthesis of a filter family by pole-parameter variation.

2.10.3 Complementary Symmetry

For a Butterworth filter of specified order, the poles located on the left-half of s-plane, on the second and third quadrant, are symmetrical about the horizontal axis and hence exhibit a mirror image symmetry. Therefore all the poles on the left-half of the s-plane can be represented just by the poles on the second quadrant only, i.e., the second quadrant poles are a representative of all the poles on the left-half of the s-plane.

Let us consider a n^{th} order Butterworth filter. The pole parameters corresponding to the second quadrant poles are given by

$$\omega_{pk} = 1 \begin{cases} k = 1, 2, ..., \frac{n}{2}, & for\ n\ even \\ k = 0, 1, ..., \frac{n-1}{2} & for\ n\ odd \end{cases} \tag{2.28}$$

and

$$\theta_{pk} = \begin{cases} \frac{(2k-1)\pi}{2n}, & k = 1, 2, ..., \frac{n}{2} \quad for\ n\ even \\ \frac{k\pi}{2n}, & k = 0, 1, ..., \frac{n-1}{2} \quad for\ n\ odd \end{cases} \tag{2.29}$$

For example if the order of the filter is 8, i.e., $n = 8$, then there will be 4 pole-phasors of magnitude unity and angles $\pi/16$, $3\pi/16$, $5\pi/16$, $7\pi/16$.

Let us consider the general case, in which all pole-phasors have a magnitude equal to ω_p (not necessarily unity), and the polar angles retained at values as given by Eqn.(2.29). Normalizing the d.c value of the transfer function $A(\omega)$ to unity such that

$A(\omega)$ at $\omega = 0$ is independent of ω_p, we can write the squared magnitude expression of the transfer function as follows:

$$A^2(\omega) = \frac{\omega_p^n}{\omega_p^{2n} + \omega^{2n}} \tag{2.30}$$

From the above expression, the pole locations can be written as

$$s_k = \omega_p \exp\left[\frac{j(2k-1)\pi}{2n}\right], \; for\; k = 1, 2, ..., \frac{n}{2}, \; \forall\, n\; even \tag{2.31}$$

and

$$s_k = \omega_p \exp\left[\frac{jk\pi}{n}\right], \; for\; k = 0, 1, 2, ..., \frac{n-1}{2}, \; \forall\, n\; odd \tag{2.32}$$

In general, for any Butterworth filter of a given odd or even order, the Butterworth poles exhibit very interesting symmetry properties with respect to both real as well as the imaginary axis. In addition, if the Butterworth filter is of even order, then the filter displays varying degrees of symmetry. These additional symmetry properties are exploited in designing the new family of transitional filters.

Here, we consider only those filters whose order is a binary power, i.e., $n = 2^k$, k being integers greater than 2 only. This is because, filters of such order possess the highest degree of symmetry and therefore it is easy to deal with such a case although it is possible to extend the same case to filters of various orders. For such class of filters, whose order is a binary power, in addition to half-plane symmetry along the real or imaginary axis, which is common to all Butterworth filters, it is also symmetric with respect to the $\pi/4$ axis, in each quadrant of the s-plane.

To discuss our case, let us consider the order of the filter to be 16, i.e., $n = 16$. Therefore we have 16 poles on the left half of the s-plane, symmetric about the real

axis. Now in general, a Butterworth filter with $n = 2^k$ will have $n/2$ poles in the second quadrant given by

$$\theta_k = \frac{(2k-1)\pi}{2n}, \forall\, k = 1, 2, ..., \frac{n}{2} \tag{2.33}$$

This is illustrated in the Fig.(2.17) for $n = 16$.

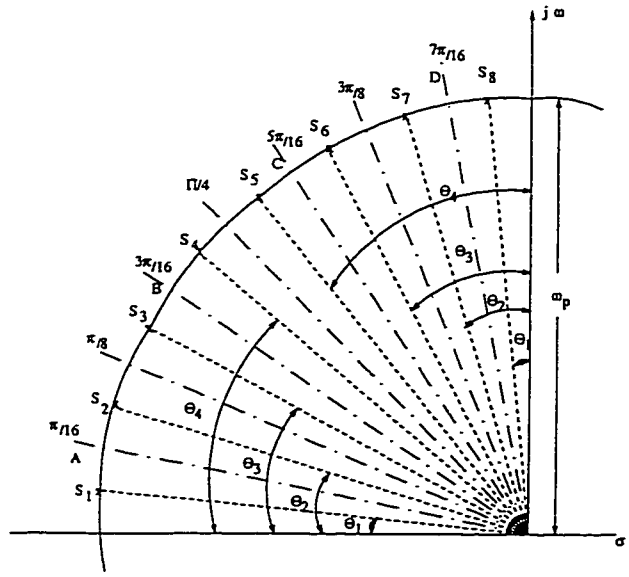

Figure 2.17: Pole plot for a 1-D filter of order $n = 16$.

Fig.(2.17) shows eight poles on the second quadrant. Since the pole positions are symmetric about the real axis, the eight poles on the second quadrant are representative of all the poles of the filter. The eight poles designated as $s_1, s_2, s_3, ..., s_8$ make angles $\theta_1, \theta_2, ..., \theta_8$ respectively to the real axis. Within the second quadrant, it is evident that the poles are symmetric about the $\pi/4$ axis and the symmetrical pole-pairs are given as follows.

$$\begin{bmatrix} \theta_1 = \frac{\pi}{32} & \theta_8 = \frac{15\pi}{32} \end{bmatrix}$$
$$\begin{bmatrix} \theta_2 = \frac{3\pi}{32} & \theta_7 = \frac{13\pi}{32} \end{bmatrix}$$
$$\begin{bmatrix} \theta_3 = \frac{5\pi}{32} & \theta_6 = \frac{11\pi}{32} \end{bmatrix} \tag{2.34}$$
$$\begin{bmatrix} \theta_4 = \frac{7\pi}{32} & \theta_5 = \frac{9\pi}{32} \end{bmatrix}$$

Also, it is clear that the polar angles of each of the above four symmetrical pole-pairs add up to $\pi/2$. In general we may write this as follows

$$(\theta_1 + \theta_8) = (\theta_2 + \theta_7) = (\theta_3 + \theta_6) = (\theta_4 + \theta_5) = \frac{\pi}{2} \tag{2.35}$$

Such pole-pairs, whose θ_p values add up to $\pi/2$ can thus be designated as "Complementary Pole Pairs(CPP's)". It can be seen that each pair of poles with θ_l and $\theta_{(n/2)-l+1}$, located symmetrically on either side of the $\pi/4$ axis, exhibit the CPP property since,

$$(\theta_1 + \theta_{(n/2)-l+1}) = \tfrac{\pi}{2}, \quad \forall\, l = 1, 2, ..., \tfrac{n}{4} \tag{2.36}$$

2.10.4 Symmetrical Swinging of Butterworth Poles Preserving the CPP Property

We shall now consider a modification in the Butterworth filter pole-pattern, which will still preserve the CPP property. Before we consider the modification, it is interesting to note that the adjacent Butterworth poles in the second quadrant possess another symmetry, this time, the adjacent pole-pairs (s_1, s_2), (s_3, s_4), (s_5, s_6) and (s_7, s_8) being symmetrical about the lines OA, OB, OC and OD which make an angle of $\pi/16$, $3\pi/16$, $5\pi/16$, $9\pi/16$, respectively.

Now, modifying the reference pole-pattern, by swinging the pole-vectors in each adjacent pole-pair by equal angles θ_0 towards the respective axes of symmetry, the new pole locations are $(s_1^{'}, s_2^{'}), (s_3^{'}, s_4^{'}), (s_5^{'}, s_6^{'})$ and $(s_7^{'}, s_8^{'})$. Therefore the new set of polar angles will be as follows

$$\begin{aligned}
&\left[\ \theta_1^{'} = (\tfrac{\pi}{32} + \theta_0) \qquad\qquad \theta_8^{'} = (\tfrac{15\pi}{32} - \theta_0)\ \right] \\
&\left[\ \theta_2^{'} = (\tfrac{3\pi}{32} - \theta_0) \qquad\qquad \theta_7^{'} = (\tfrac{13\pi}{32} + \theta_0)\ \right] \\
&\left[\ \theta_3^{'} = (\tfrac{5\pi}{32} + \theta_0) \qquad\qquad \theta_6^{'} = (\tfrac{11\pi}{32} - \theta_0)\ \right] \\
&\left[\ \theta_4^{'} = (\tfrac{7\pi}{32} - \theta_0) \qquad\qquad \theta_5^{'} = (\tfrac{9\pi}{32} + \theta_0)\ \right]
\end{aligned} \tag{2.37}$$

This is illustrated in the Fig.(2.18).

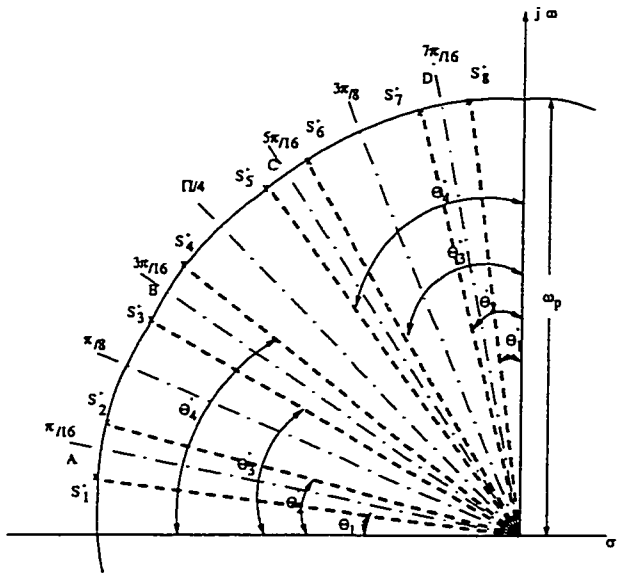

Figure 2.18: Pole parameter swinging and shifting of the adjacent pole-pair towards each other.

By varying the value of θ_0, a family of transitional filters can be obtained. Therefore, in general, for a Butterworth filter of order $n = 2^k$ the modified polar angles can be given by the following general expression.

$$\theta_k^{'} = \frac{(2k-1)\pi}{2n} + (-1)^{k-1}\theta_0, \quad \forall\, k = 1, 2, ..., \frac{n}{2} \tag{2.38}$$

It can also be seen that the modified pole-pattern as given by the Eqn.(2.38) still possesses the CPP property as we get

$$(\theta_l^{'} + \theta_{(n/2)-l+1}^{'}) = \frac{\pi}{2}, \quad \forall\, l = 1, 2, ..., \frac{n}{4} \tag{2.39}$$

from Eqn.(2.36). Thus it is seen that, the symmetrical swinging of the pole-phasors, equally on both sides conserves the net angle contributed by the adjacent pole-phasors, the net angle being $\pi/2$. This symmetrical swinging of adjacent pole-phasors can be both in the positive or negative direction, being towards or away from the respective axes of symmetry, such that $\theta_0 > 0$ *or* $\theta_0 < 0$ and $|\theta_0|_{max} = \frac{\pi}{2n}$. These family of filters obtained by modifications in the pole-pattern may be referred to as the CPP Filters.

The squared magnitude function of an n^{th} order CPPF can now be obtained as a product of the component squared magnitudes of each CPPF. The second order transfer function corresponding to the complex conjugate pole-pair given by the pole-parameters ω_{pk} and $\pm\theta_{pk}$ can be written as follows:

$$T_k(s) = \frac{\omega_{pk}^2}{s^2 + 2\omega_{pk}\cos(\theta_{pk})s + \omega_{pk}^2} \tag{2.40}$$

From Eqn.(2.40) the squared magnitude function is thus written as

$$A_k^2(\omega) = T_k(s)T_k(-s)\Big|_{s=j\omega} = \frac{\omega_{pk}^4}{\omega^4 + 2\omega_{pk}^2\cos(2\theta_{pk})\omega^2 + \omega_{pk}^2} \tag{2.41}$$

From Eqn.(2.41), the squared magnitude function of each CPPF can be obtained individually and the final squared magnitude function can be obtained by taking the product of all the individual magnitude expressions.

For our case, say $n = 16$, we know that all the CPP's have the same polar magnitude $\omega_{pk} = \omega_p$. Also from the CPP property, within the 2nd quadrant the adjacent pole-pairs are symmetrical. Therefore

$$(\theta_1' + \theta_4') = (\theta_2' + \theta_3') = \frac{\pi}{4} \tag{2.42}$$

We also have the symmetry property that

$$\theta_1' + \theta_2' = \frac{\pi}{8} \tag{2.43}$$

Using Eqn.(2.41) the squared magnitude function for the poles (s_1', s_8'), (s_2', s_7'), (s_3', s_6') and (s_4', s_5') can be written individually and using the above symmetry properties, they can be eventually combined as follows

$$A^2(\omega) = \left[A_{1,8}^2(\omega) \cdot A_{4,5}^2(\omega)\right] \cdot \left[A_{2,7}^2(\omega) \cdot A_{3,6}^2(\omega)\right] \tag{2.44}$$

$$= \frac{\omega_p^{32}}{\omega^{32} - 2\omega_p^{16}\cos 16\theta_1'\omega^{16} + \omega_p^{32}}$$

From Eqn.(2.44), it is possible to deduce the final expression for the magnitude

function for a general order $n = 2^k$ as

$$A^2(\omega) = \frac{\omega_p^{2n}}{\omega^{2n} - 2\omega_p^n \cos(n\theta_1')\omega^n + \omega_p^{2n}} \tag{2.45}$$

The value θ_0 is a free parameter, offering another additional degree of freedom. It affects all the θ_p''s and hence the Q_p's including the critical one of the new family of filters that we have designated as the Complementary Pole Pair Filters(CPPF's).

2.10.5 Low-Q Filters(LQF)

Low-Q filters are CPPF's corresponding to $\theta_1' > \frac{\pi}{2n}$. This swings the CPP's of the Butterworth filters towards the $\pi/4$ axis in the second quadrant. All the coefficients of $A^2(\omega)$ as in Eqn.(2.45) will be positive, since $\cos(n\theta_1') < 0$. Therefore the denominator expression increases monotonically with respect to ω and therefore $A^2(\omega)$ becomes monotonically decreasing, although not maximally flat. The analysis is more clear if we compare it with a Butterworth filter of the same order. Also the comparison is categorized into two different categories based on two factors:

(a) both the filters having the same pass-band attenuation.

(b) both the filters having the same value of ω_p.

Let us consider a Butterworth filter and a Low-Q filter of the same order. Based on the first factor let us consider that the filters have identical pass-band attenuation, i.e.,

$$A_{CB} = A_{CL} \tag{2.46}$$

where A_{CB} and A_{CL} are respectively, the magnitudes of the Butterworth filter and the Low-Q filter at cut-off $\omega = 1$. From Eqn.(2.30), (2.45) and (2.46), with ω_B and

ω_L as the pole frequencies of the Butterworth filter and the Low-Q filter respectively, we have

$$\omega_L^{2n} + 2\omega_B^{2n}\omega_L^n \cos(n\theta_1') - \omega_B^{2n} = 0 \tag{2.47}$$

Solving the above equation for ω_L, we obtain,

$$\omega_L^n = -\omega_B^n \cos(n\theta_1') \pm \sqrt{1 + \omega_B^{2n}\cos^2(n\theta_1')} \tag{2.48}$$

As we know here that $\cos(n\theta_1') < 0$ for LQF and also that the filters needed are for practical applications, the value of ω_L may be derived as

$$\omega_L = \omega_B \left[\omega_B^n \left|\cos(n\theta_1')\right| + \sqrt{1 + \omega_B^{2n}\cos^2(n\theta_1')}\right]^{1/n} \tag{2.49}$$

From Eqn.(2.49), we can deduce that

$$\omega_L > \omega_B \tag{2.50}$$

This means that, in order to maintain identical maximum pass-band attenuation as in Eqn.(2.46), the pole-frequency ω_L of the LQF should be chosen larger than the pole-frequency ω_B of Butterworth filter. Next, one can compare the slopes at cut-off for the Butterworth and the Low-Q filters, where the slope S_c is given by

$$S_c = \left.\frac{dA(\omega)}{d\omega}\right|_{\omega=1} \tag{2.51}$$

and deduce that

$$\frac{S_{CB}}{S_{CL}} = \left(\frac{\omega_L}{\omega_B}\right)^{2n} \left[\frac{1}{1 + \omega_L^n \left|\cos(n\theta_1')\right|}\right] > 1 \tag{2.52}$$

where S_{CB} and S_{CL} are slopes at cut-off, corresponding to the Butterworth filter and the Low-Q filter respectively. Thus we can summarize that

(a) the magnitude response of a LQF is strictly monotonic, while that of the Butterworth filter is maximally flat.

(b) pole-frequency of the LQF is larger than that of the Butterworth filter.

(c) slope at cut-off of the Butterworth filter is larger than that of the LQF.

(d) critical pole-Q of the Butterworth filter is larger than that of the LQF.

Another case is when both filters have identical ω_p values, (i.e. $\omega_B = \omega_L$). It can be shown that

$$A_{CB} > A_{CL} \tag{2.53}$$

and also

$$\theta_{CB} > \theta_{CL} \tag{2.54}$$

where θ_{CB} and θ_{CL} are, respectively, the critical angles of the Butterworth filter and the Low-Q filter, respectively.

2.10.6 High-Q Filters(HQF)

High-Q filters are CPPF's corresponding to $\theta_1' < \frac{\pi}{2n}$. This swings the CPP's of the Butterworth pole-phasors away from the $\pi/4$ axis in the second quadrant. Due to the above condition, $\cos(n\theta_1') > 0$ and the denominator expression of Eqn.(2.45) exhibits maxima and minima at certain values of ω. The magnitude response of HQF is thus non-monotonic with a single peak occuring at ω_m given by

$$\omega_{mH}^n = \omega_H^n \cos(n\theta_1') \tag{2.55}$$

where ω_H is the pole-frequency of the HQF.

From Eqn.(2.45) and Eqn.(2.55) the corresponding peak squared magnitude can be evaluated as

$$A_{mH}^2 = \frac{1}{\sin^2(n\theta_1')} \tag{2.56}$$

which is independent of the pole-frequency.

The magnitude ratio in the pass-band for the HQF can be written as

$$a_{pH} = \frac{A_{mH}}{A_{cH}} \tag{2.57}$$

where A_{cH} is the magnitude of the HQF response at cut-off. Similarly, the magnitude ratio in the pass-band for the Butterworth filter is given by,

$$a_{pB} = \frac{1}{A_{cB}} \tag{2.58}$$

where A_{cB} is the magnitude of the Butterworth filter at cut-off, the peak magnitude of the filter being unity. However, the peak-magnitude of the HQF is not unity. To facilitate easy comparison, we can change the d.c. value of the HQF response to $\left\{\sin(n\theta_1')\right\}$, so that the peak value of the response becomes unity for this case too. Incorporating this normalization in Eqn.(2.45) the squared magnitude response of the HQF can be derived as

$$A_H^2(\omega) = \frac{\omega_H^{2n}\sin^2(n\theta_1')}{\omega^{2n} - 2\omega_H^n\cos(n\theta_1')\omega^n + \omega_H^{2n}} \tag{2.59}$$

Analytically it can be shown that the stop-band response of the HQF is much

better than that of the Butterworth filter and it can be deduced that

$$A_{cH}^2 \leq \sin^2(n\theta_1') \tag{2.60}$$

It can thus be summarized that

(a) the slope at cut-off of the HQF is larger than that of the Butterworth filter.

(b) pole-frequency of the HQF is smaller than that of the Butterworth filter, i.e., $\omega_H < \omega_p$.

(c) critical-pole-Q of the HQF is larger than that of the Butterworth filter.

2.10.7 Implementation of Pole Parameter Transformation

The program for the implementation of the pole parameter transformations has been written in MATLAB using the different built-in subroutines(Program A4). The program consists of the following main steps.

1. A Butterworth filter of order $n = 8$ is first designed and its poles are plotted.

2. The magnitude function of the Butterworth filter is then obtained and plotted.

3. The poles of the filter are shifted by an angle of five degrees positive and negative and the new magnitude function is obtained using Eqn.(2.45) for each of the above case.

4. The magnitude function of the shifted pole filter is plotted and compared with that of the original filter.

5. For a positive five degree shift the magnitude function corresponded to a Low-Q filter and for a negative five degree shift the magnitude function corresponded to a High-Q filter.

Program A4

```
%% BUTTERWORTH LOWPASS FILTER ( 1-D)
    %% CPPF and effects of changing the phasor angle
    %% Order of the filter
    n1=8;
    %% To obtain and plot the poles of the filter
    i=1;
    if rem(n1,2)==0
    for k1=(n1+2)/2 : (3*n1)/2
    a1 = cos(((2*k1)-1)*pi/(2*n1));
    b1 = sin(((2*k1)-1)*pi/(2*n1));
    s1(1,i)= a1+j*b1;
    i=i+1;
    axis([-1 0 0 1 ]);
    plot(a1,b1,'yo');
    hold on;
    end
    else
    for k1=(n1+3)/2:((3*n1)+1)/2
    a1=cos((k1-1)*pi/n1);
    b1=sin(((k1-1)*pi)/n1);
    s1(1,i)= a1+j*b1;
    i=i+1;
    axis([-1 0 0 1 ]);
    plot(a1,b1,'yo');
    hold on;
    end
    end
    title('Plot of poles of the Butterworth filter');
    xlabel('Real axis');
    ylabel('Imag.axis');
    grid on;
    print -dps buttpole.ps;
    s1'
    %%%% To obtain the polar phasor
    Mag_cp=abs(s1');
```

```
ang_cp=angle(s1');
degree=180*ang_cp/pi;
%%%% To display the polar phasor w.r.t quadrant-2
for k1=1:n1
if degree(k1)>0
degree_disp(k1)=180-degree(k1);
end
if degree(k1)<0
degree_disp(k1)=-180-degree(k1);
end
end
degree_disp'
%%%% To obtain the magnitude function for the butterworth filter %%%%%
Nmr=Mag_cp(1)^(2*n1);
Dnr(1,1)=1;
Dnr(1,n1)=-2*(Mag_cp(1)^(n1))*cos(n1*ang_cp(1));
Dnr(1,2*n1)=Mag_cp(1)^(2*n1);
c1=0;
for w=0:0.01:2
c1=c1+1;
Dnrval(c1)=(Dnr(1,1)*w^(2*n1)) + (Dnr(1,n1)*(w^n1)) + (Mag_cp(1)^(2*n1));
Mod(c1)=sqrt(Nmr/Dnrval(c1));
end
%% SHIFT of poles by theta  =  5degrees
for k2=1:2:n1
new_deg_5(k2) = degree(k2) - 5;
new_deg_5(k2+1) = degree(k2+1) + 5;
end
ang_cp_5 = (new_deg_5)*pi/180;
%% To display the angle w.r.t. quadrant 2
for k3=1:n1
if new_deg_5(k3)<0
new_deg_5_disp(k3)=-180 - new_deg_5(k3);
end
if new_deg_5(k3)>0
new_deg_5_disp(k3)=180 - new_deg_5(k3);
end
```

```
end
new_deg_5_disp'
%% To obtain and plot the magnitude function after 5degshift
Nmr_5 = Mag_cp(1)^(2*n1);
Dnr_5(1,1) = 1;
Dnr_5(1,n1) = -2*(Mag_cp(1)^(n1))*cos(n1*ang_cp_5(1));
Dnr_5(1,2*n1) = Mag_cp(1)^(2*n1);
c1 = 0;
for w = 0:0.01:2
c1 = c1+1;
Dnrval_5(c1)=(Dnr_5(1,1)*w^(2*n1)) + (Dnr_5(1,n1)*(w^n1)) + (Mag_cp(1)^(2*n1));
Mod_5(c1)=sqrt(Nmr_5/Dnrval_5(c1));
end
%% SHIFT of poles by theta  =  -5 degrees
for k2=1:2:n1
new_deg_m5(k2) = degree(k2) + 5 ;
new_deg_m5(k2+1) = degree(k2+1) - 5;
end
ang_cp_m5 = new_deg_m5*pi/180;
%% To display the pole phasors w.r.t quadrant2
for k4=1:n1
if new_deg_m5(k4)<0
new_deg_m5_disp(k4)=-180 - new_deg_m5(k4);
end
if new_deg_m5(k4)>0
new_deg_m5_disp(k4)=180 - new_deg_m5(k4);
end
end
new_deg_m5_disp'
%% To obtain and plot the magnitude function after -5degshift
Nmr_m5 = (Mag_cp(1)^(2*n1))*((sin(n1*ang_cp_m5(1)))^2);
Dnr_m5(1,1) = 1;
Dnr_m5(1,n1) = -2*(Mag_cp(1)^(n1))*cos(n1*ang_cp_m5(1));
Dnr_m5(1,2*n1) = Mag_cp(1)^(2*n1);
c1 = 0;
for w = 0:0.01:2
c1 = c1+1;
```

```
Dnrval_m5(c1)=(Dnr_m5(1,1)*w^(2*n1)) + (Dnr_m5(1,n1)*(w^n1)) + (Mag_cp(1)^(2*n1));
Mod_m5(c1)=sqrt(Nmr_m5/Dnrval_m5(c1));
end
%%To plot the polar plot showing the shift in angle by 5degrees.
figure;
polar(ang_cp,Mag_cp,'y*');
hold on;
polar((ang_cp_5)',Mag_cp,'r+');
hold on;
polar((ang_cp_m5)',Mag_cp,'go');
legend('no shift','5deg shift','-5deg shift');
print -dps polarp.ps;
%% End of program
```

The results are plotted and the respective plots are shown.

Figs.(2.19(a) and (b)) show the pole placement in the different axis domains and Fig.(2.20) shows a comparative study of the magnitude responses.

The results have been summarized in Table(2.3)

Filters : Pole shift(in degrees)	ω_p(rad)	θ_p(degrees)	Q_c
LQF : $\theta_0 = 5^o$	1.0785	16.25^o 28.75^o 61.25^o 73.75^o	1.7868
HQF : $\theta_0 = -5^o$	0.9580	6.25^o 38.75^o 51.25^o 83.75^o	4.59270

Table 2.3: Summary of the results obtained due to the analysis of the pole parameter transformation filters.

The above method of pole-parameter transformation can be readily extended to the 2-D case as it is a simple and straight forward extension of the 1-D case, the magnitude functions being product separable.

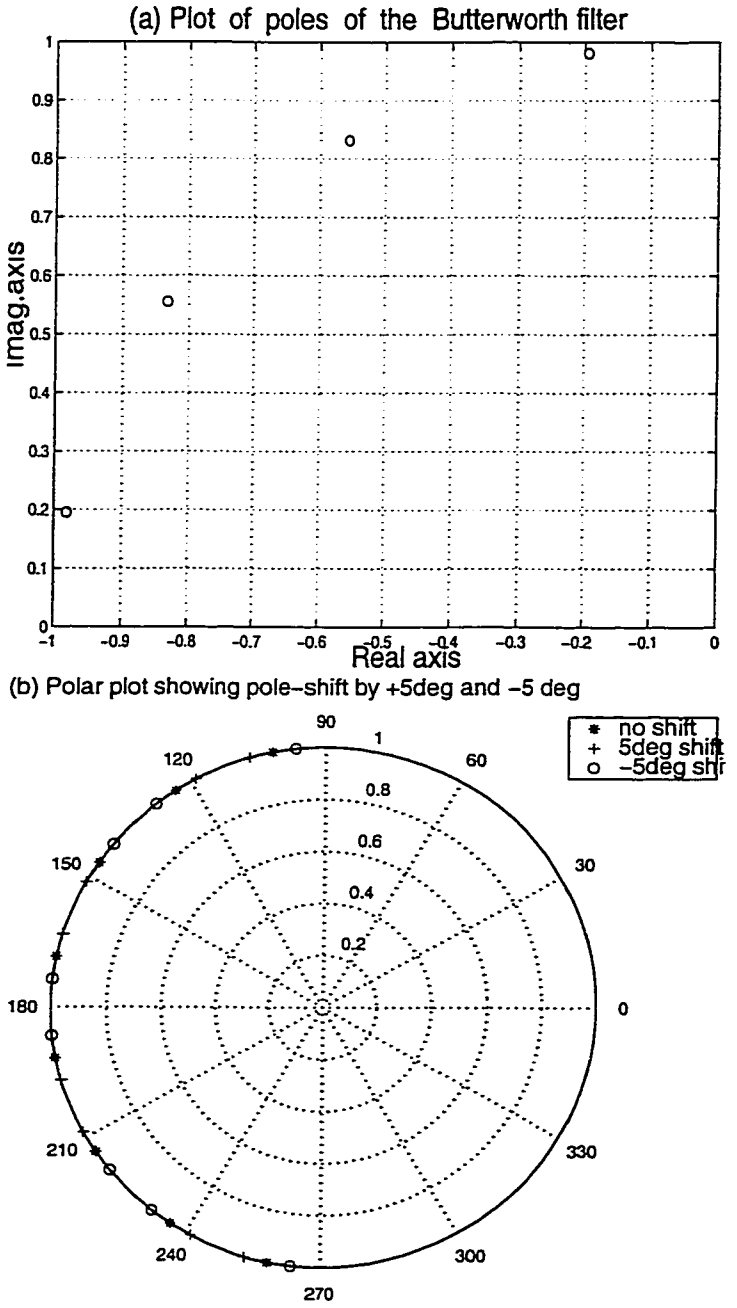

Figure 2.19: (a) Polar plot for 1-D filter of order $n = 8$. (b) Shifting of the poles by $\pm 5°$.

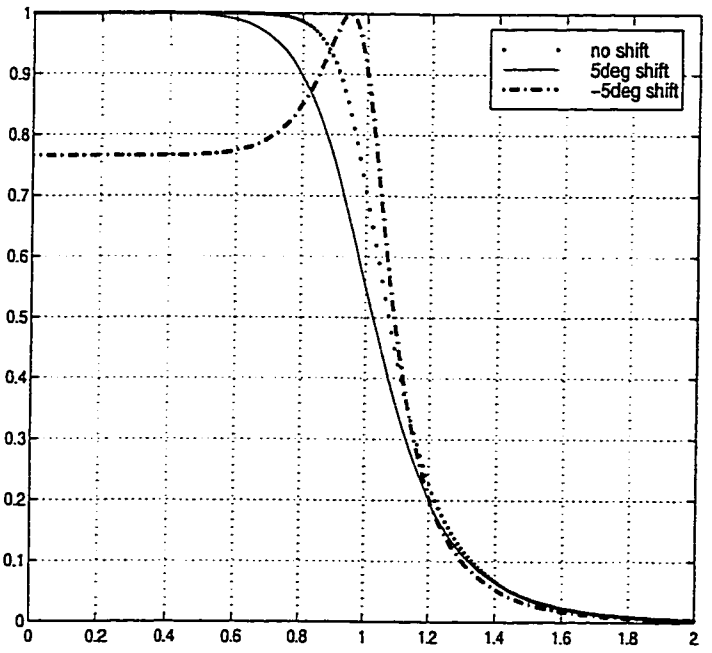

Figure 2.20: Magnitude response of the CPP filters : comparitive study

2.10.8 Two-dimensional CPPF

With the above review in 1-D, we shall extend the same to the construction of complementary pole-pair filters to the 2-D case also. In this case, the 2-D CPPF is simply obtained as a product of two cascaded 1-D filters as an independent product. This means that variation of pole parameters in each dimension is independent too.

For the sake of simplicity in performing arithematic calculations, the concept of 2-D CPPF has been studied using the same transfer function that was used in the first program in this chapter(Program A1). The transfer function used in that case is taken and the roots are determined as follows.

Let $T_1(s_1) = \frac{1}{g_1(s_1)+f_1(s_1)}$ where $g_1(s_1)$ is a third order butterworth polynomial given by

$g_1(s_1) = s_1^3 + 2s_1^2 + 2s_1 + 1$ and $f_1(s_1) = k_1$.

Similarly for $g_2(s_2)$ and $f_2(s_2)$ in the second dimension, the expressions to obtain $T_2(s_2)$ are given by

$g_2(s_2) = s_2^3 + 2s_2^2 + 2s_2 + 1$ and $f_2(s_2) = k_2$.

The above transfer function gives two complex poles on the 2^{nd} and 3^{rd} quadrant respectively forming angles of $+60^o$ and -60^o respectively with the X-axis in the negative direction. The value of $k = k_1 = k_2$ is chosen as the optimum value for circular symmetry as was derived from Program A3. It has thus been chosen to be -0.3 and the poles (P_1) are determined based on the transfer function that includes the above value of k.

The poles are then shifted by an angle $\pm 5^o$ as shown in Fig.(2.21), giving rise to two different pole-pairs $(P1', P2')$ and $(P1'', P_2'')$, making angles of $\pm 65^o$and $\pm 55^o$ respectively with the negative real axis.

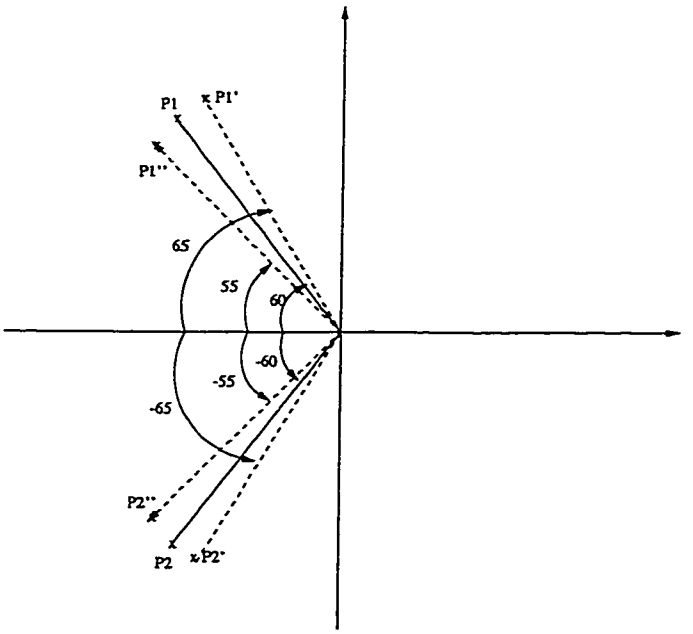

Figure 2.21: Shift of poles by angle of $\pm 5^o$ for the two independent transfer functions.

The poles for these angles are then calculated and the transfer function is determined. The optimum range of k, for stability, for these two transfer functions is found to be

(a) For positive shift in pole of 5° (away from each other) : $-1 < k < 1.7279$

(b) For negative shift in pole of 5°(towards each other) : $-1 < k < -0.6689$

From the above results the optimum value of k for circular symmetry is determined using Program A2 and Program A3 and it is thus found that for $k = -0.48$, the positive pole shift of 5^o, exhibits circular symmetry and for $k = -0.67$, the negative pole shift of 5^o, exhibits circular symmetry.

The Program for the 2-D case follows the same pattern as the 1-D case and therefore has not been shown. Fig.(2.22(a) and (b)) show the 2-D filter response before any pole parameter transformation has been applied to it.

Fig.(2.23(a)-(e)) show the 2-D filter response after a pole shift of +5° has been applied to it. Applying Program A3 to these responses(Fig.(2.24(a)-(e)), it has been found that at $k = -0.48$, it exhibits near circular symmetry for the magnitude range $0.49 < Mag < 0.51$. This has been shown only for this case, as an illustration. The same procedure has however been used in determining the value of k for all the cases of pole shifts discussed in this section.

Fig.(2.25(a)-(e)) show the the 2-D filter response after a pole shift of −5° has been applied to it. Here it is seen that near circular symmetry has been obtained at a value of $k = -0.67$.

For both positive and negative pole-parameter shifting, it has been found that circular symmetry can still be achieved within the optimum stability range for k. The same can be achieved for different values of θ_o, i.e., for different values of shift

in the angle and therefore different values of k. The plots that follow show the above simulation for values of $\theta_o = \pm 3^o, \pm 7^o$.

Fig.(2.26(a)-(e)) show the the 2-D filter response after a pole shift of $+3°$ has been applied to it. Here it is seen that near circular symmetry has been obtained at a value of $k = -0.08$.

Fig.(2.27(a)-(e)) show the the 2-D filter response after a pole shift of $-3°$ has been applied to it. Here it is seen that near circular symmetry has been obtained at a value of $k = -0.04$.

Fig.(2.28(a)-(e)) show the the 2-D filter response after a pole shift of $+7°$ has been applied to it. Here it is seen that near circular symmetry has been obtained at a value of $k = -0.2$.

Fig.(2.29(a)-(e)) show the the 2-D filter response after a pole shift of $-7°$ has been applied to it. Here it is seen that near circular symmetry is not a possibilty in any magnitude range.

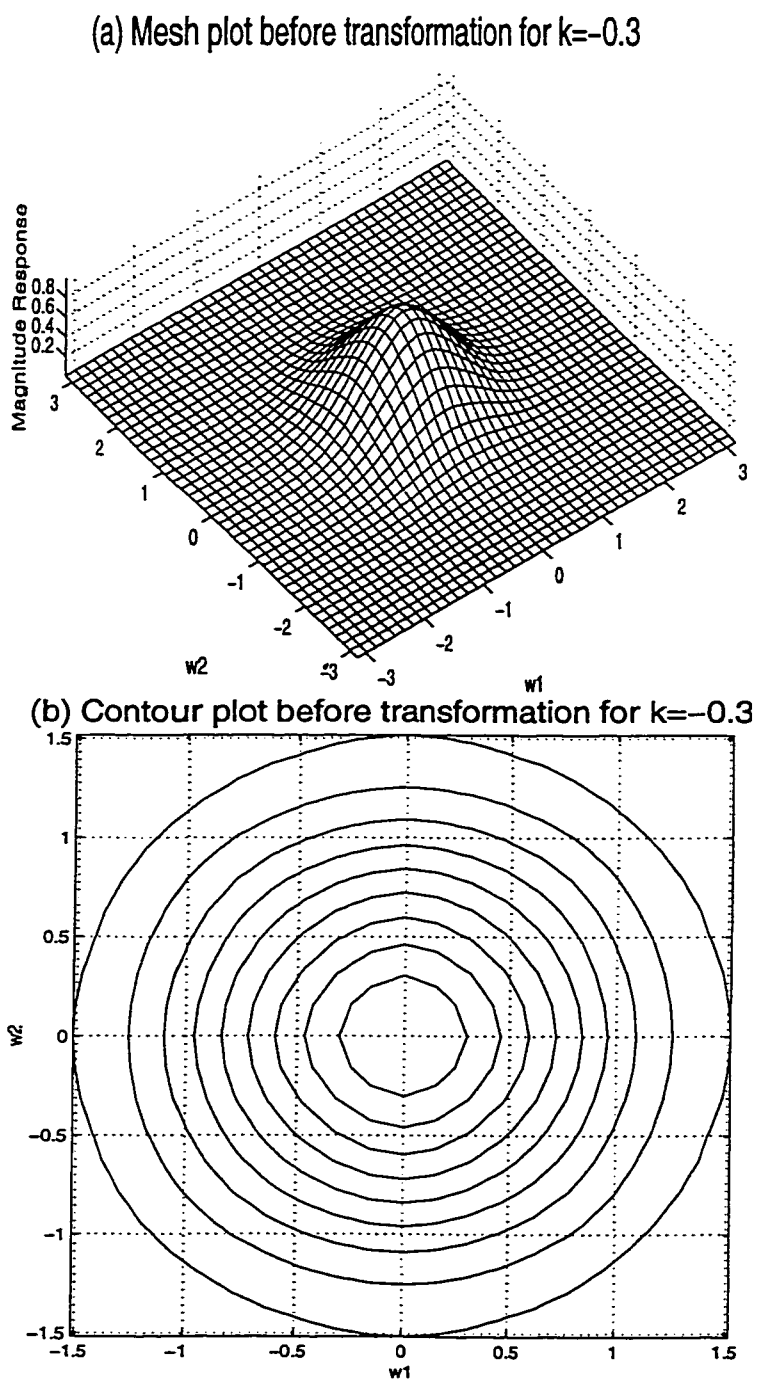

Figure 2.22: 2-D CPPF before pole parameter transformation showing near circular symmetry at $k = k_1 = k_2 = -0.3$. (a) Magnitude Plot (b) Contour Plot

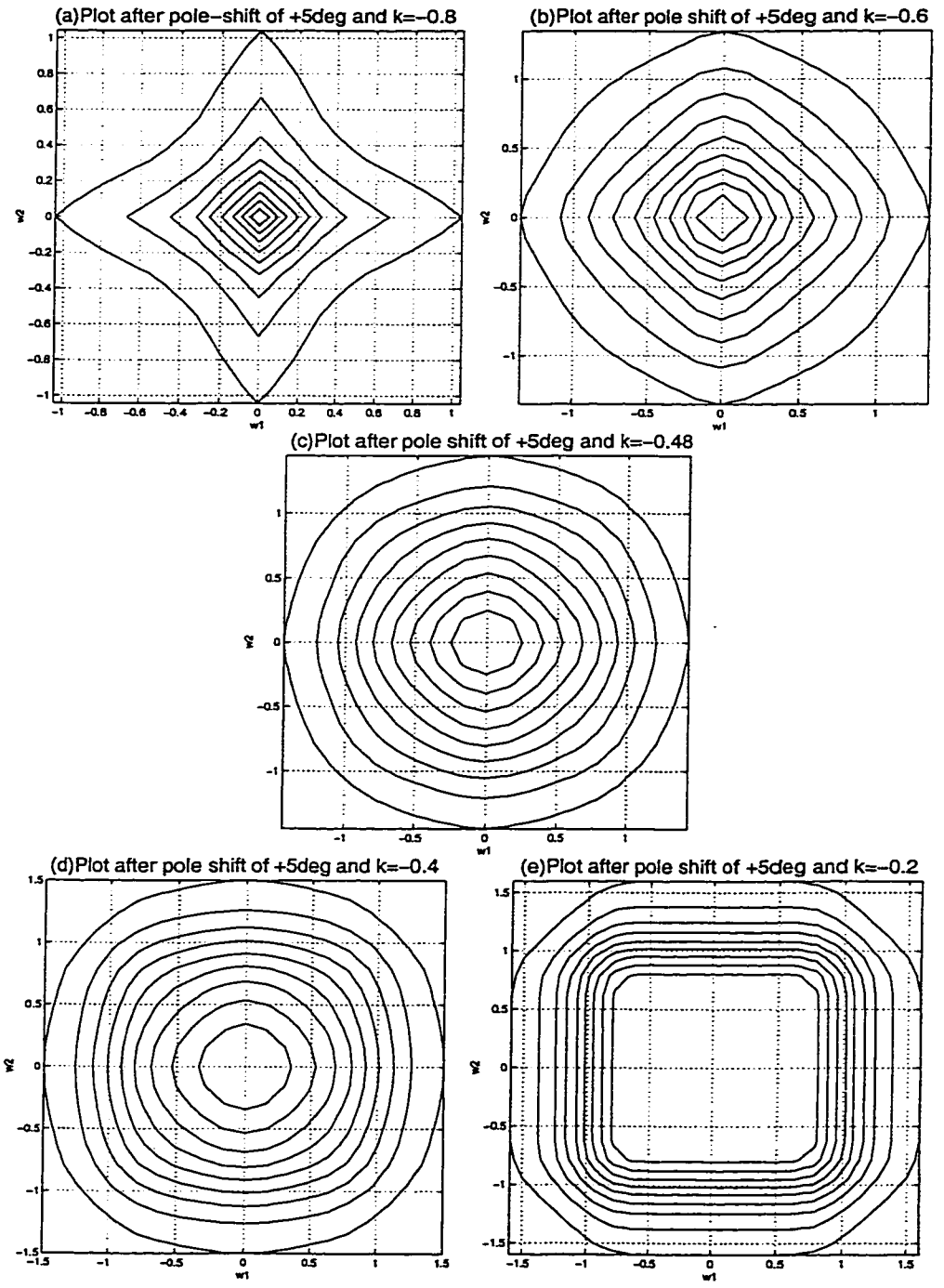

Figure 2.23: 2-D CPPF after pole parameter transformation of $\theta_o = +5^o$ showing near circular symmetry at $k = k_1 = k_2 = -0.48$.

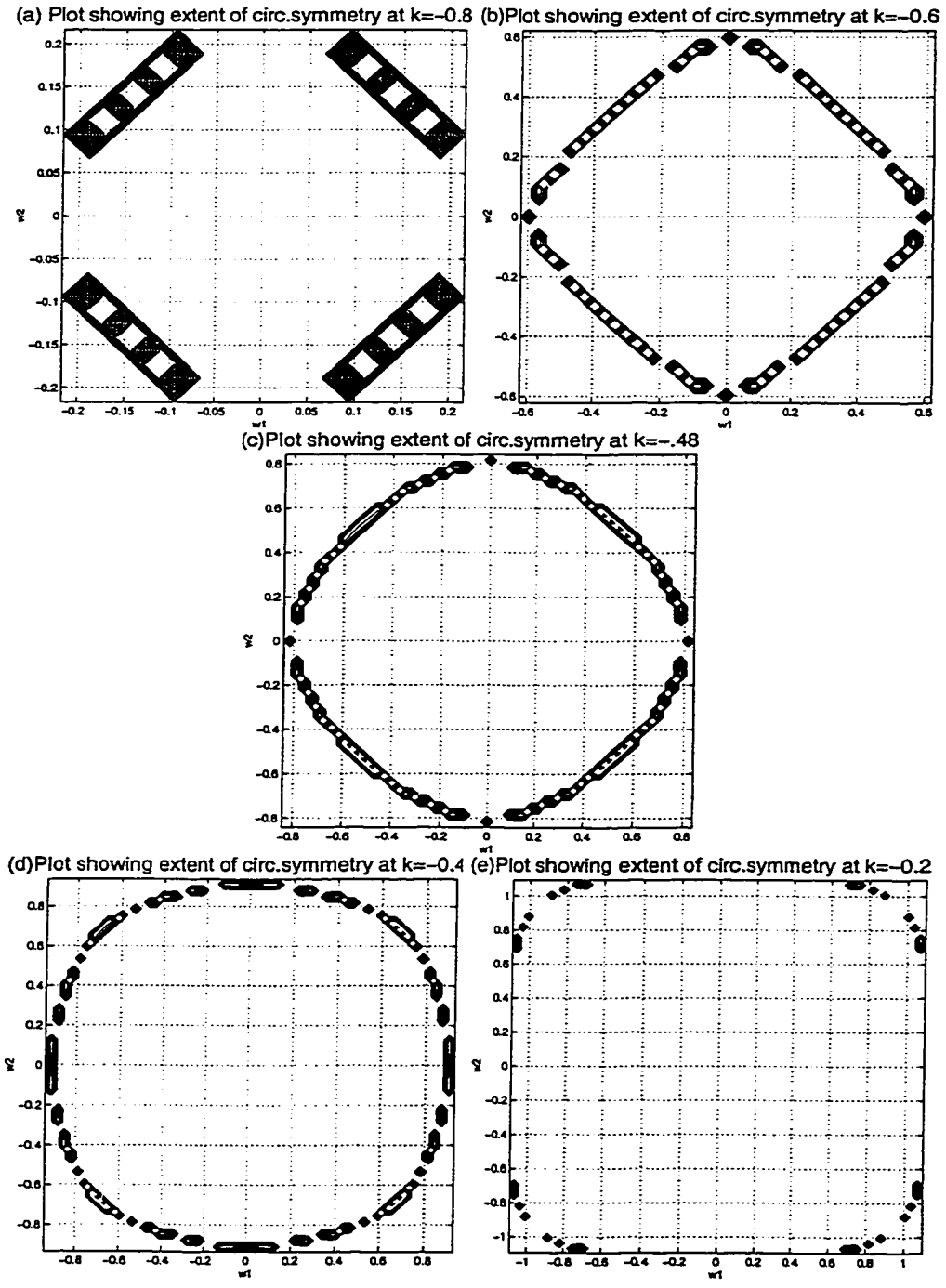

Figure 2.24: Plots to illustrate the extent of circular symmetry obtained after shifting the poles of the original transfer function by $+5^o$.

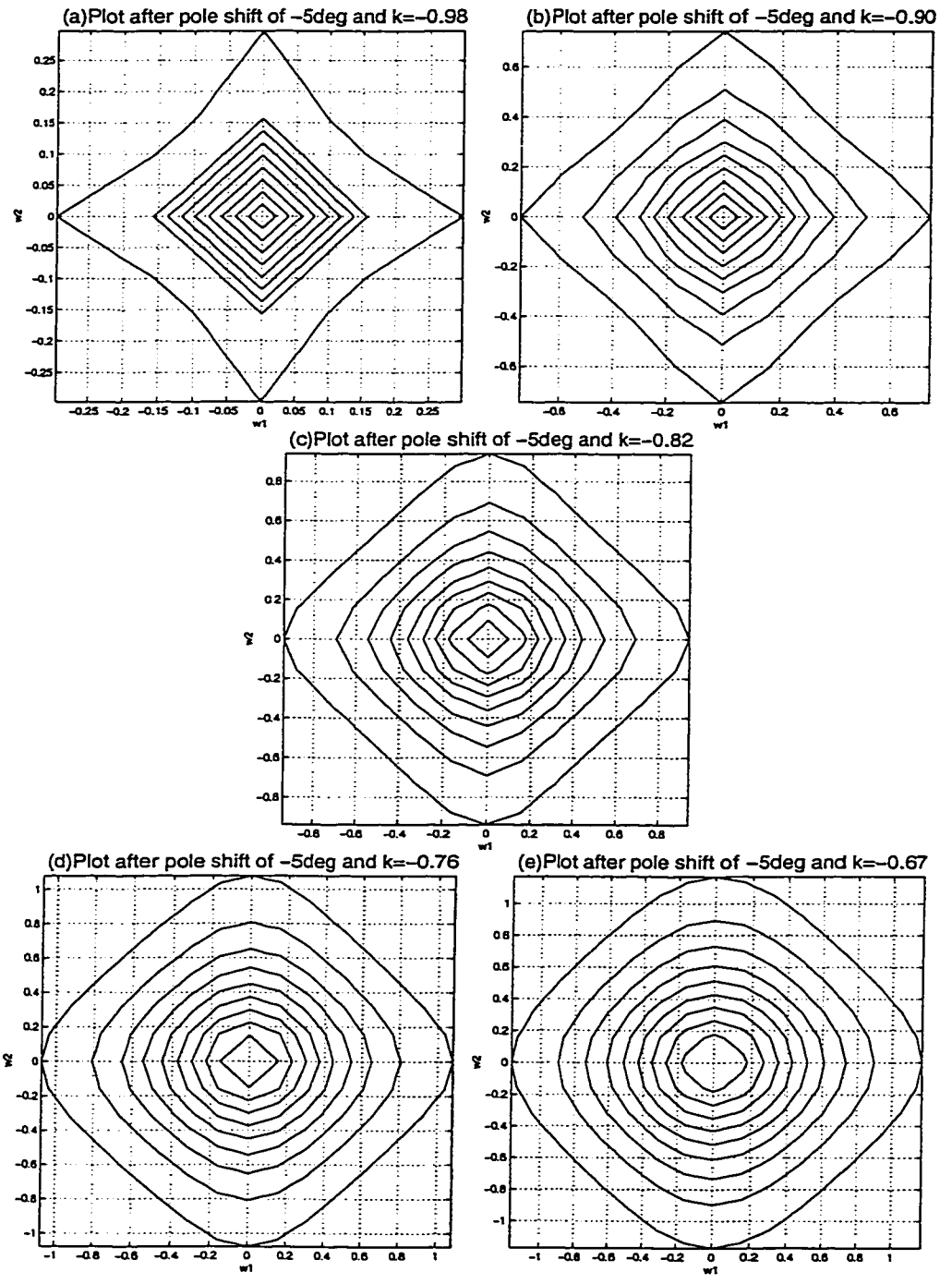

Figure 2.25: 2-D CPPF after pole parameter transformation of $\theta_o = -5^o$ showing near circular symmetry at $k = k_1 = k_2 = -0.67$.

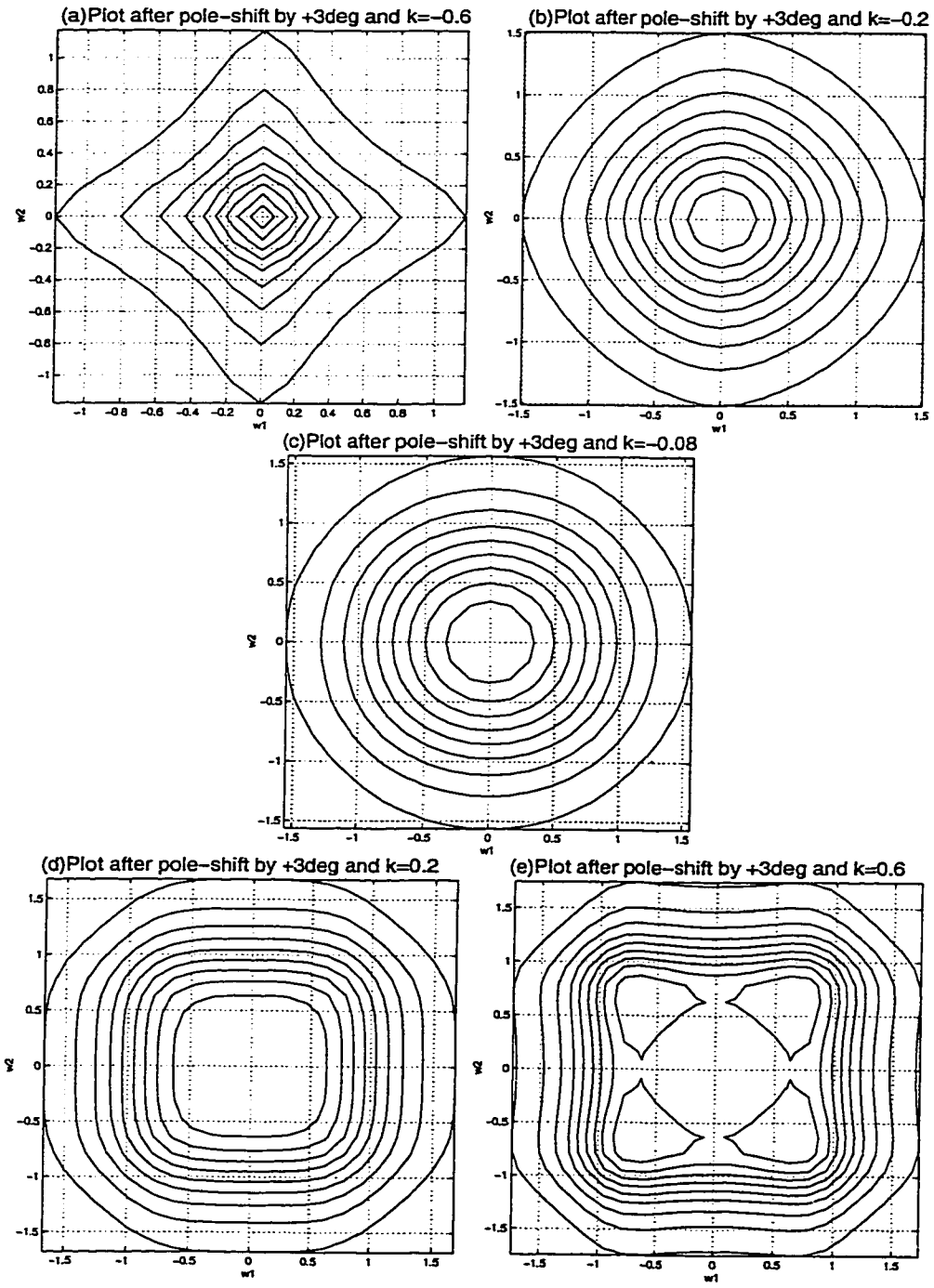

Figure 2.26: 2-D CPPF after pole parameter transformation of $\theta_o = +3^o$ showing near circular symmetry at $k = k_1 = k_2 = -0.08$.

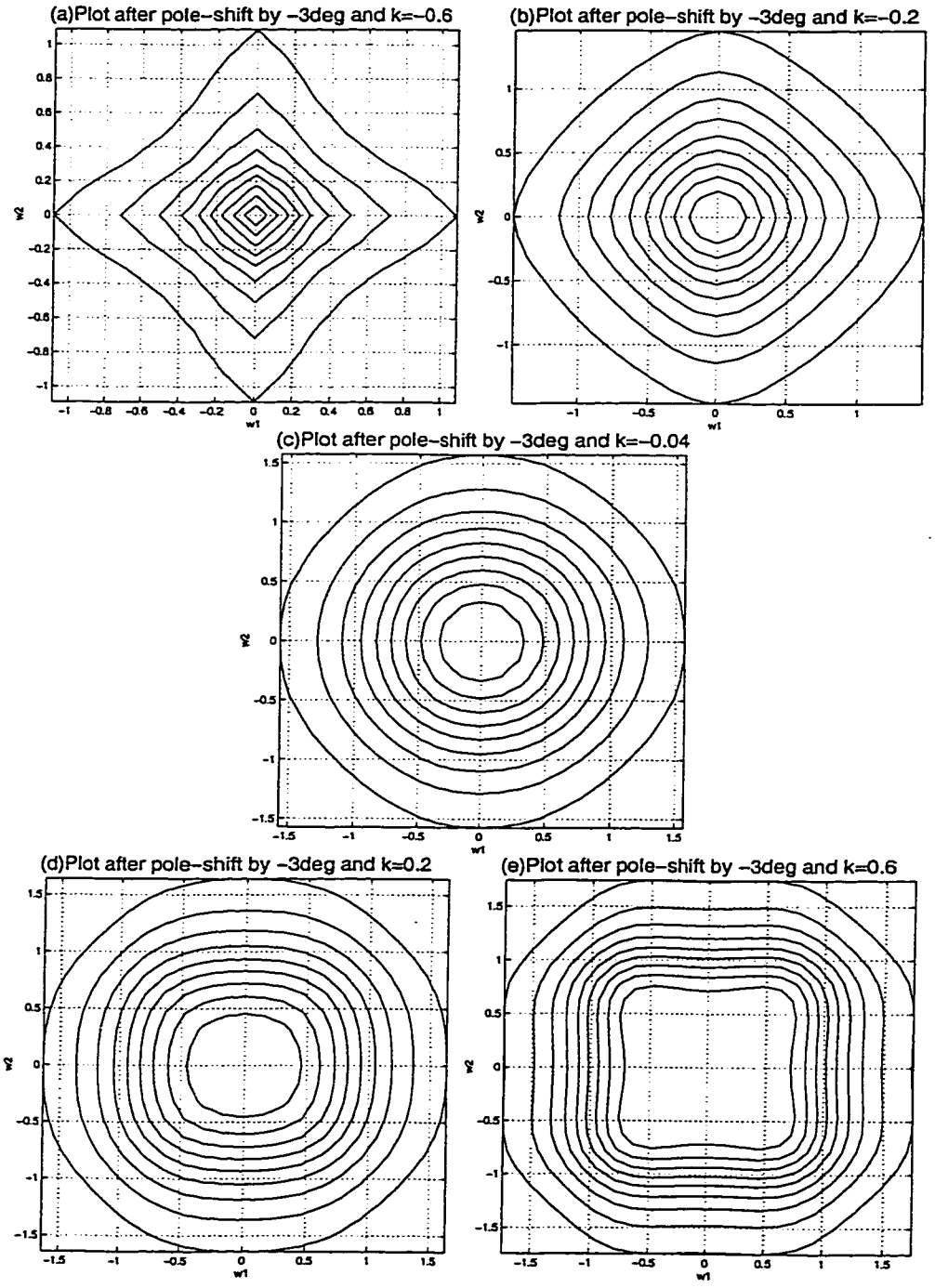

Figure 2.27: 2-D CPPF after pole parameter transformation of $\theta_o = -3^o$ showing near circular symmetry at $k = k_1 = k_2 = -0.04$.

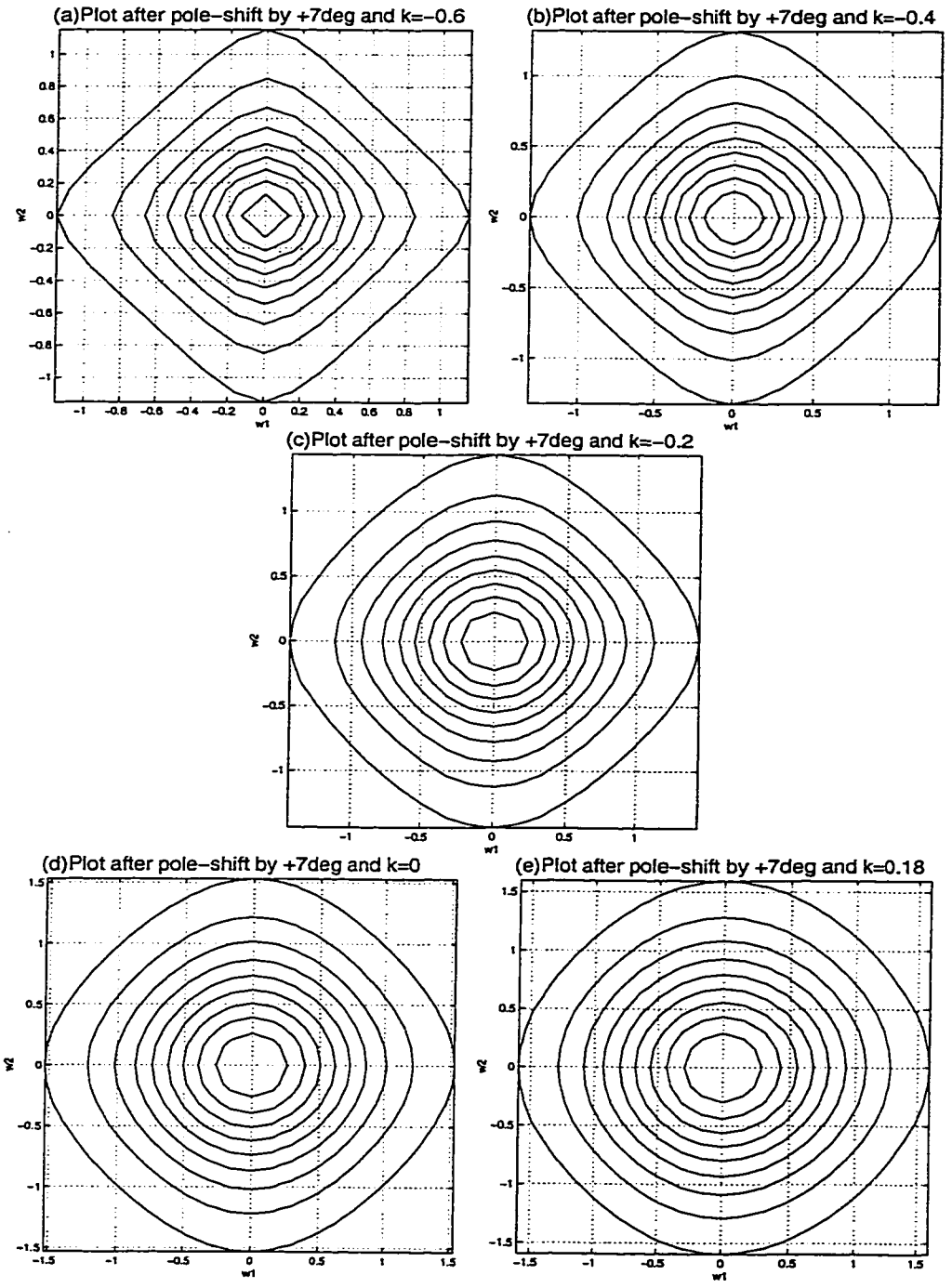

Figure 2.28: 2-D CPPF after pole parameter transformation of $\theta_o = +7^o$ showing near circular symmetry at $k = k_1 = k_2 = 0.18$.

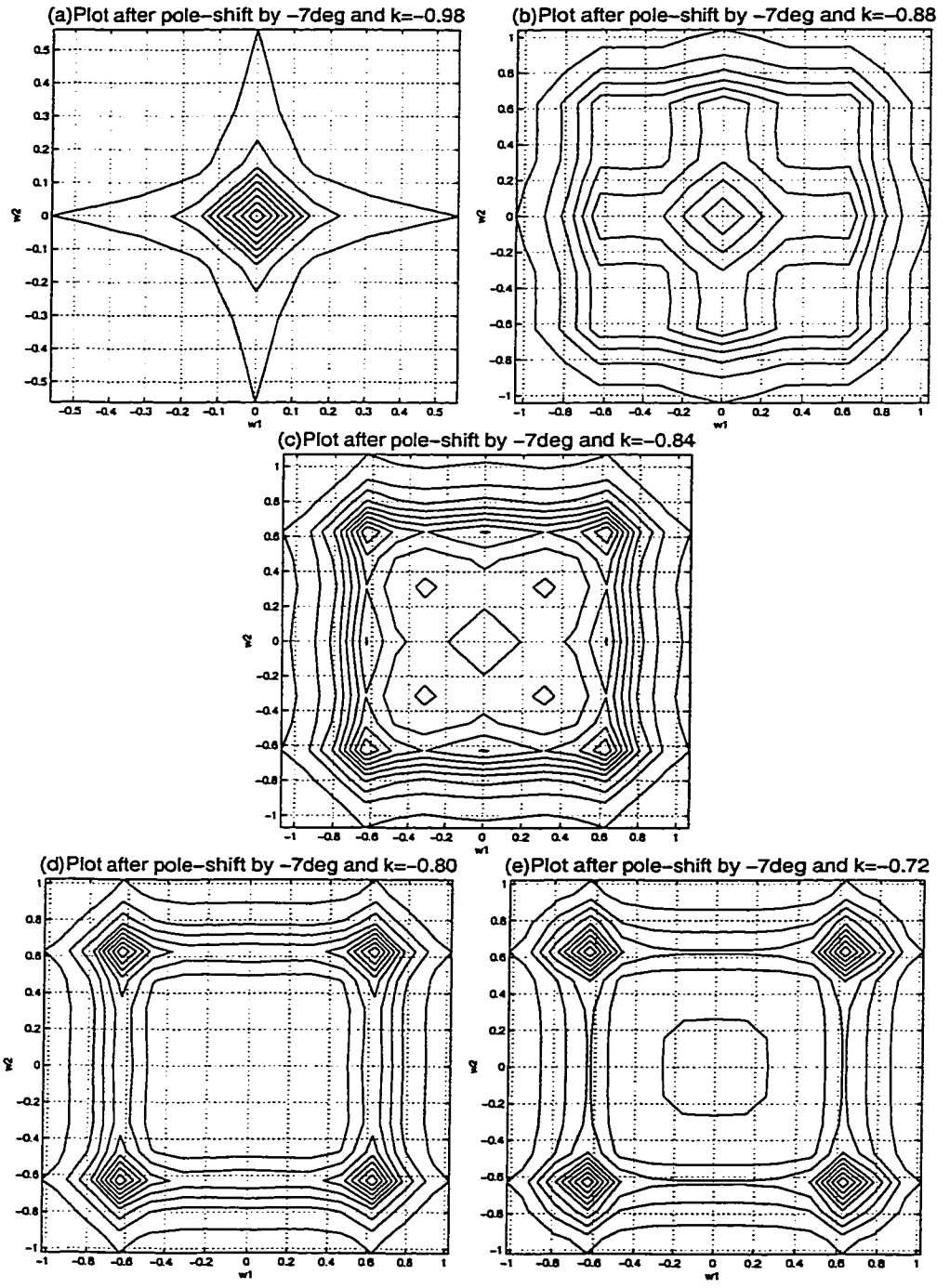

Figure 2.29: 2-D CPPF after pole parameter transformation of $\theta_o = -7^o$. It is noted that there is clearly no circular symmetry in this case.

As it can be seen, for different values of angular shift in the complex poles in each of the cases, the value of k also shifts correspondingly for near circular symmetry. However, with greater increase in the value of the angular shift it can be seen that the filter loses its circular symmetry within the stable region of k, .i.e., comparing the circular symmetric characteristic for $\theta_o = \pm 3^o, \pm 5^o and \pm 7^o$, it can be easily deduced that for $\theta_o = \pm 7^o$ the circular symmetric property reduces considerably and shifts towards the outer limits of k.

Table (2.4) summarizes the results for the six cases that has been discussed.

Angular Shift(in degrees)	Stability range of k	Value of k for circular symmetry
$\theta_o = -7$	$-1 < k < -0.7134$	No value
$\theta_o = -5$	$-1 < k < -0.6689$	k=-0.6700(approx. outer limit)
$\theta_o = -3$	$-1 < k < 6.7056$	k=+0.0400
$\theta_o = +3$	$-1 < k < 4.9936$	k=-0.0800
$\theta_o = +5$	$-1 < k < 1.7277$	k=-0.4800(approx. outer limit)
$\theta_o = +7$	$-1 < k < 0.0189$	k=+0.1800(outer limit)

Table 2.4: Summary of the results achieved due to different values of angular shift in the complex poles and their corresponding values of k for circular symmetry. The range of magnitude chosen for all the above cases is 0.49<Mag<0.51.

2.10.9 Summary and Discussion

In summary, this chapter has shown in detail the approximation to circular symmetry that can be achieved in stable, 2-D Lowpass transfer functions, starting from, two 1-D transfer functions. The study has been done using both Butterworth and Chebyshev transfer functions. Another interesting aspect of filter design namely the effect of pole parameter transformation on circular symmetry has been studied in the 2-D case and the results have been shown.

In the study of Butterworth filters, extensive simulations have been done for the

third order filter and results have been plotted. An algorithm to determine the extent of circular symmetry in specific magnitude ranges has been written and this has been used in all the above cases, as a tool to determine the range and value of the feedback factor k for circular symmetry for each of the above cases. It has been found from the results obtained that, circular symmetry varies with the the value of k, within stability limits. Specific magnitude ranges has been chosen for all the cases, so as to be consistent with the comparative study.

In the Chebyshev study, it has been proved that the value of k for circular symmetry, varies as a function of ripple width ϵ. For the same order and different value of ripple width, results have been plotted and tabulated.

The effect of pole-parameter transformation on circular symmetry has been studied with six different cases of pole-parameter transformation and the results have been tabulated. It has been proved from the results that, the greater the deviation from the original poles of the transfer functions, the smaller the value of k for stability and thus circular symmetry.

Thus, in this Thesis, this chapter is an important work towards the study of 2-D near circular symmetric filters possessing separable denominator transfer functions.

Chapter 3

Generation of Stable 2-D Bandpass, Bandstop and Highpass Filters and their Approximation to Circular Symmetry

The previous chapter dealt with the implementation of 2-D Lowpass Filter design only. In this chapter, the implementation of other types of filters namely Highpass filter, Bandpass filter and Bandstop filter and their approximation to circular symmetry will be discussed. We will restrict our discussion, in this chapter, to the Butterworth filter design only.

3.1 Bandpass Filter

Bandpass filters have a specific band or range of frequencies above and below which they attenuate signals. Thus, very low and very high frequency components of a signal are attenuated and the signals within the specified pass-band range possess a high gain.

The design of 2-D IIR Butterworth Bandpass filter is carried out in the same manner as the Lowpass design, in principle, by first designing the 1-D Butterworth filter and then combining two similar 1-D transfer functions as a product. The code has been written using MATLAB (Program B1) using the different built-in subroutines to achieve the filter specifications. The following procedure has been adopted to design the filter:

(1) The required specifications namely the order of the filter (N) and the upper and lower pass-band edges (W_n), as a 1x2 matrix, are first defined. The filter chosen in this case has an analog cut-off frequency of [0.3, 1] and is of the fourth order.

(2) The numerator and denominator polynomials of the analog transfer function are determined using the MATLAB function *"butter"* for the Bandpass filter design. This gives the transfer function for the FIR filter.

In this case, the fourth order Bandpass transfer function(1D) is given by

$$H_{FIR}(s) = \frac{0.2401s^4}{(s^8 + 1.8292s^7 + 2.8730s^6 + 2.5426s^5 + 1.7839s^4 + 0.7628s^3 + 0.2586s^2 + 0.0494s + 0.0081)} \tag{3.1}$$

Having determined the numerator and denominator polynomials for the analog transfer function of the FIR filter, the IIR filter transfer function (1D) is then deter-

mined, as from Eqn.(2.19). This is given by

$$H_{IIR}(s) = \frac{0.2401s^4}{(s^8 + 1.8292s^7 + 2.8730s^6 + 2.5426s^5 + (1.7839 + 0.2401k)s^4 + 0.7628s^3 + 0.2586s^2 + 0.0494s + 0.0081)} \quad (3.2)$$

Now in order for Eqn.(3.2) to be stable, the range of k needs to be determined. Following the same method suggested in Chapter-2 and from Eqn.(2.20) we have

$$\frac{m(s) + m_1(s)}{n(s)} = \frac{s^8 + 2.8730s^6 + (1.7839 + 0.2401k)s^4 + 0.2586s^2 + 0.0081}{1.8292s^7 + 2.5426s^5 + 0.7628s^3 + 0.0494s} \quad (3.3)$$

Now Eqn.(3.3) can be split into partial fractions as follows:

$$K_\infty s + \sum_i \frac{K_i s}{s^2 + \beta_i^2} + \frac{K_0}{s} = \frac{s^8 + 2.8730s^6 + (1.7839 + 0.2401k)s^4 + 0.2586s^2 + 0.0081}{1.8292s(s^2 + 1.0002)(s^2 + 0.3)(s^2 + 0.09)} \quad (3.4)$$

where $\beta_1 = 1.0002, \beta_2 = 0.3, \beta_3 = 0.09$ are the roots of the denominator of Eqn.(3.3).

For Eqn.(3.4) to be a strictly Hurwitz polynomial, $K_i > 0$.

Therefore, we find the values of K_i such that $K_i > 0$ and from the equations obtained, we find the range of k for stability.

From Eqn.(3.4), we have the following equations from which we determine the range of k.

$$K_0 = \frac{0.0081}{1.8292} > 0 \quad (3.5)$$

$$K_1 = \frac{s^8 + 2.8730s^6 + (1.7839 + 0.2401k)s^4 + 0.2586s^2 + 0.0081}{1.8292s^2(s^2 + 0.3)(s^2 + 0.09)} \mid s^2 = 1.0002 \quad > 0 \quad (3.6)$$

$$K_2 = \frac{s^8 + 2.8730s^6 + (1.7839 + 0.2401k)s^4 + 0.2586s^2 + 0.0081}{1.8292s^2(s^2 + 1.0002)(s^2 + 0.09)} \mid s^2 = 0.3 \quad > 0 \tag{3.7}$$

$$K_3 = \frac{s^8 + 2.8730s^6 + (1.7839 + 0.2401k)s^4 + 0.2586s^2 + 0.0081}{1.8292s^2(s^2 + 1.0002)(s^2 + 0.3)} \mid s^2 = 0.09 \quad > 0 \tag{3.8}$$

Solving the Eqns.(3.6), (3.7) and (3.8), we have the following ranges of k respectively, for which Eqn.(3.2) is stable.

$$k < 1.4169, k > -1.0048, k < 1.3684 \tag{3.9}$$

Thus, the resultant range of k for which Eqn.(3.2) is stable is given by

$$-1.0048 < k < 1.3684 \tag{3.10}$$

(3) Bilinear transformation is then performed to determine the digital counter part. This is done using the MATLAB function *"bilinear"*. Refer to Program B2.

(4) Now we have the digital transfer function of the 1-D filter. The same procedure as above, is extended to the second dimension and the transfer function for the second dimension is obtained independently.

(5) The product of the two 1-D polynomials is then determined.

(6) A general subroutine suitable for any order of the filter has been written to determine the frequency response of the 2-D filter. Refer Program B2. The corresponding contour plots are plotted using the MATLAB function *"contour"*.

The MATLAB program namely, Program B1 and B2 have been written for the Bandpass filter specifications given by

$W_n1 = W_n2$	$N1 = N2$
[0.3 1]	4

All frequencies are in radians. The scripts 1 and 2 refer to the first and second dimensions, respectively.

Program B1

```
%% 2D-BANDPASS BUTTERWORTH FILTER
clear all;
close all;
N1=4;
Wn1=[0.3 1];
N2=N1;
Wn2=Wn1;
[B1,A1] = butter(N1,Wn1,'s');
[B2,A2] = butter(N2,Wn2,'s');
for k1=-1.0:0.1:1.36
zz=garg_rama_mag(B1,A1,k1);
lim=pi;
interval=pi/50;
w1=0:interval:lim;
w2=0:interval:lim;
[ww1,ww2]=meshgrid(w1,w2);
figure;
contour(ww1,ww2,zz);
axis('image');
xlabel('w1');
ylabel('w2');
zlabel('Magnitude Response');
title('2-D Butterworth BPF');
grid on;
print -dps bandpasscont.ps;
end
```

Program B2

```
%% Function to determine the transfer function of the filter for
```

```
%% a given k1,k2
function [zz] = garg_rama_mag(B1,A1,k1);
k2=k1;
B2=B1;
[R C]=size(A1);
A1((C+1)/2) = A1((C+1)/2) + k1*B1((C+1)/2);
A2=A1;
%% Bilinear transformation of the transfer function
[N1,D1]=bilinear(B1,A1,1);
[N2,D2]=bilinear(B2,A2,1);
%% To determine the 2-D transfer function of the IIR Filter
for m=1:1:size(N1,2)
for n=1:1:size(N2,2)
N(m,n)= N1(m)*N2(n);
end
end
for m=1:1:size(D1,2)
for n=1:1:size(D2,2)
D(m,n)= D1(m)*D2(n);
end
end
lim=pi;
interval=pi/50;
c1=0;
for w1 = 0:interval:lim
c2=0;
c1=c1+1;
for w2 = 0:interval:lim
c2=c2+1;
for col=1:1:size(N2,2)
NRow(1,col)=(cos(w2) + j *sin(w2))^(size(N2,2)-col);
end
for row=1:1:size(N2,2)
NCol(row,1)=(cos(w1) + j *sin(w1))^(size(N1,2)-row);
end
NR = NRow * N' * NCol;
a=real(NR);
```

```
b=imag(NR);
for col=1:1:size(D2,2)
DRow(1,col)=(cos(w2) + j *sin(w2))^(size(D2,2)-col);
end
for row=1:1:size(D2,2)
DCol(row,1)=(cos(w1) + j *sin(w1))^(size(D1,2)-row);
end
DR = DRow * D' * DCol;
c=real(DR); d=imag(DR);
MOD(c1,c2) = (sqrt((a*c + b*d)^2 + (b*c - a*d)^2))/(c^2+d^2);
end
end
w1=0:interval:lim; w2=0:interval:lim;
[ww1,ww2]=meshgrid(w1,w2);
zz=MOD/(max(max(MOD)));
%% End of Program
```

The results of the algorithm, namely the contour plots for the first quadrant are shown in Fig.(3.1(a)-(e)). A large number of plots for all possible values of k within the stability ranges were plotted. Only the plots of interest have been shown. As it can be seen from the these plots, there is a certain range of k for which near circular symmetry is exhibited in the frequency response for specific magnitude ranges. From Section 2.8 using Program A3 the extent of circular symmetry is determined for the above responses and the optimum value of k for which we have the closest proximity to circular symmetry is determined.

The plots in Fig.(3.2) show the extent of circular symmetry for the responses shown in Fig.(3.1). The plot for $k = -1.36$ is not shown since there are no points within this magnitude range which approximate to circular symmetry.

It is evident from the above plots that at $k = -0.14$, the response exhibits near circular symmetry and for other values of k above and below the value -0.14, circular symmetry gradually ceases to exist.

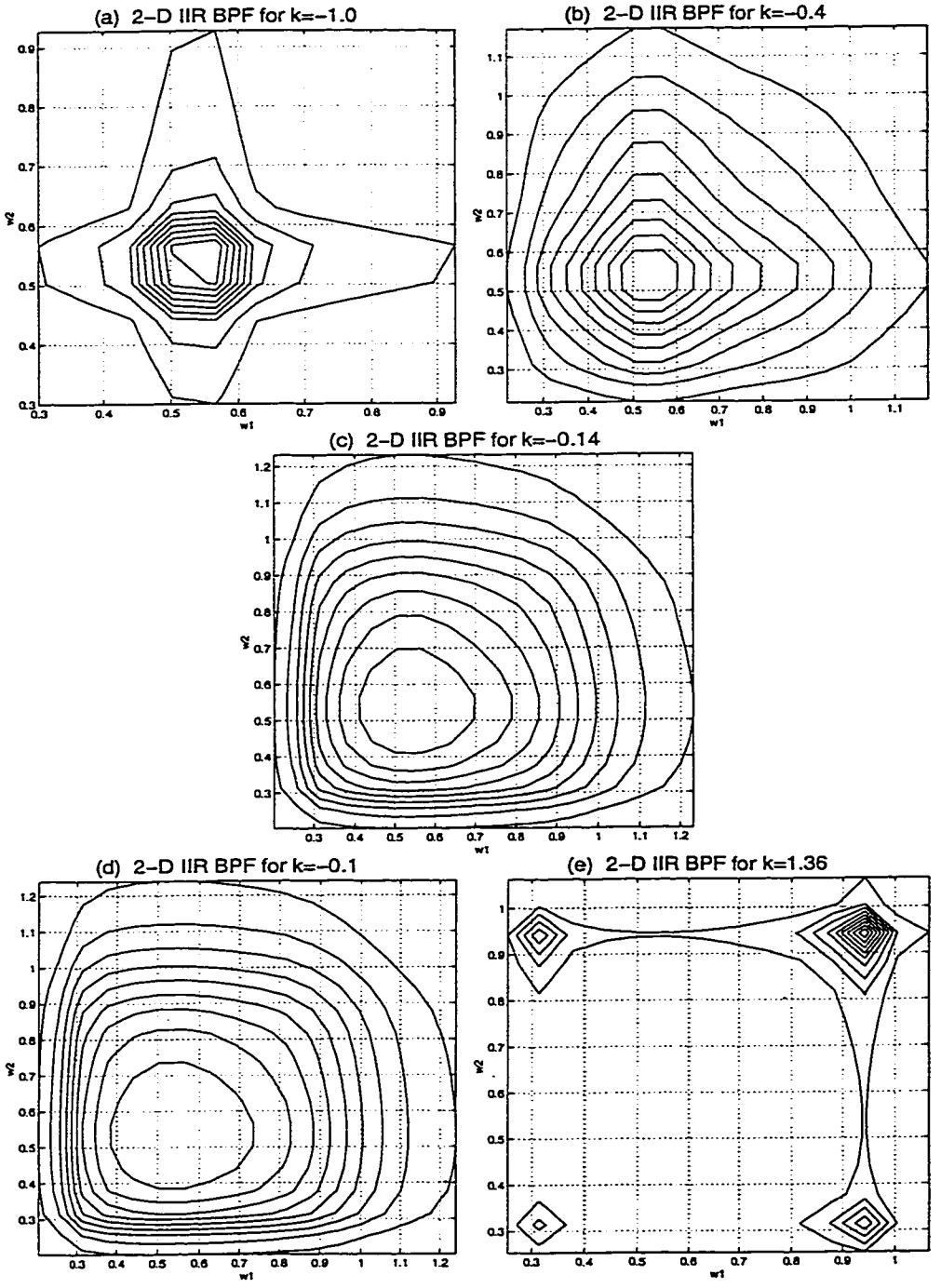

Figure 3.1: 2-D IIR Butterworth Bandpass filter of 4^{th} order - contour plots.

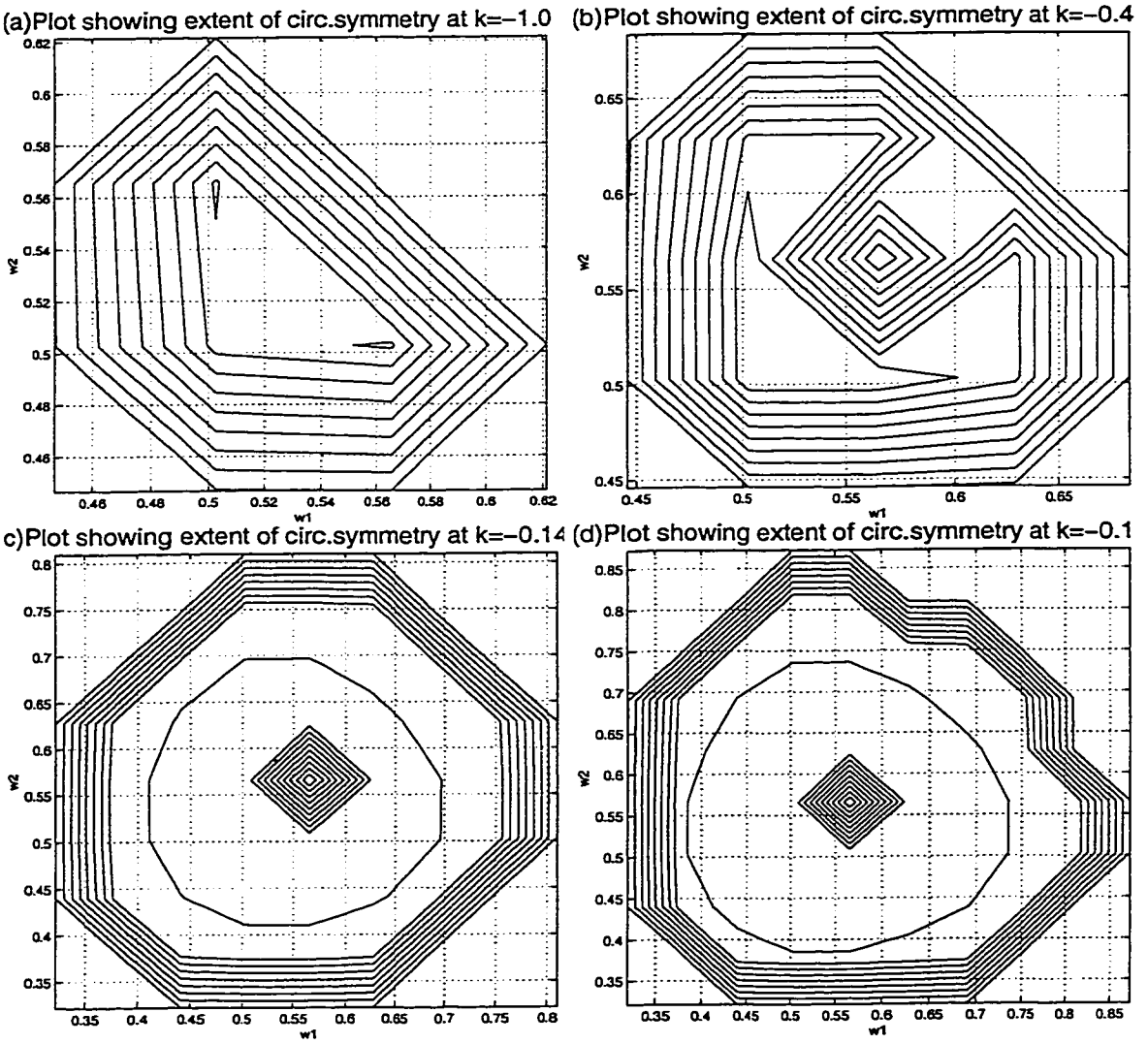

Figure 3.2: Plots to show the extent of circular symmetry of the responses shown in Fig.(3.1). The magnitude range under consideration is 0.8<Mag<1.

3.2 Bandstop Filter

Bandstop filters have a specific band or range of frequencies within which they attenuate signals. Thus, very low and very high frequency components of signals have a high gain and the signals within the specified attenuation range have very low gain.

The design of 2-D IIR Butterworth Bandstop filter is carried out in the same manner as the Bandpass design, in principle, by first designing the 1-D Butterworth filter and then combining two similar 1-D transfer functions as a product. The code has been written using MATLAB(Program B3) using the different built-in subroutines to achieve the filter specifications. The following procedure has been adopted to design the filter:

(1) In this case, the required specifications namely the order of the filter N and the upper and lower pass-band edges (W_n), as a 1x2 matrix, are first defined. The filter chosen has an analog cut-off frequency of [0.3, 1] and is of the fourth order. This means that frequencies beyond this range have high gain.

(2) The numerator and denominator polynomials of the analog transfer functions are determined using the MATLAB function *"butter"* for the Bandstop filter design. This gives the transfer function for the FIR filter.

In this case, the 4^{th} order Bandstop transfer function (1D) is given by

$$H_{IIR}(s) = \frac{s^8 + 1.2s^6 + 0.54s^4 + 0.1080s^2 + 0.0081}{(s^8 + 1.8292s^7 + 2.8730s^6 + 2.5426s^5 + 1.7839s^4 + 0.7628s^3 + 0.2586s^2 + 0.0494s + 0.0081)} \tag{3.11}$$

Having determined the numerator and denominator polynomials for the analog transfer function of the FIR filter, the IIR filter transfer function(1D) is then deter-

mined, as from Eqn.(2.19). This is given by

$$H_{IIR}(s) = \frac{s^8 + 1.2s^6 + 0.54s^4 + 0.108s^2 + 0.0081}{\begin{array}{c}(s^8 + 1.8292s^7 + 2.8730s^6 + 2.5426s^5 + 1.7839s^4 + \\ 0.7628s^3 + 0.2586s^2 + 0.0494s + 0.0081 + \\ k(s^8 + 1.2s^6 + 0.54s^4 + 0.108s^2 + 0.0081))\end{array}} \tag{3.12}$$

Now for Eqn.(3.12) to be stable, the range of k needs to be determined. Following the same method suggested in Chapter- 2 and from Eqn.(2.20) we have

$$\frac{m(s) + m_1(s)}{m(s)} = \frac{\begin{array}{c}(s^8 + 2.8730s^6 + 1.7839s^4 + 0.2586s^2 + 0.0081 + \\ k(s^8 + 1.2s^6 + 0.54s^4 + 0.108s^2 + 0.0081))\end{array}}{1.8292s^7 + 2.5426s^5 + 0.7628s^3 + 0.0494s} \tag{3.13}$$

Now Eqn.(3.13) can be split into partial fractions as follows

$$K_\infty s + \sum_i \frac{K_i s}{s^2 + \beta_i^2} + \frac{K_0}{s} = \frac{\begin{array}{c}(s^8 + 2.8730s^6 + 1.7839s^4 + 0.2586s^2 + 0.0081 + \\ k(s^8 + 1.2s^6 + 0.54s^4 + 0.108s^2 + 0.0081))\end{array}}{1.8292s(s^2 + 1.0002)(s^2 + 0.3)(s^2 + 0.09)} \tag{3.14}$$

where $\beta_1 = 1.0002$, $\beta_2 = 0.3$, $\beta_3 = 0.09$ are the roots of the denominator of Eqn.(3.13).

For Eqn.(3.14) to be a strictly Hurwitz polynomial, $K_i > 0$.

Therefore we find the values of K_i such that $K_i > 0$ and from the equations obtained, we find the range of k for stability.

From Eqn.(3.14), we have the following equations from which we determine the

range of k.

$$K_0 = \frac{0.0081(1+k)}{1.8292} > 0 \tag{3.15}$$

$$K_1 = \frac{\begin{array}{c}(s^8 + 2.8730s^6 + 1.7839s^4 + 0.2586s^2 + 0.0081 + \\ k(s^8 + 1.2s^6 + 0.54s^4 + 0.108s^2 + 0.0081))\end{array}}{1.8292s^2(s^2+0.3)(s^2+0.09)} \mid s^2 = 1.0002 \ > 0 \tag{3.16}$$

$$K_2 = \frac{\begin{array}{c}(s^8 + 2.8730s^6 + 1.7839s^4 + 0.2586s^2 + 0.0081 + \\ k(s^8 + 1.2s^6 + 0.54s^4 + 0.108s^2 + 0.0081))\end{array}}{1.8292s^2(s^2+1.0002)(s^2+0.09)} \mid s^2 = 0.3 \ > 0 \tag{3.17}$$

$$K_3 = \frac{\begin{array}{c}(s^8 + 2.8730s^6 + 1.7839s^4 + 0.2586s^2 + 0.0081 + \\ k(s^8 + 1.2s^6 + 0.54s^4 + 0.108s^2 + 0.0081))\end{array}}{1.8292s^2(s^2+1.0002)(s^2+0.3)} \mid s^2 = 0.09 \ > 0 \tag{3.18}$$

Solving the Eqns.(3.15), (3.16), (3.17) and (3.18), we have following ranges of k respectively, for which Eqn.(3.12) is stable.

$$-1 < k < \infty, \ no\ range, \ k < 1.4138, \ k < 1.3685 \tag{3.19}$$

Thus, the resultant range of k for which Eqn.(3.12) is stable is given by

$$-1 < k < 1.3685 \tag{3.20}$$

(3) Bilinear transformation is then performed to determine the digital counterpart. This is done using the MATLAB function *"bilinear"*. Refer to Program B4.

(4) Now we have the digital transfer function of the 1-D filter. The same procedure as above is extended to the second dimension and the transfer function for the second

dimension is obtained independently.

(5) The product of the two 1-D polynomials is determined.

(6) A general subroutine, suitable for any order of the filter has been written to determine the frequency response of the 2-D filter. Refer Program B4. The corresponding contour plots are plotted using the MATLAB function *"contour"*.

The MATLAB program namely, Program B3 and B4 has been written for the Bandstop filter specifications given by

$W_n1 = W_n2$	$N1 = N2$
[0.3 1]	4

All frequencies are in radians. The scripts 1 and 2 refer to the first and second dimensions respectively.

Program B3

```
%% 2D-BAND-STOP BUTTERWORTH FILTER
clear all;
close all;
N1=4;
Wn1=[0.3 1];
N2=N1;
Wn2=Wn1;
[B1,A1] = butter(N1,Wn1,'stop','s');
[B2,A2] = butter(N2,Wn2,'stop','s');
for k1=-1.0:0.1:1.36
zz=garg_rama_mag(B1,A1,k1);
lim=pi;
interval=pi/50;
w1=0:interval:lim;
w2=0:interval:lim;
[ww1,ww2]=meshgrid(w1,w2);
figure;
contour(ww1,ww2,zz);
```

```
axis('image');
xlabel('w1');
ylabel('w2');
zlabel('Magnitude Response');
title('2-D Butterworth BPF');
grid on;
print -dps bandstopcont.ps;
end
```

Program B4

```
%% Function to determine the transfer function of the filter for
%% a given k1,k2
function [zz] = garg_rama_mag(B1,A1,k1);
k2=k1;
B2=B1;
[R C]=size(A1);
for t=0: 2:C-1
A1(C-t) = A1(C-t) + k1*B1(C-t);
end
A2=A1;
%% Bilinear transformation of the transfer function
[N1,D1]=bilinear(B1,A1,1);
[N2,D2]=bilinear(B2,A2,1);
%% To determine the 2-D transfer function of the IIR Filter
for m=1:1:size(N1,2)
for n=1:1:size(N2,2)
N(m,n)= N1(m)*N2(n);
end
end
for m=1:1:size(D1,2)
for n=1:1:size(D2,2)
D(m,n)= D1(m)*D2(n);
end
end
lim=pi;
interval=pi/50;
c1=0;
```

```
for w1 = 0:interval:lim
c2=0;
c1=c1+1;
for w2 = 0:interval:lim
c2=c2+1;
for col=1:1:size(N2,2)
NRow(1,col)=(cos(w2) + j *sin(w2))^(size(N2,2)-col);
end
for row=1:1:size(N2,2)
NCol(row,1)=(cos(w1) + j *sin(w1))^(size(N1,2)-row);
end
NR = NRow * N' * NCol;
a=real(NR);
b=imag(NR);
for col=1:1:size(D2,2)
DRow(1,col)=(cos(w2) + j *sin(w2))^(size(D2,2)-col);
end
for row=1:1:size(D2,2)
DCol(row,1)=(cos(w1) + j *sin(w1))^(size(D1,2)-row);
end
DR = DRow * D' * DCol;
c=real(DR);
d=imag(DR);
MOD(c1,c2) = (sqrt((a*c + b*d)^2 + (b*c - a*d)^2))/(c^2+d^2);
end
end
w1=0:interval:lim;
w2=0:interval:lim;
[ww1,ww2]=meshgrid(w1,w2);
zz=MOD/(max(max(MOD)));
%% End of Program
```

The results of the algorithm namely the contour plots for the first quadrant are as shown in Fig.(3.3(a)-(e)). A large number of plots for all possible values of k within the stability ranges were plotted. Only the plots of interest have been shown. As it can be seen from Fig.(3.3), there is a certain range of k for which circular symmetry is exhibited in the frequency response for specific magnitude ranges. From Section 2.8, using Program A3, the extent of circular symmetry is determined for the above responses and the optimum value of k for which we have the closest proximity to circular symmetry is determined.

The plots in Fig.(3.4) show the extent of circular symmetry for the responses shown in Fig.(3.3). The plot for $k = 1.36$ is not shown since there are no points within this magnitude range which approximate to circular symmetry.

It is evident from the above plots that at $k = -0.40$, the response exhibits near circular symmetry and for other values of k above and below -0.40, the circular symmetry gradually ceases to exist. For the above study of Bandstop filter, near-circular symmetry has been considered for both the lower and upper pass-band in order to evaluate the optimum value of k.

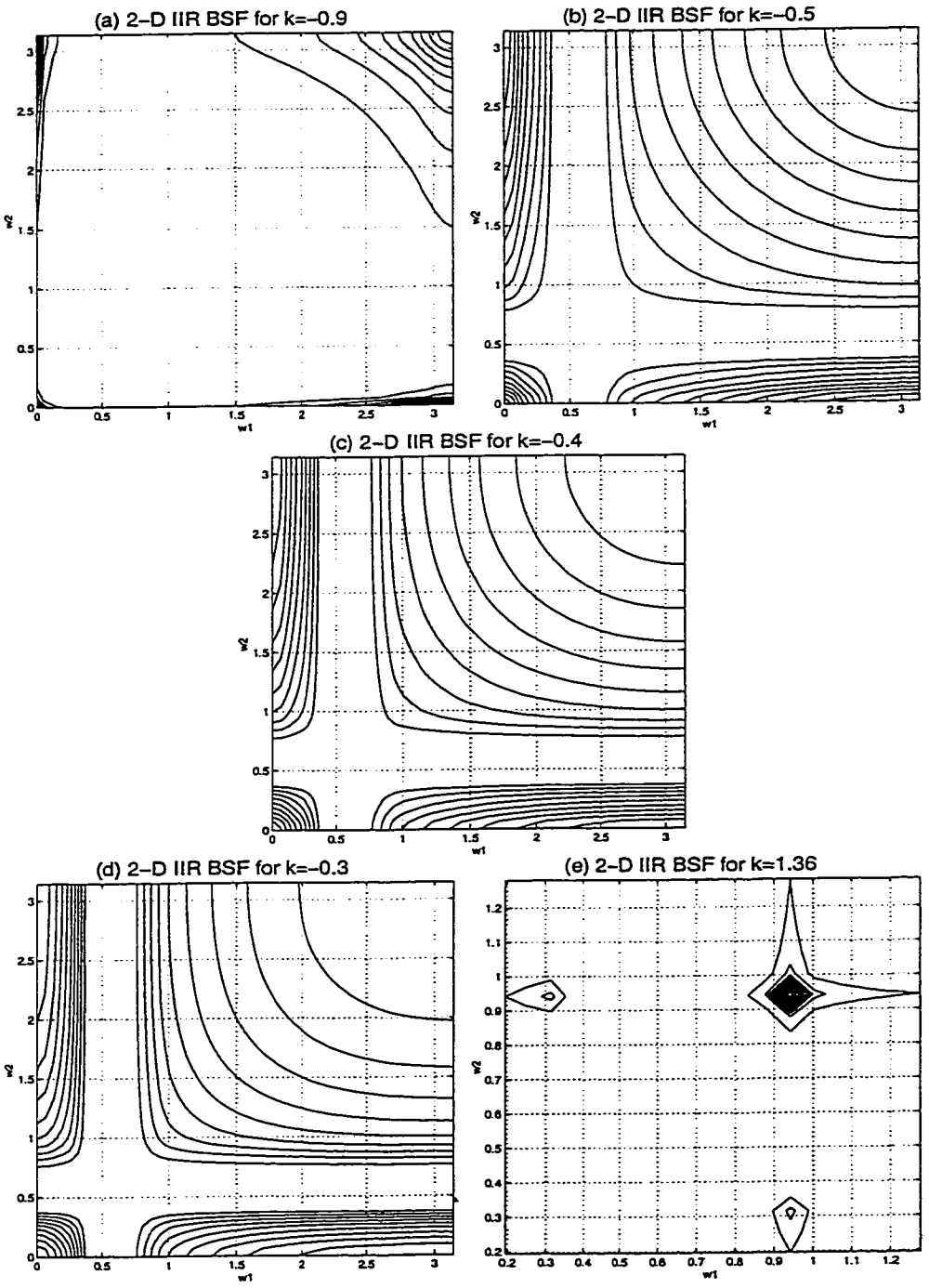

Figure 3.3: 2-D IIR Butterworth Bandstop Filter of 4th order-contour plots.

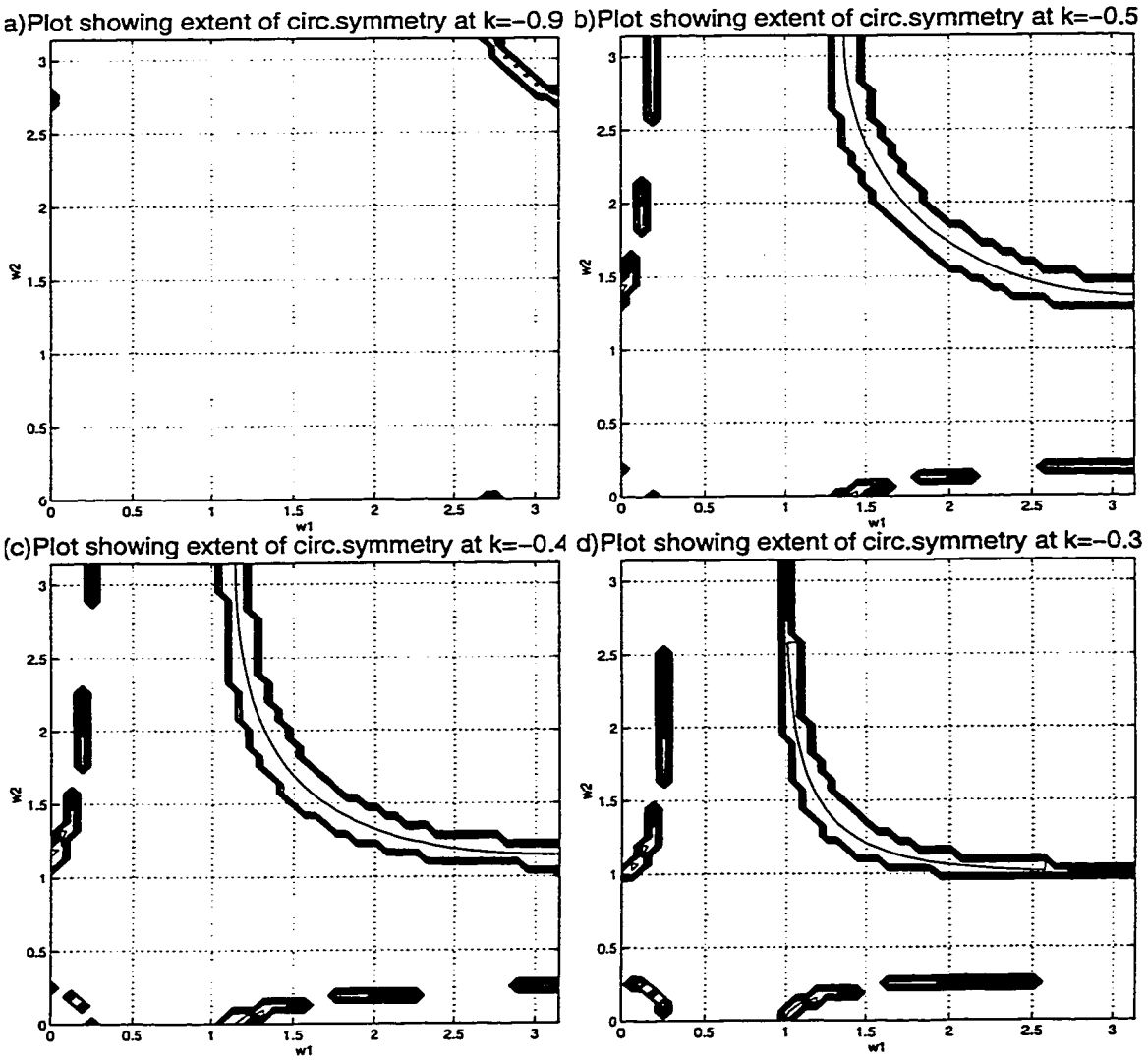

Figure 3.4: Plots to show the extent of circular symmetry of the responses shown in Fig.(3.3). The magnitude range under consideration is 0.45<Mag<0.55.

3.3 Highpass Filter

Highpass filters have a specific value of frequency above which they allow signals. Thus, low frequency components of signal are attenuated and the signals above the specified range have a high gain.

The design of 2-D IIR Butterworth Highpass filter is carried out in the same manner as the Lowpass design, in principle, by first designing the 1-D Butterworth filter and then combining two similar 1-D transfer functions as a product. The code has been written using MATLAB(Program B5) using the various built-in subroutines, to achieve the filter specifications. The following procedure has been adopted to design the filter:

(1) The required specifications namely the pass-band edge(W_1) and the order of the filter N are first defined. The filter chosen has an analog cut-off frequency of [0.3] and it has been chosen to be of the fourth order.

(2) The numerator and denominator polynomials of the analog transfer functions are determined using the MATLAB function *"butter"* for the Highpass filter design. This gives the transfer function for the FIR filter.

In this case, the 4^{th} order Highpass transfer function(1D) is given by

$$H_{FIR}(s) = \frac{s^4}{s^4 + 0.7839s^3 + 0.3073s^2 + 0.0706s + 0.0081} \tag{3.21}$$

Having determined the numerator and denominator polynomials for the analog transfer function of the FIR filter, the IIR filter transfer function(1D) is then determined,

as from Eqn.(2.19). This is given by

$$H_{IIR}(s) = \frac{s^4}{s^4(1+k) + 0.7839s^3 + 0.3073s^2 + 0.0706s + 0.0081} \tag{3.22}$$

Now for Eqn.(3.22) to be stable, the range of k needs to be determined. Following the same method suggested in Chapter-2 and from Eqn.(2.20) we have

$$\frac{m(s) + m_1(s)}{n(s)} = \frac{s^4(1+k) + 0.3073s^2 + 0.0081}{0.7839s^3 + 0.0706s} \tag{3.23}$$

Now Eqn.(3.33) can be split into partial fractions as follows :

$$K_\infty s + \sum_{i=1} \frac{K_i s}{s^2 + \beta_i^2} + \frac{K_0}{s} = \frac{s^4(1+k) + 0.3073s^2 + 0.0081}{0.7839s(s^2 + 0.0901)} \tag{3.24}$$

where $\beta_1 = 0.0901$ is the root of the denominator polynomial of Eqn.(3.23).

For Eqn.(3.24) to be a strictly Hurwitz polynomial, $K_i > 0$.

Therefore, we find the values of K_i such that $K_i > 0$ and from the equations obtained, we find the range of k for stability.

From Eqn.(3.24) we have the following equations from which we determine the range of k.

$$K_0 = \frac{0.0081}{1.8292} > 0 \tag{3.25}$$

$$K_\infty = 1 + k > 0 \tag{3.26}$$

$$K_1 = \frac{s^4(1+k) + 0.3073s^2 + 0.0081}{0.7839s} \mid s^2 = 0.0901 \quad > 0 \tag{3.27}$$

Solving the Eqns.(3.26) and (3.27), we have the following ranges of k, for which

Eqn.(3.22) is stable

$$-1 < k < \infty, \quad k < 1.4134 \tag{3.28}$$

Thus, the resultant range of k for which Eqn.(3.22) is stable is given by

$$-1 < k < 1.4134 \tag{3.29}$$

(3) Bilinear transformation is then performed to determine the digital counterpart. This is done using the MATLAB function *"bilinear"*. Refer to Program B6.

(4) Now we have the digital transfer function of the 1-D filter. The same procedure as above, is extended to the second dimension and the transfer function for the second dimension is obtained independently.

(5) The product of the two 1-D polynomials is determined.

(6) A general subroutine suitable for any order of the filter was written to determine the frequency response of the 2-D filter. Refer Program B32. The corresponding contour plots are plotted using the matlab function *"contour"*.

The MATLAB program namely, Program B5 and B6 has been written for the Highpass filter specifications given by

$W_n1 = W_n2$	$N1 = N2$
[0.3]	4

All frequencies are in radians. The scripts 1 and 2 refer to the first and second dimensions respectively.

Program B5

```
%% 2D-HIGHPASS BUTTERWORTH FILTER
clear all;
close all;
N1=4;
Wn1=[0.3 ];
N2=N1;
Wn2=Wn1;
[B1,A1] = butter(N1,Wn1,'high','s');
[B2,A2] = butter(N2,Wn2,'high','s');
for k1=-1.0:0.1:1.4
zz=garg_rama_mag(B1,A1,k1);
lim=pi;
interval=pi/50;
w1=0:interval:lim;
w2=0:interval:lim;
[ww1,ww2]=meshgrid(w1,w2);
figure;
contour(ww1,ww2,zz);
axis('image');
xlabel('w1');
ylabel('w2');
zlabel('Magnitude Response');
title('2-D Butterworth BPF');
grid on;
print -dps highpasscont.ps;
end
```

Program B6

```
%% Function to determine the transfer function of the filter for
%% a given k1,k2
function [zz] = garg_rama_mag(B1,A1,k1);
k2=k1;
B2=B1;
[R C]=size(A1);
A1(1) = A1(1) + k1*B1(1);
A2=A1;
```

```
%% Bilinear transformation of the transfer function
[N1,D1]=bilinear(B1,A1,1);
[N2,D2]=bilinear(B2,A2,1);
%% To determine the 2-D transfer function of the IIR Filter
for m=1:1:size(N1,2)
for n=1:1:size(N2,2)
N(m,n)= N1(m)*N2(n);
end
end
for m=1:1:size(D1,2)
for n=1:1:size(D2,2)
D(m,n)= D1(m)*D2(n);
end
end
lim=pi;
interval=pi/50;
c1=0;
for w1 = 0:interval:lim
c2=0;
c1=c1+1;
for w2 = 0:interval:lim
c2=c2+1;
for col=1:1:size(N2,2)
NRow(1,col)=(cos(w2) + j *sin(w2))^(size(N2,2)-col);
end
for row=1:1:size(N2,2)
NCol(row,1)=(cos(w1) + j *sin(w1))^(size(N1,2)-row);
end
NR = NRow * N' * NCol;
a=real(NR);
b=imag(NR);
for col=1:1:size(D2,2)
DRow(1,col)=(cos(w2) + j *sin(w2))^(size(D2,2)-col);
end
for row=1:1:size(D2,2)
DCol(row,1)=(cos(w1) + j *sin(w1))^(size(D1,2)-row);
end
```

```
DR = DRow * D' * DCol;
c=real(DR); d=imag(DR);
MOD(c1,c2) = (sqrt((a*c + b*d)^2 + (b*c - a*d)^2))/(c^2+d^2);
end
end
w1=0:interval:lim; w2=0:interval:lim;
[ww1,ww2]=meshgrid(w1,w2);
zz=MOD/(max(max(MOD)));
%% End of Program
```

The results of the algorithm namely, the contour plots for the first quadrant are as shown in Fig.(3.5(a)-(e)). A large number of plots for all possible values of k within the stability ranges were plotted. Only the plots of interest have been shown. As it can be seen from the above plots, there is a certain range of k for which circular symmetry is exhibited in the frequency response for specific magnitude ranges. From Section 2.8 using Algorithm A3, the extent of circular symmetry is determined for the above responses and the optimum value of k for which we have the closest proximity to circular symmetry is determined.

The plots in Fig.(3.6) show the extent of circular symmetry for the responses shown in Fig.(3.5). The plot for $k = 1.4$ has not been shown since there are no values that exhibit near-circular symmetry within the chosen magnitude range. It is evident from the above plots that at $k = -0.8$, the response exhibits near circular symmetry and for other values of k above and below -0.8, the circular symmetry gradually ceases to exist. However, it is noted that, specifically for a Highpass filter, since the pass-band range extends to infinity, it is really not possible to define a circular symmetric response all over the pass-band. In this section, strictly, near-circular symmetry has been demonstrated in the transition band.

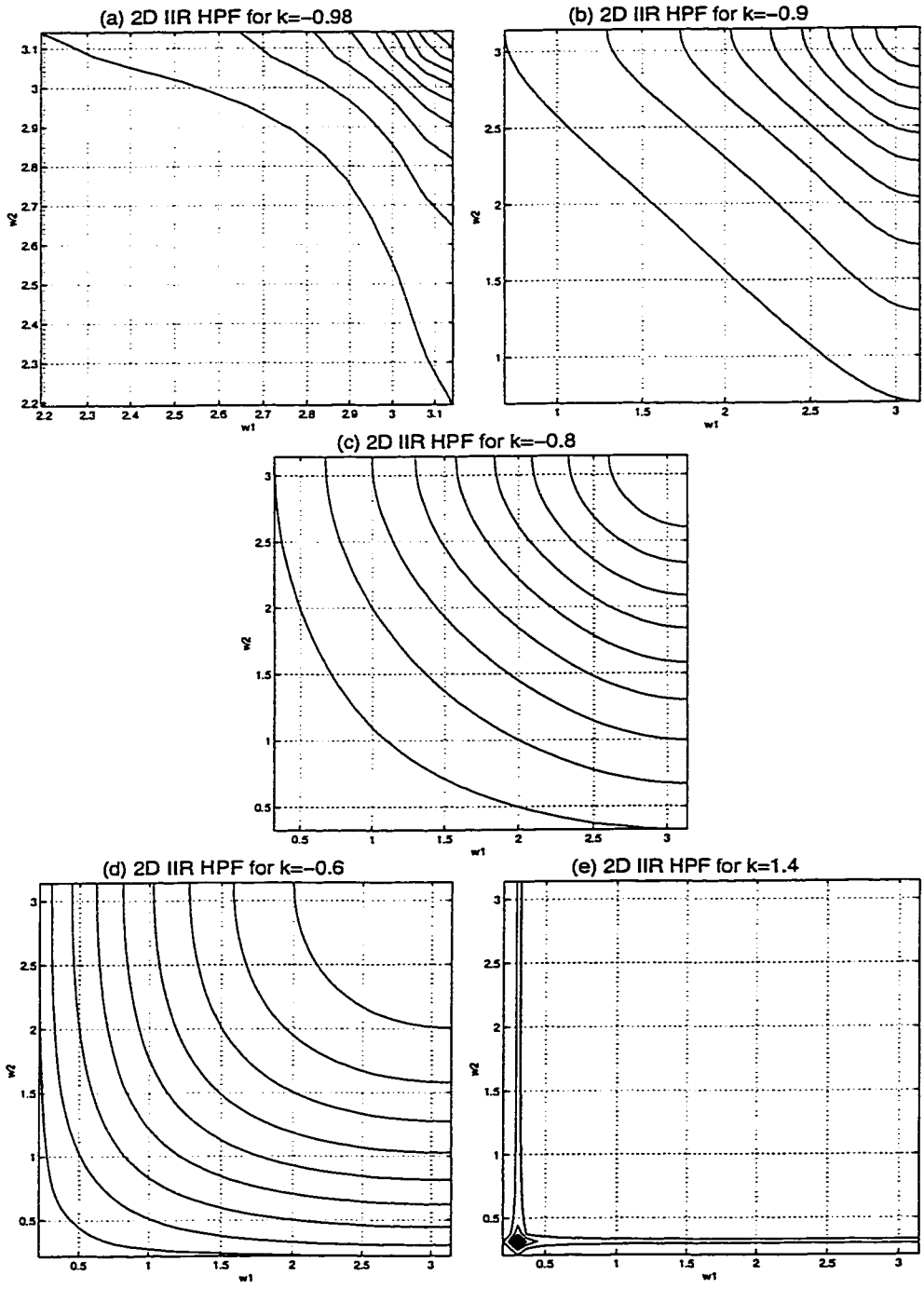

Figure 3.5: 2-D IIR Butterworth Highpass Filter of 4th order-contour plots.

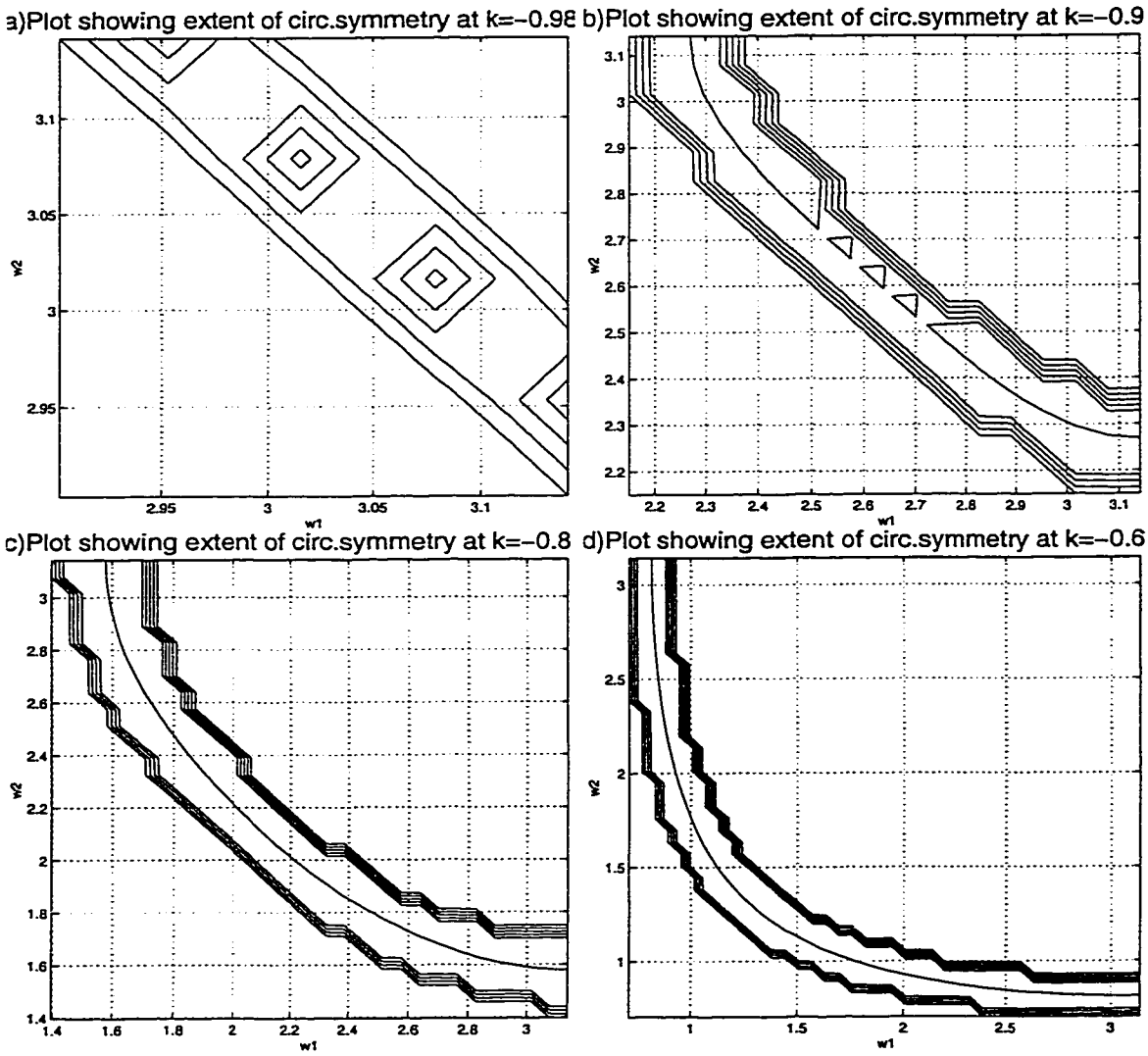

Figure 3.6: Plots to show the extent of circular symmetry of the responses shown in Fig.(3.5). The magnitude range under consideration is 0.45<Mag<0.55.

3.4 Summary and Discussion

This chapter has dealt with the design of 2-D Bandpass, Bandstop and Highpass IIR Butterworth filters and their approximation to circular symmetry within stability limits.

For the Bandpass filter, near circular symmetry has been obtained corresponding to a single quadrant of the filter response. This is because the Bandpass response is obviously a closed response within a quadrant, and circular symmetry in one quadrant means corresponding symmetry in all the four quadrants.

For the Bandstop filter, near circular symmetry can be seen in the two transition regions(lower and upper) and depending on the requirement, the study can be extended to a more specific region. Here too, the example shown takes into account the circular symmetry for both these regions of interest. In the lower transition region and below, circular symmetry study can be extended due to the response from all the four quadrants. The upper transition band and higher, however extend to infinity and therefore, this study can only be restricted to the lower part of the upper transition region.

For the Highpass filter, however, as has been mentioned before, the circular symmetry study can only be studied in the lower transition region due to the infinite bound of the pass-band region.

In general, from the results obtained from above, it can be seen that near circular symmetry has been obtained in certain frequency ranges for a particular value of a magnitude range. Depending on the required application, it is possible to change the specification in such a manner that circular symmetry for a different magnitude range can be studied and analysed.

Chapter 4

Combination Filters

Certain applications require specific types of symmetric response which may be uniquely obtained by combination of two or more filters of the same or different kind. This has been carried out before in different ways in 1-D analysis. This chapter deals with such types of combination filters, extended to the second dimension. In this chapter, it will be shown that transfer functions of one or more filters can be arithmetically added and/or subtracted to achieve a specific type of response. It is also intended here to study the extent of circular symmetry that can be achieved by such types of combination filters.

In this chapter we will deal with three different types of combination filters, namely:

1. Lowpass and Bandpass combination.
2. Bandpass Filter obtained as a result of the subtraction of two Lowpass filters.
3. Bandstop Filter obtained as a result of adding a Lowpass and a Highpass filter.

The above filters are achieved by combining the transfer functions of the two different types of filters.

4.1 Lowpass and Bandpass Combination Filter

First we will consider one of the the most elementary types of combination namely, the combination of a Lowpass and a Bandpass filter to form a specific type of response, in which the pass-band of the eventual combination filter will have variable gain depending upon how the transition regions of the Lowpass and the Bandpass filter add up. Fig.(4.1) shows the one-dimensional interpretation of the Lowpass and Bandpass combination filter. The design procedure is very simple in its sense. Firstly the

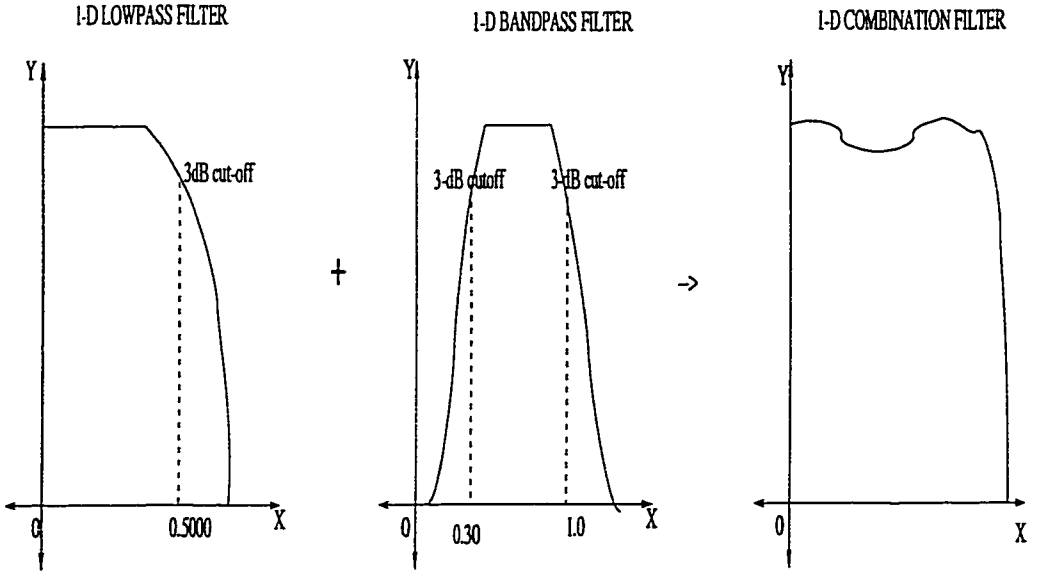

Figure 4.1: A one-dimensional interpretation of the Lowpass+Bandpass combination.

individual filters, namely the Lowpass and the Bandpass filter have been designed separately based on the design parameters shown in Table (4.1). The individual

Table 4.1: Combination filter parameters - Lowpass + Bandpass Filter.

	Lowpass Filter	Bandpass Filter
Order	4	4
Cut-off(rad)	0.5	[0.3 1]

filters are designed and analysed separately for their respective responses.

Another important aspect of this study, has been to analyse the extent of circular symmetry of the combination filter when the individual filters are themselves approximated to circular symmetry.

In this case, the Lowpass and the Bandpass filters have been separately analysed for circular symmetry following the same procedure in Chapter-3. Following that analysis, we have the results as follows.

Lowpass Transfer function= $\frac{0.0625}{s^4+1.3066s^3+0.8536s^2+0.3266s+0.0625}$

Range of k for stability $= -1 < k < 1.4143$.

Value of k for near circular symmetry $= -0.26$.

The plots in Fig.(4.2) show the response for the Lowpass filter corrected for near circular symmetry.

The Bandpass filter considered here, has the same response as the one shown in Section 3.1. Refer Section 3.1 for figures.

The effective response of the combination filter which is obtained as a result of adding the Lowpass and the Bandpass transfer functions is shown below.

The response of the combination filter as shown in Fig.(4.3), has then been studied to test its closeness to circular symmetry using Program A3(Chapter-2). This study reveals the plot on Fig.(4.4).

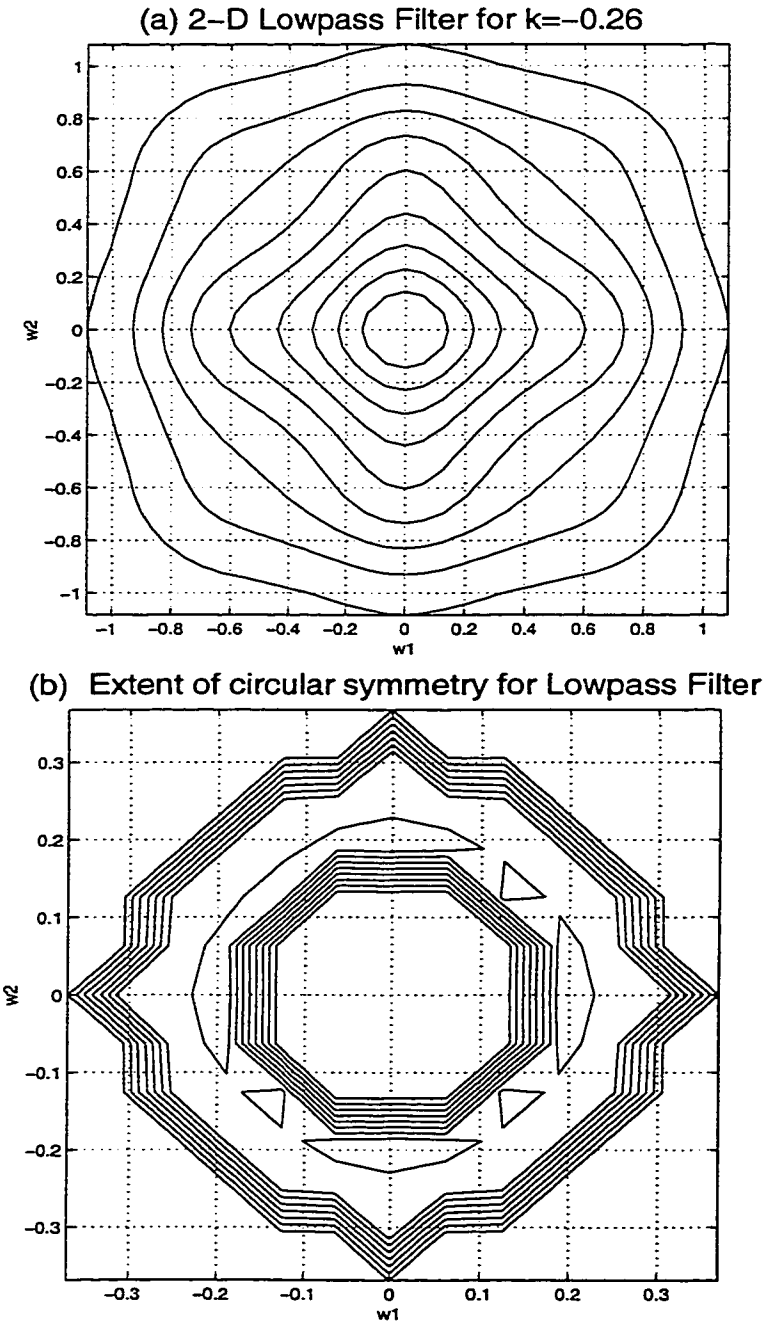

Figure 4.2: Plots showing (a) the response of the Lowpass filter (b) approximation to circular symmetry between magnitude range [0.7,0.9](normalised) derived from Program A3.

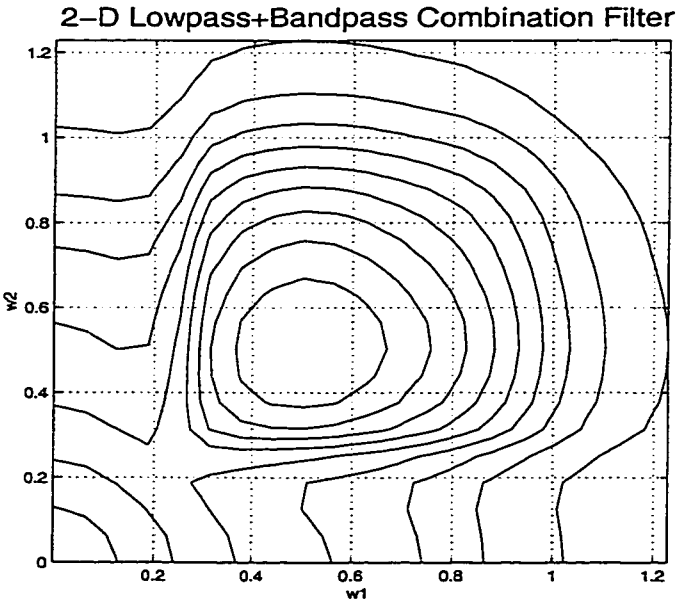

Figure 4.3: Plot showing the response of the combination filter.

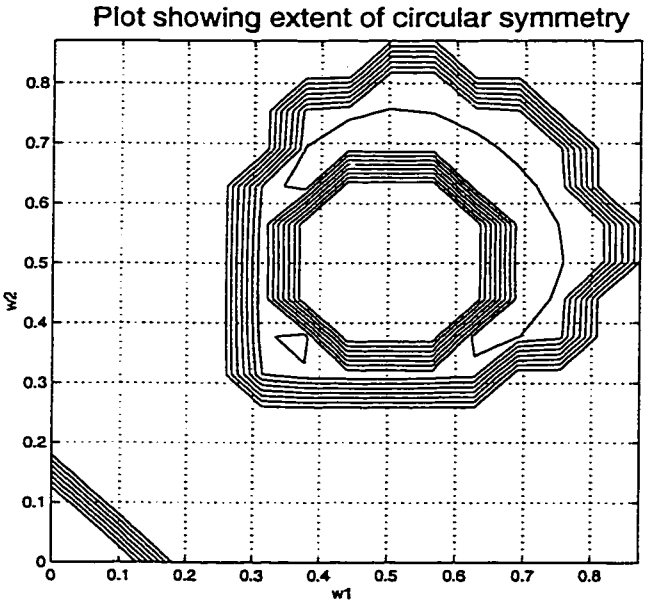

Figure 4.4: Plot showing the extent of circular symmetry in the combination of a Lowpass and a Bandpass filter. Magnitude range under study=[0.7 0.9](normalised) derived from Program A3.

It is evident from Fig.(4.4) that, near circular symmetry cannot be obtained in the transition region, although the individual filters are near-circularly symmetric in their respective transition regions. Circular symmetry is however, found possible in the pass-band regions of the combination filter within which the individual Lowpass and Bandpass pass-band regions are not affected by the magnitude response of each other. It is seen that the Bandpass region of the combination filter exhibits near circular symmetry to an extent.

The Program to obtain the above results has been written in MATLAB and is shown below in Program C1.

Program C1

```
%% 2-D LOWPASS+BANDPASS COMBINATION BUTTERWORTH FILTER
clear all; close all;
%%2-D LOWPASS BUTTERWORTH FILTER
Lk1=-0.26; LN1=4; LWn1=0.5; L N2=LN1; LWn2=LWn1;
[LB1,LA1] = butter(LN1,LWn1,'s');
[LB2,LA2] = butter(LN2,LWn2,'s');
LPTF = garg_rama_mag(LB1,LA1,Lk1);
%%2-D BANDPASS BUTTERWORTH FILTER
Bk1=-0.14; BN1=4; BWn1=[0.3 1]; BN2=BN1; BWn2=BWn1;
[BB1,BA1] = butter(BN1,BWn1,'s');
[BB2,BA2] = butter(BN2,BWn2,'s');
BPTF=garg_rama_mag(BB1,BA1,Bk1);
TTF=LPTF+BPTF;
TTF=TTF/(max(max(TTF)));
lim=pi; interval=pi/50;
w1=0:interval:lim; w2=0:interval:lim;
[ww1,ww2]=meshgrid(w1,w2);
figure;
contour(ww1,ww2,(TTF));
axis('image'); xlabel('w1'); ylabel('w2'); zlabel('Magnitude Response');
title('2-D Butterworth Lowpass+Bandpass Combination Filter');
grid on;
```

4.2 Lowpass and Lowpass Combination Filter

Next we will consider a more interesting combination namely, the combination of two Lowpass filters to form an eventual Bandpass response. Fig.(4.5) shows the one-dimensional interpretation of the two Lowpass combination filter. It shows that when two Lowpass filters of different cut-off frequencies (the first one higher than the second one) are subtracted from each other, we get an eventual Bandpass response. The de-

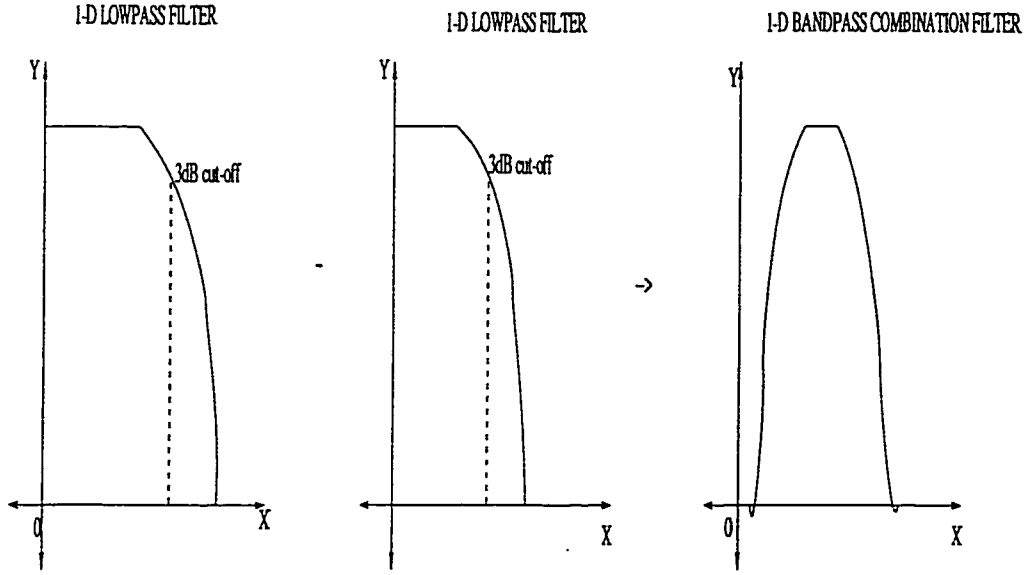

Figure 4.5: A one-dimensional interpretation of the two Lowpass filter combination.

sign procedure is simple. First, the individual Lowpass filters are designed separately based on the design parameters shown in Table (4.2). The most important aspect of this study has been to analyse the extent of circular symmetry of the combination filter when the individual filters are themselves approximated to circular symmetry.

In our case, both the Lowpass filters have been separately analysed for circular symmetry following the same procedure as in Chapter-3. Note that the first Lowpass filter that has been considered here for illustration follows the same design as the one

Table 4.2: Combination filter parameters - Lowpass - Lowpass Filter.

	Lowpass Filter1	Lowpass Filter2
Order	4	4
Cut-off(rad)	0.5	0.2

that was chosen in Section 4.1. The analysis of the Lowpass filters are as follows:

Lowpass Transfer function(1) = $\frac{0.0625}{s^4+1.3066s^3+0.8536s^2+0.3266s+0.0625}$

Range of k for stability = $-1 < k < 1.4143$.

Value of k for near circular symmetry for Filter 1 = -0.26.

Lowpass Transfer function(2) = $\frac{0.0016}{s^4+0.5226s^3+0.1366s^2+0.0209s+0.0016}$

Range of k for stability = $-1 < k < 1.4360$.

Value of k for near circular symmetry for Filter 2 = -0.01.

The plots in Fig.(4.6) show the response for the Lowpass filters corrected for near circular symmetry for a specific magnitude range(from Program A3). It is seen that the individual filters exhibit near circular symmetry within the specific magnitude range.

The effective response of the combination filter which is obtained as a result of subtracting the Lowpass filter(2) from Lowpass Filter(1) is shown in Fig.(4.7). This figure shows both the mesh and contour plots of the combination filter which approximates to a Bandpass response. The extent of circular symmetry has been tested for this combination filter and it has been seen that the combination filter exhibits near circular symmetry in the outer range of subtraction. Theoretically, the subtraction of two Lowpass filters should result in a Bandpass filter. From the combination filter plots, it is seen that a Bandpass filter with a short pass-band region has been obtained. Near circular symmetry is possible in the outer boundary of this pass-band

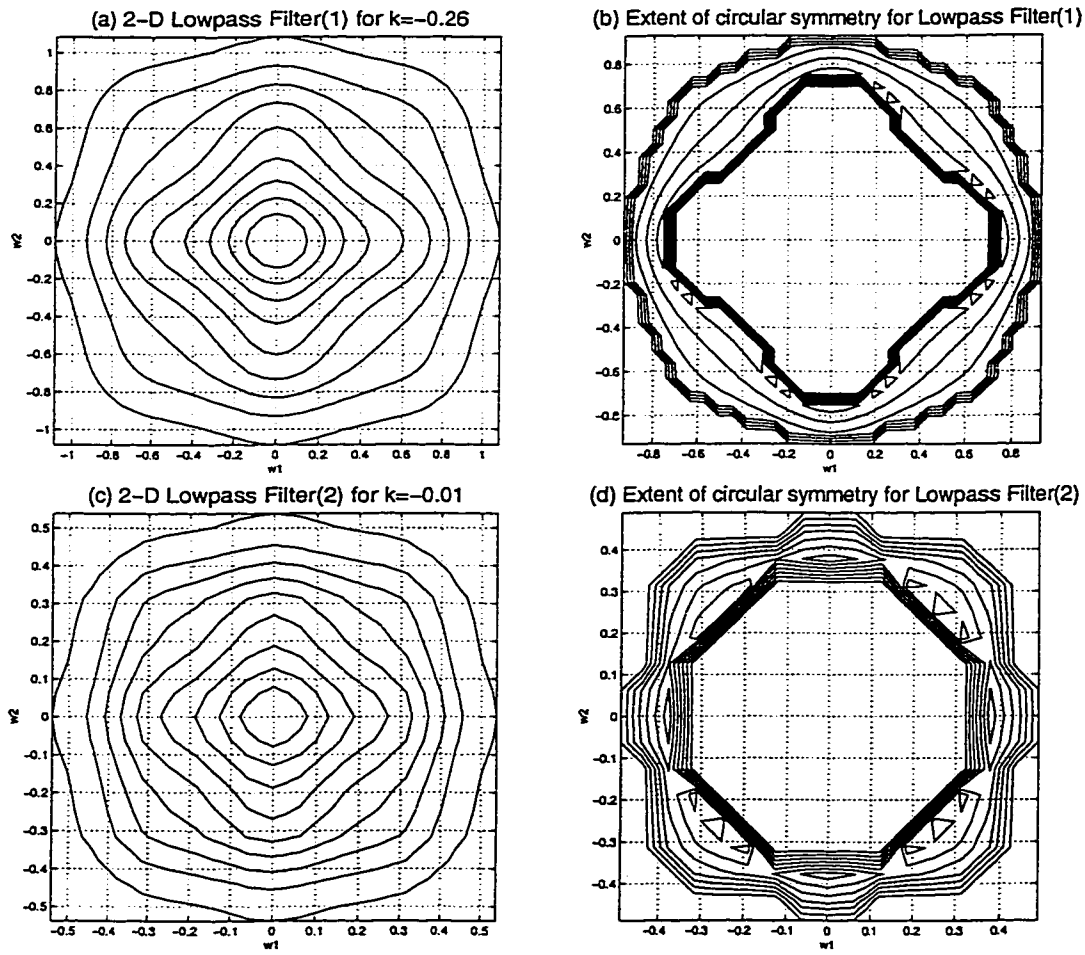

Figure 4.6: Plots (a) and (c) showing the response of the Lowpass filters (1) and (2) respectively and plots (b) and (d) showing their approximation to circular symmetry for a specific magnitude range [0.2, 0.4](normalised) derived from Program A3.

region. Circular symmetry exists for certain magnitudes in the pass-band regions of the individual filters which are not affected by the magnitude response of each other.

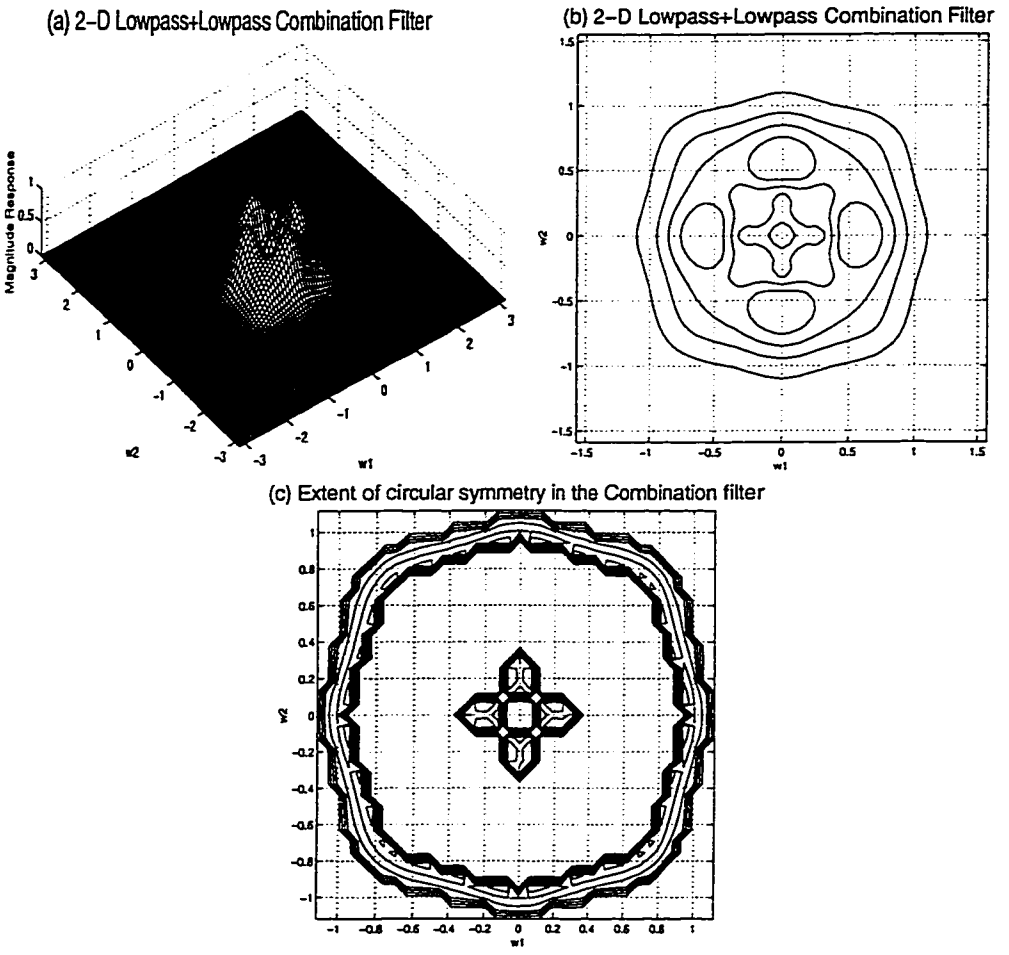

Figure 4.7: Plots (a) and (b) showing the response of the combination filter(magnitude and contour plots respectively) and plot (c) showing the extent of circular symmetry in this response between the magnitude range[0.2, 0.4](normalised) derived from Program A3.

The Program to obtain the above results has been written in MATLAB and is shown below in Program C2.

Program C2

```
%% 2-D LOWPASS+LOWPASS COMBINATION BUTTERWORTH FILTER
clear all;
close all;
%%2-D LOWPASS BUTTERWORTH FILTER - 1
Lk1=-0.26; LN1=4; LWn1=0.5; LN2=LN1; LWn2=LWn1;
[LB1,LA1] = butter(LN1,LWn1,'s');
[LB2,LA2] = butter(LN2,LWn2,'s');
LPTF = garg_rama_mag(LB1,LA1,Lk1);
LPTF = LPTF/max(max(LPTF));
%%2-D LOWPASS BUTTERWORTH FILTER - 2
lk1=0; lN1=4; lWn1=0.2; lN2=lN1; lWn2=lWn1;
[lB1,lA1] = butter(lN1,lWn1,'s');
[lB2,lA2] = butter(lN2,lWn2,'s');
lPTF=garg_rama_mag(lB1,lA1,lk1);
lPTF = lPTF/max(max(lPTF));
TTF=LPTF-lPTF;
TTF=TTF/(max(max(TTF)));
lim=pi; interval=pi/50;
w1=-lim:interval:lim;
w2=-lim:interval:lim;
[ww1,ww2]=meshgrid(w1,w2);
figure;
mesh(ww1,ww2,(TTF));
axis('image');
xlabel('w1');
ylabel('w2');
zlabel('Magnitude Response');
title('2-D Butterworth Lowpass+Lowpass Combination Filter');
grid on;
%%print -dps bandpasscont.ps;
```

4.3 Lowpass and Highpass Combination Filter

We will now consider another type of combination filter which effectively yields a Bandstop filter by combining arithematically, the responses of a Lowpass and Highpass filters. We will consider the Lowpass and Highpass filters with near circular symmetric responses on their outer limits so that the Bandstop filter can also be studied for its extent of circular symmetry by the combination of the above filters. Fig.(4.8) shows the one-dimensional interpretation of the Lowpass and Highpass combination filter. The design procedure, here again, is very simple in its sense. Firstly

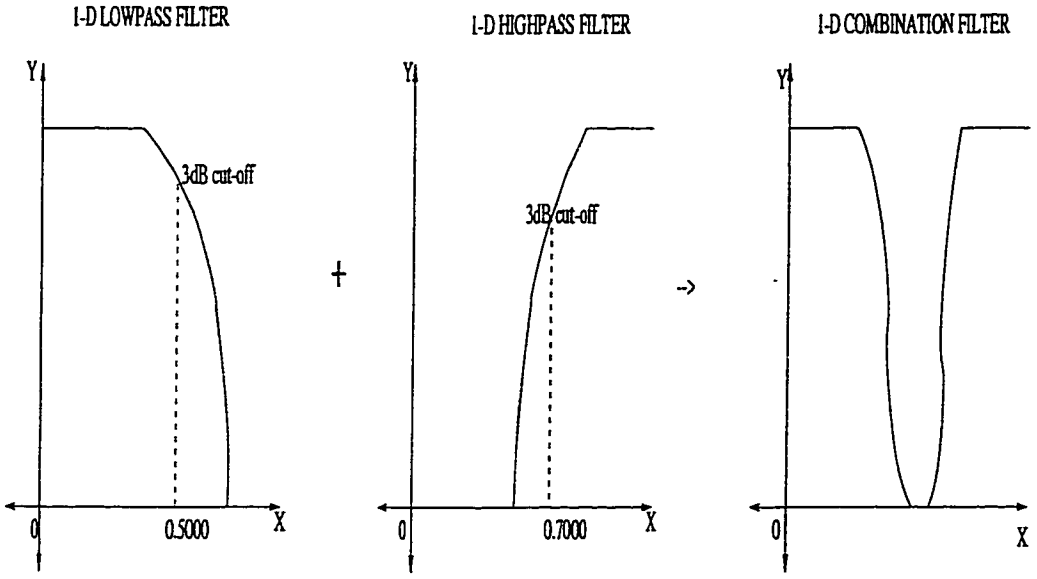

Figure 4.8: A one-dimensional interpretation of the Lowpass+Highpass combination.

the individual filters, namely the Lowpass and the Highpass filter have been designed separately based on the design parameters shown in Table (4.3). The individual filters are designed and analysed separately for their respective responses.

Another important aspect of this study has been to analyse the extent of circular symmetry of the combination filter when the individual filters are themselves

Table 4.3: Combination filter parameters - Lowpass + Highpass filter.

	Lowpass Filter	Highpass Filter
Order	4	4
Cut-off(rad)	0.5	0.7

approximated to circular symmetry.

In our case, the Lowpass and the Highpass filters have been separately analysed for circular symmetry following the same procedure as in Chapter-3. Following that analysis, we have the following results:

Lowpass Transfer function= $\frac{0.0625}{s^4+1.3066s^3+0.8536s^2+0.3266s+0.0625}$

Range of k for stability = $-1 < k < 1.4143$.

Value of k for near circular symmetry = -0.26.

Note that the Lowpass filter considered here, follows the same design as that considered in Section 4.1.

The plots in Fig.(4.9) show the response for the Lowpass filter corrected for near circular symmetry. The Highpass filter considered here, has a cut-off frequency of 0.7 leaving a stop-band range for the combination filter between [0.5, 0.7]. The Highpass filter is first studied independently, for circular symmetry following the same method as suggested in Section 3.3. Following that analysis we have the following results:

Highpass Transfer function= $\frac{s^4}{s^4+1.8292s^3+1.6730s^2+0.8963s+0.2401}$

Range of k for stability = $-1 < k < 1.4167$.

Value of k for near circular symmetry = -0.52.

The response of the Highpass filter after its test for stability due to variation in parameter k is as shown in Fig.(4.10). The response of the combination filter is as shown in Fig.(4.11) has then been tested for its extent of circular symmetry using Program A3(Chapter-2). This study reveals the following plots. The reason why the

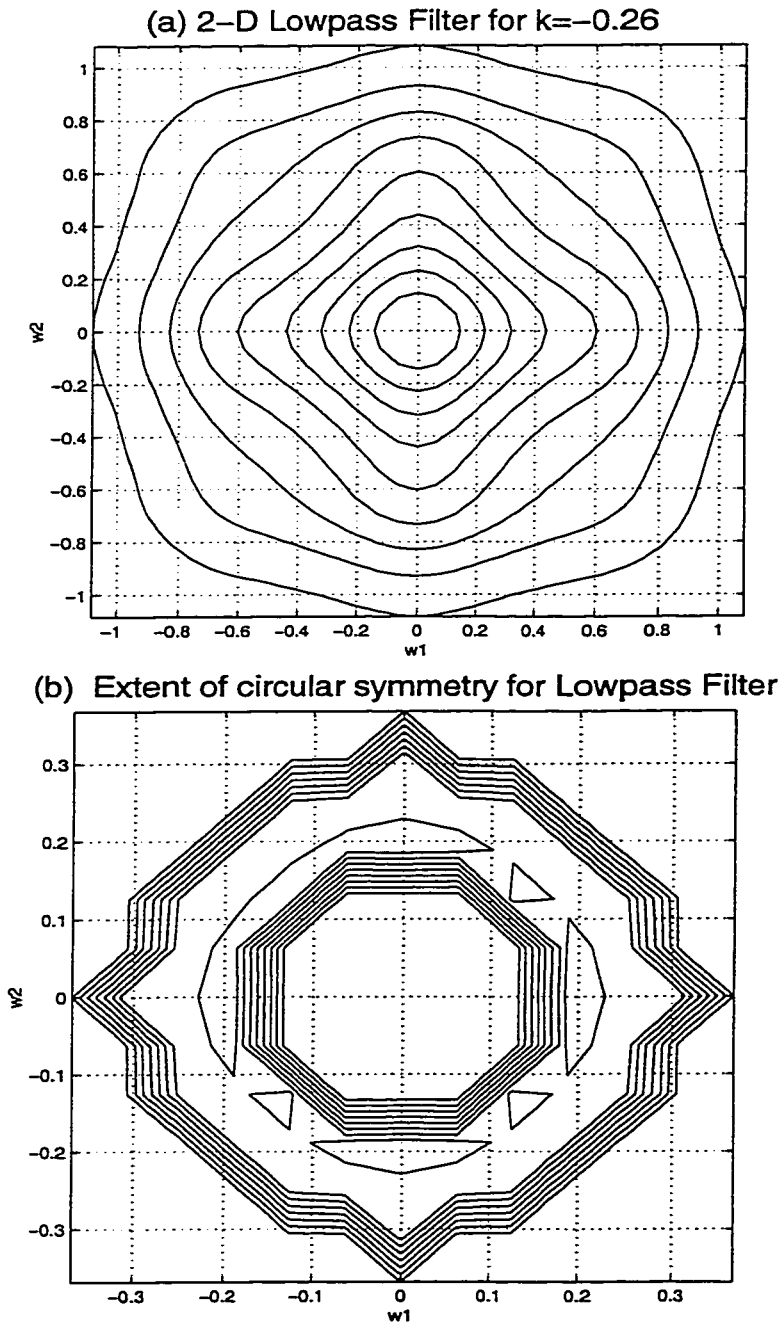

Figure 4.9: Plot (a) showing the response of the Lowpass filter and plot (b) showing its approximation to circular symmetry between magnitude range [0.2, 0.4](normalised) derived from Program A3.

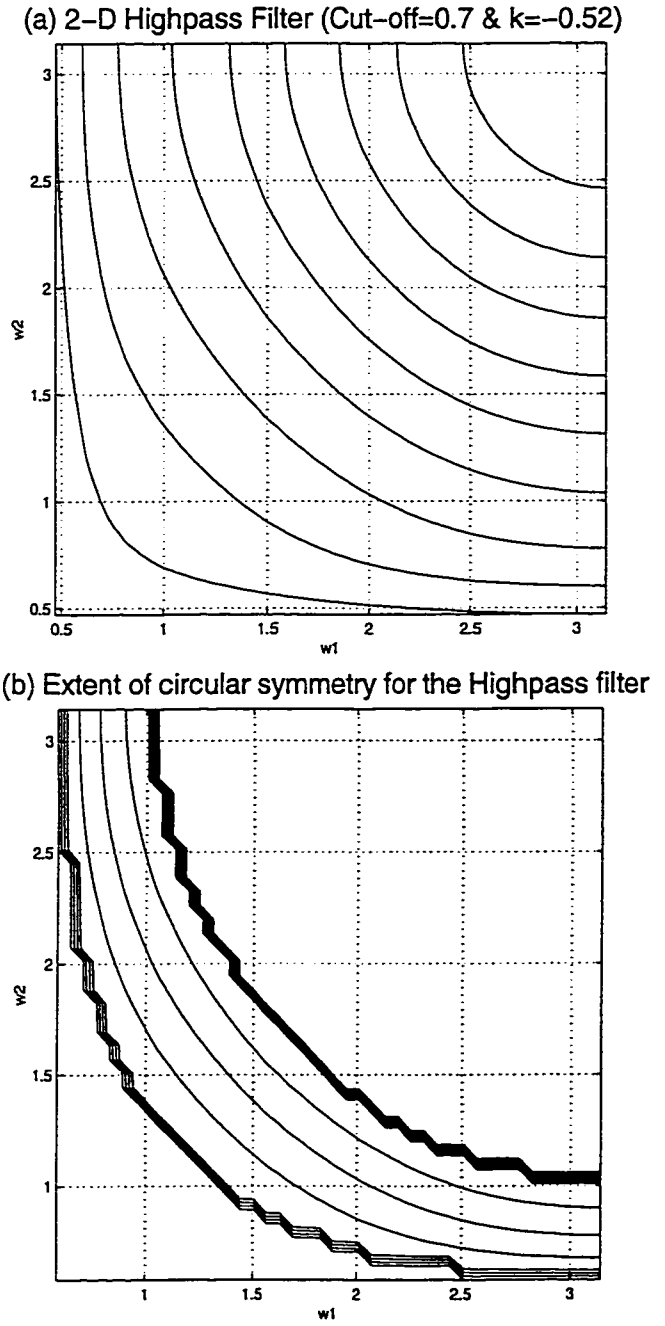

Figure 4.10: Plot (a) showing the response of the Highpass filter and plot (b) showing its extent of circular symmetry for $k = -0.52$ and in the magnitude range [0.2, 0.4](normalised) derived from Program A3.

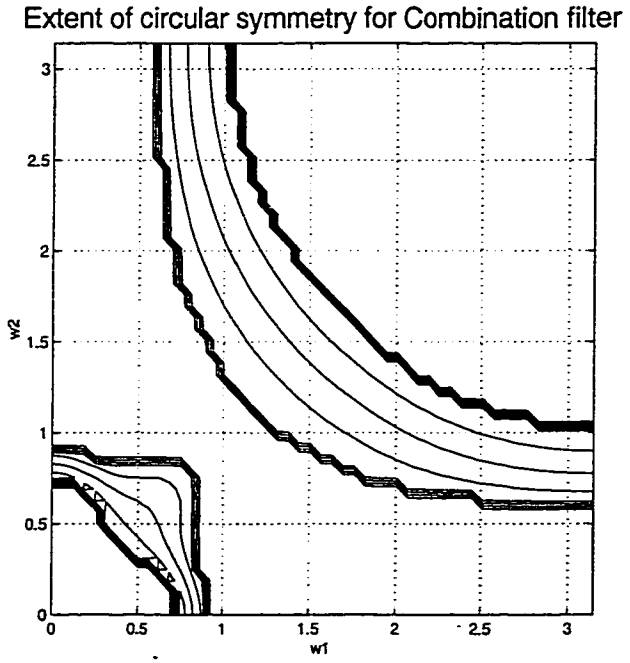

Figure 4.11: Plot to show the extent of circular symmetry in the combination of a Lowpass and a Highpass filter. Magnitude range under study=[0.2 0.4](normalised) derived from Program A3.

magnitude range of [0.2, 0.4] is chosen for study of circular symmetry is that, the transition regions of the individual filters lie around this value of magnitude range. It is evident from Fig.(4.11) that near circular symmetry can still be obtained in the transition region of the combination filter. Circular symmetry is also not affected by the responses of the filters in their respective pass-bands due to the effect of their combined magnitudes.

The Program to obtain the above results were written in MATLAB and is shown below in Program C3.

Program C3

```
%% 2-D LOWPASS+HIGHPASS COMBINATION BUTTERWORTH FILTER
clear all;
close all;
Lk1=-0.26; LN1=4; LWn1=0.5; LN2=LN1; LWn2=LWn1;
[LB1,LA1] = butter(LN1,LWn1,'s');
[LB2,LA2] = butter(LN2,LWn2,'s');
LPTF = garg_rama_mag_LP(LB1,LA1,Lk1);
%%2-D HIGHPASS BUTTERWORTH FILTER
Hk1=-0.52; HN1=4; HWn1=0.7; HN2=HN1; HWn2=HWn1;
[HB1,HA1] = butter(HN1,HWn1,'high','s');
[HB2,HA2] = butter(HN2,HWn2,'high','s');
HPTF=garg_rama_mag_HP(HB1,HA1,Hk1);
TTF=LPTF+HPTF;
TTF=TTF/(max(max(TTF)));
lim=pi; interval=pi/50;
w1=0:interval:lim; w2=0:interval:lim;
[ww1,ww2]=meshgrid(w1,w2);
figure;
mesh(ww1,ww2,(TTF));
axis('image');
xlabel('w1'); ylabel('w2');
zlabel('Magnitude Response');
title('2-D Butterworth Lowpass+Highpass Combination Filter','FontSize',18');
grid on;
figure;
contour(ww1,ww2,(TTF));
axis('image');
xlabel('w1'); ylabel('w2');
zlabel('Magnitude Response');
title('2-D Butterworth Lowpass+Highpass Combination Filter','FontSize',18');
grid on;
```

4.4 Summary and Discussion

In this chapter, we have dealt with three different types of combination filters. The purpose of this chapter has been to study the effect of combining individual filters which have near circular symmetry in their transition regions. The effective combination filter has been studied and analysed to see if the circular symmetry still exists in its response.

The first combination filter to be studied was the effect of a Lowpass and a Bandpass filter to form a Lowpass filter of larger pass-band. This study revealed that near circular symmetry in the combination filter can only be obtained in the individual pass-band regions of the two filters and the transition region does not exhibit circular symmetry.

The second combination filter to be studied was the effect of combining(subtracting) two Lowpass filters of different pass-band widths, to obtain a Bandpass filter. Here it has been shown that circular symmetry exists to an extent in the transition regions of the Bandpass combination filter. Circular symmetry also exists in the individual filter's pass-band regions where-in the responses of the individual filters do not affect each other.

The third combination filter to be studied was the effect of combining a Lowpass and a Highpass filter to form a Bandstop combination filter. Here again, it has been proven that circular symmetry exists in the transition region of the Bandstop combination filter response.

This chapter is just the first step towards the study of combining filter responses to obtain unique and user-specific responses. Modern image processing softwares use this feature to obtain specific responses towards enhancing image quality.

Chapter 5

Conclusions

Multi-dimensional system and analysis is a topic that is developing in great pace and specifically 2-D systems are used widely in modern image processing software and analysis. One of the main uses that 2-D system finds itself in, are the 2-D filters. Modern image processing softwares[6] require sufficient amount of pre-processing of the raw image data that is being used for analysis.. These pre-processing steps comprise mainly of filtering noise and smoothening defects that might otherwise cause serious implications in image analysis. This pre-processing stage largely uses Butterworth filters of a given order to correct the image and mould it for efficient image analysis. Image processing itself, in its true sense, uses different kinds of filters for various image manipulation purposes such as sharpening, smoothening, edge detection and other arithematic operations. In all these cases we deal with image data which is truly two-dimensional in its sense. Thus it becomes necessary that we deal with 2-D filters which do not have any preferential orientation towards data manipulation because the image signal itself, does not have any preferential spatial direction. This fact has been the main motivation behind this thesis work. This study, in all

its chapters, focuses mainly on the extent of circular symmetry of 2-D filters obtained as a result of simplistic design procedures. Other interesting aspects such as pole-parameter transformation and their effect on circular symmetry and the effect of combining different types of 2-D filter functions have also been studied and analysed.

5.1 Circular Symmetry of 2-D Filters

We have implemented a simple method of designing 2-D IIR filters, namely using the product of two 1-D IIR transfer functions. The most important factor to be considered for filter design is the stability of the filters. It is necessary to test stability for any filter design, inorder that the filter does not become unstable for bounded input frequency. It is a known fact that Finite Impulse Response(FIR) filters are inherently stable. However there is more flexibility with IIR Filters in terms of parameter modifications to obtain a required set of filters. The main problem, however, affecting the design of IIR filters is the stability of the filters. Bringing the filter into the second dimension also increases the complexity to test stability. This again is one of the main reasons why 2-D filters obtained as the product of two, 1-D filters have been used in this thesis. Methods have already been proposed[30] to perform a stability check on such types of separable denominator transfer functions in two dimensions. In this thesis, these have been used , to test the designed filter for stabilty, before further analysis. This ensures that the filter is stable and can withstand the various parameter modifications that it undergoes for approximation to circular symmetry. It has also been shown in[30], that it is possible to have variable magnitude characteristics for 2-D filters by changing the feedback factor k in the IIR filter transfer function, within stability limits, and obtain responses close to circular symmetry. This is the most important

factor used in this thesis to study the different possibilities of circular symmetry. The circular symmetry study in this thesis can be divided into four different groups based on the nature and type of filters that have been used, namely Lowpass filter study, study of filters obtained due to pole-parameter variation, study of the other common types of filters namely Highpass, Bandpass and Bandstop filters and the study of combination of these common types of filters. All the filter transfer function considered in the above study have an infinite impulse response. In what follows, we will have a summary of the various conclusions we have obtained as a result of this study.

5.1.1 Study of Circular Symmetry in Lowpass Filters

In Chapter-2, we have concentrated on the two most commonly used filter transfer functions, namely, the Butterworth and the Chebyshev transfer functions. These are used to approximate 2-D circular symmetry.

Butterworth Filters

The transfer function that has been used in this thesis for this type of filter is of third order. The point here is to adhere to the lowest order possible that can easily illustrate the effect of circular symmetry. Higher order filters can be used for the same kind of analysis but will involve more complexity in terms of design, computer programming and time of execution. It is thus sufficient to consider a third order transfer function to illustrate the approximation to circular symmetry.

2-D filters have been plotted first, simply as a product of two 1-D filters and it has been clearly shown that circular symmetry is not a possibility(Fig.(2.1)), without

further effort. The feedback factor k is then tested for stability limits($-1 < k < 3$) and for this specific third order transfer function (Eqn.(2.20)) various filters are plotted between these limits and the transfer function is analysed. It has been found that circular symmetry exists(Fig.(2.5)) at a value of $k = -0.3$. A separate program has been written using MATLAB to study the magnitude charateristic of each of these filters obtained as a function of k and circular symmetry has been studied between the normalised magnitude range of $0.49 < Mag < 0.51$. It is from this program that the accurate value of k (Fig.(2.8)) is determined for closest proximity to circular symmetry. It is possible to study a different magnitude range of interest and for each of these range, there will exist a different value of k for near circular symmetry.

Chebyshev Filters

There are two transfer functions that have been used to study the case of Chebyschev filters. These two transfer functions are different from each other based on the single most important factor of distinction between filters of this type namely, the ripple width. The transfer function of the filters that have been used to study these cases is of third order. The ripple widths that have been considered are $\epsilon = 0.1526$ and $\epsilon = 0.3493$.

For the first case, where the ripple width is $\epsilon = 0.1526$, it has been found that circular symmetry exists for a value of $k = -0.64$, if the magnitude range range under study is $0.28 < Mag < 0.32$.

For the second case, where the ripple width is $\epsilon = 0.3493$, it has been found that circular symmetry exists for a value of $k = -0.25$, if the magnitude range range under study is $0.49 < Mag < 0.51$.

In effect, for the parameters chosen in their respective cases, the first case(Fig.(2.13c)) exhibits better circular symmetry than the second case(Fig.(2.15c)). Hence, for a given ripple width and order of a chebyshev filter, it is possible to determine the value of k (within stability limits) and the range of magnitude response over which the circular symmetry is possible.

5.1.2 Study of Circular Symmetry in Complementary Pole-pair Filters

Complementary pole-pair filters are a unique set of filters obtained as a result of change in the pole-parameters. In this case the pole-parameter that has been chosen for study of different kinds of filters is the polar angle of the poles of these filters. This study has been illustrated in one dimension to explain the nature of these types of filters[15] and it has then been extended to the second dimension for the purpose of meeting the objectives of this thesis.

Circular symmetry study here has been carried out for different cases based on the change in the polar angle and accordingly, extensive simulations have been done for specific change in polar angles of $\pm 3°, \pm 5°$ *and* $\pm\ 7°$. It is seen from Fig.(2.23c), Fig(2.25c), Fig.(2.26c), Fig.(2.27c), Fig.(2.28c) and Fig.(2.29c) that the best possible circular symmetries that can be obtained within the magnitude range $0.49 < Mag < 0.51$, are for the respective values of k as shown in the each plot. It can also be observed that circular symmetry gradually ceases to exist, as the angle of the pole-parameter variation increases. The same can also be proved for a different magnitude range under study. In this case we will have different values of k for circular symmetry for each of the angle variation but the effective disintegration in circular symmetry

will still be experienced for greater increase in the polar angle.

5.1.3 Study of Circular Symmetry in 2-D Highpass, Bandpass and Bandstop Filters

Common types of filters that are used in practice, apart from the Lowpass filters, are the Highpass, Bandpass and Bandstop filters. In Chapter-3, the extent of circular symmetry on 2-D filters of the above types have been studied.

Bandpass Filters

The Bandpass filter that has been studied in this case has an analog cut-off frequency between [0.3, 1.0] and has been chosen to be fourth order. The IIR transfer function of such a filter is then determined(Eqn.(3.1)) and the values of k for which the filter is stable is found to be in the range $-1.0048 < k < 1.3684$. Within these limits, it has been found that the filter exhibits near circular symmetry only in high magnitude ranges $0.8 < Mag < 1.0$ and for a value of $k = -0.14$(Fig.(3.1c)), near circular symmetry has been obtained within the specified magnitude range. It is noted that the study of circular symmetry for Bandpass filter has been shown only for one quadrant. This is due to the fact that, 2-D filters with separable denominator polynomials exhibit symmetry about the X and Y axis and circular symmetry is a possibility within only one of the quadrants. It is also seen that for higher values of k, circular symmetry completely ceases to exist.

Bandstop Filters

The Bandstop filter that has been studied in this case has an analog cut-off frequency of [0.3, 1.0] and has been chosen to be of fourth order. This means that the filter has high gain beyond this region. The IIR transfer function of such a filter is then determined(Eqn.(3.11)) and the values of k for which the filter is stable is found to be in the range $-1 < k < 1.3685$. Within these limits, it has been found that the filter exhibits near circular symmetry only in high magnitude ranges $0.45 < Mag < 0.55$ and for a value of $k = -0.40$(Fig.(3.4c)), near circular symmetry has been obtained within the specified magnitude range. Here too, the study of circular symmetry has been shown only for one quadrant. Although it is possible that for frequencies lower than the lower cut-off frequencies, circular symmetry can exist covering all four quadrants. It is noted that near circular symmetry can only be seen within the lower cut-off region in both dimensions, since for the higher cut-off region, there cannot be a closed response covering all four quadrants, as the response extends to infinity. For higher values of k, even this extent of circular symmetry ceases to exist.

Highpass Filters

The Highpass filter that has been used in this case is a fourth order filter with a cut-off beyond 0.3. For a Highpass filter, since the pass-band region exists from a certain cut-off frequency to infinity it is entirely not possible to define circular symmetry in the passband. It can only be defined for a single quadrant(half a semicircle) and it has to be assumed that the symmetry exist upto infinity. Having defined the transfer function from the known parameters mentioned above(Eqn.(3.21)), the range of k for stability of the filter is given by $-1 < k < 1.4134$. It has been found that there exists

a symmetry that can be approximated to a circle, at infinity for a vlaue of $k = -0.80$. Beyond this value this symmetry cease to exist. Although circular symmetry cannot be visualised for a Highpass filter with separable denominator transfer function, it has been proved that there exists a symmetry that approximates to a circle at infinity in the transition region of the filter.

5.1.4 Study of Circular Symmetry in 2-D Combination Filters

Another interesting aspect that has been considered in Chapter-4 of this work is to combine some common filters that have already been approximated for circular symmetry and study the extent of circular symmetry on the combination filters. There are three such combinations which have been considered.

Combination of Lowpass and Bandpass Filter

In this case a Lowpass and a Bandpass filter which have been already considered in Chapter-2 and Chapter-3 respectively, have been used to form a combination response which resembles a Lowpass response with non-uniform gain in its pass-band region. This has been obtained by adding the individual responses of the filters. It is seen here that circular symmetry does not exist in the combination filter in the transition region but still exists in certain parts of the response which are not an effect of the combination.(Fig.(4.3)).

Combination of Lowpass and Lowpass Filter

In this case, two Lowpass filters of different cut-off frequencies, 0.5 and 0.2 respectively, have been used to form a combination response which resembles a Bandpass

response. This has been obtained by subtracting the two responses. It is seen here that circular symmetry is a distinct possibilty in the region shown in (Fig.(4.7c)). This study can also be extended to different magnitude regions to see how the subtraction of two near circular symmetric filters affect the symmetry.

Combination of Lowpass and Highpass Filter

In this case a Lowpass and a Highpass filter which have analog cut-off frequencies of 0.5 and 0.7 respectively, have been used to form a combination response which resembles a Bandstop response. It is seen here too that circular symmetry only exists in certain regions of the filters which are not entirely affected by the individual reponse of each other(Fig.(4.11)). In this case the Lowpass response and the Highpass response show their individual closeness to circular symmetry and we do not see the same in the transition band.

Thus, the overall purpose of this thesis has been to study the effect of circular symmetry on separable denominator 2-D transfer functions. Four of the most common types of filters have been chosen and studied. It has been seen largely that circular symmetry is possible in the Lowpass and the Bandpass responses and is not a distinct possibility in the Highpass and Bandpass responses due to the unlimited response range. The different filters and cases considered have been obtained after number of simulations. However it is possible to vary the value of k or the magnitude range under study to obtain innumerable instances of near circular symmetry in these cases. There is a lot of scope for future work in this respect.

From the foregoing, it is clear that it is possible to obtain 2-D circular symmetric filters, starting from 1-D filters. These could be Lowpass, Highpass, Bandpass or

Bandstop filters, obtained either directly or by a combination of other filters. Apart from the configuration considered in Fig.(2.2), it appears possible that there may exist other configurations exhibiting circular symmetry and this is a suggestion for further work.

An interesting investigation would be to start from two Allpass filters which give rise to complementary filters. This is a suggestion for future work.

Bibliography

[1] Rabiner, R.L. and Gold, B. " Theory and Application of Digital Signal Processing " Prentice Hall, 1975.

[2] Jury, E.I. "Inners and Stability of Dynamic Systems", John Wiley and Sons, 1974.

[3] Gargour, C.S. and Ramachandran, V. "Generation of very strictly Hurwitz polynomials and Applications to 2-D Filter Design", Control and Dynamic Systems, Academic Press Inc.Vol.69, pp.211-254, 1995.

[4] Goodman,D. "Some difficulties with Double Bilinear Transformation in 2-D Digital Filter Design", Proc.IEEE, Vol.66, July 1978.

[5] Tzafestas, S.G. "Multidimensional Systems:Techniques and Applications", 1986.

[6] Matrox Imaging Library(MIL)-User Guide, Matrox Electronic System Inc. Montreal.

[7] Karivaratharajan,P., and Swamy, M.N.S., "Symmetry Constraints on two-dimensional Half-Plane Digital Transfer Functions". IEEE Trans. on Acoustics, speech and signal processing, 27(5):506-511, 1979.

[8] Shanks, J.L., Treitel, S. and Justice, J.H., "Stability of two-dimensional Recursive Filters". IEEE Trans. Audio-Acoustics, Vol. AU-20, June 1972.

[9] Mitra, S.K., Sagar, A.D. and Pendergrass, N.A. "Realization of two-dimensional Recursive Digital Filters". IEEE Trans. on Circuits and Systems, Vol.CAS-22, No.3, 1975.

[10] Swamy, M.N.S., Thyagarajan, K.S., and Ramachandran,V., "Two-dimensional wave digital filters using doubly terminated two variable LC-ladder configurations", Journal of the Franklin Institute, Vol.304, No.4/5, pp.201-215.

[11] McClellan, J.H. : "The design of two-dimensional digital filters by transformations". Proc. of the 7th Annual Princeton conference on information sciences and systems, pp.247-251, 1973.

[12] Bernabli, M., Cappellini, V., and Emiliani, P.M. : "A method for designing 2-D recursive digital filters having a circular symmetry". Proc. of Florence conference on digital signal processing, Sept.11th-13th, pp.196-203, 1975.

[13] Karivaratharajan,P., and Swamy, M.N.S. : "Quadrantal symmetry associated with two-dimensional digital transfer functions", ibid., CAS-25, pp.340-343, 1978.

[14] Karivaratharajan, P., and Swamy, M.N.S. : "Some results on the nature of a two-dimensional filter function possessing certain symmetry in its magnitude response", IEE J.Electronic Circuits & Systems, 2, (5), pp.147-153, September 1978.

[15] Pai,K.R., Murthy,K.V.V., Ramachandran,V., "Complementary Pole-Pair Filters And Pole Parameter Transformations", J.Circuits & Systems and Computers, Vol.6, No.4, pp.319-350, 1996.

[16] O.Hermann, "On the approximation problem in non-recursive digital Filter design", IEEE Trans. on Circuit Theory, Vol. CT-18, pp.411-413, May 1971.

[17] J.F.Kaiser, "Design subroutine(MXFLAT) for symmetric FIR Lowpass digital filters, with maximally-flat pass and stop-bands," in Programs for Digital Signal Processing, IEEE Press, 1979.

[18] P.P.Vaidyanathan, "On Maximally-Flat Linear-Phase FIR Filters", IEEE Trans. on Circuits & Systems, Vol.CAS-31, No.9, September 1984.

[19] Ramachandran,V. and Gargour,C.S. "Generation of very strict Hurwitz polynomials and applications to 2-D filter design". Control and Dynamic Systems, Vol.69, pp.211-253, 1995.

[20] Goodman,D. " Some stability properties of two-dimensional linear shift-invariant digital filters," IEEE Transactions on Circuits and Systems, Vol.CAS-24, No.4, pp.201-208, April 1977.

[21] Huang. T.S., "Stability of two-dimensional recursive filters", IEEE Transactions in Audio Electroacoustics, Vol.AU-20, pp.158-163, 1972.

[22] Mersereau, R.M., Mecklenbrauker, W.F.G. and Quatieri.Jr, T.F., "McClellan transformations for 2-D digital filtering: I.Design", IEEE Transactions in Circuits Systems, Vol.CAS-23, No.7, pp.405-414, 1976.

[23] Hu, J.V. and Rabiner, L.R., "Design techniques for two-dimensional digital filters", IEEE Transactions in Audio Electroacoustics, Vol.AU-20, No.1, pp249-257, 1972.

[24] Harris, D.B. and Mersereau, R.M., " A Comparison of algorithms for minimax design of two-dimensional linear phase FIR digital filters", IEEE Transactions in Acoustic Speech Signal Processing., Vol.ASSP-25, No.6, pp.492-500, 1977.

[25] Huang, T.S., "Two-dimensional windows", IEEE transactions in Electro Acoustics, vol.AU-20, No.1, pp.88-89, 1972.

[26] Kaiser,J.F., "Digital Filters", in system Analysis by Digital Computer.(Kuo,F.F. and Kaiser, J.F., Eds.), Wiley, New York, 1966.

[27] Hilberg, W., and Rothe, P.G., "The general uncertainity relation for real signals in the communication theory", Information and Control, Vol.18, pp.103-125, 1971.

[28] Cappellini, V. and Constantinides, A.G. and Emiliani,P.L., "Digital Filters and their applications", Academic Press, New York, 1978.

[29] Costa, J.M. and Venetsanopoulos, A.N., "Design of circulary symmetric two-dimensional filters", IEEE Transactions in Acoustic Speech Signal Processing, Vol.ASSP-22, no.6, pp.432-443, 1974.

[30] Gargour, C.S. and Ramachandran,V., "Generation of Stable 2-D Transfer Functions Having Variable magnitude characteristics", Control and Dynamic Systems, Academic Press Inc. Vol.69, pp.255-297, 1995.

[31] Su, K.L, "Analog Filters", Chapman and Hall, 1996.